Klara Treusch, Dipl.-Ing. BSc.

Continuous Hydrodeoxygenation of Liquid Phase Pyrolysis Oil

DOCTORAL THESIS

to achieve the university degree of

Doktorin der technischen Wissenschaften

submitted to

Graz University of Technology

Supervisor

Priv.-Doz. Dipl.-Ing. Dr.techn. Nikolaus Schwaiger

Institute of Chemical Engineering and Environmental Technology

Graz, March 2019

AFFIDAVIT

I declare that I have authored this thesis independently, that I have not used other than the declared sources/resources, and that I have explicitly indicated all material which has been quoted either literally or by content from the sources used. The text document uploaded to TUGRAZonline is identical to the present doctoral thesis.

01.03.2019	
Date	Signature

'...we are all facing dark and difficult times... the time should come when you have to make a choice between what is right, and what is easy...'

– Albus Percival Wulfric Brian Dumbledore

Joanne K. Rowling, Harry Potter and the Goblet of Fire

Acknowledgements

I want to express my appreciation to all the people who contributed to this thesis in one way or another. My gratitude goes to:

Nikolaus Schwaiger	for not only for being the best first time doctoral thesis supervisor or as I would like to call it "Jedi master", but also for being the most patient and promoting mentor I could imagine in the last seven years and for becoming a true friend.
Matthäus Siebenhofer	for being the person with seemingly infinite knowledge, for having an open door and open mind whenever I needed a piece of advice and for leveling my publications up in record time.
Peter Pucher	for showing me my strengths and weaknesses, for being honest and straightforward, for providing a perfect working environment to focus on this thesis and for encouraging me to believe in myself.
Edgar Ahn	for enabling and promoting my academic career as another one in a long list of young researchers graduating in the environment of BDI.
Daniela Painer	for being the best new project leader and for the enjoyable collaboration in the last year of the project.
BDI, especially R&D	for the best work environment I could have asked for, they make going to work every day feel a little more like coming back to see friends.
All Master-, Bachelor and project students	for the laboratory work, without which the experiments would not have been possible, for sharing good and bad times and for the lessons I have learned.
My TU colleagues	for all the enjoyable coffee breaks and helpful exhilarating conversations in difficult moments.
My family, my grandmother, my sisters and my father, especially my mother	for always taking care of me as the youngest sister, for supporting me in any way, for all the crucial life lessons and for enabling and promoting a good education.
Markus	for taking care of me now, for supporting me, for tolerating and listening to me in my grumpy and confused PhD phases and for helping me with the acknowledgements.

ABSTRACT

Science is racing against time to stop global warming sooner rather than later, keeping the status quo of living standard. This includes a change from fossil to sustainable biogenous resources for energy provision. This doctoral thesis follows the approach of biogenous liquid fuel production via liquid phase pyrolysis of lignocellulosic biomass and subsequent hydrodeoxygenation of liquid phase pyrolysis oil. During liquid phase pyrolysis in the bioCRACK pilot plant, 20 to 26 wt% of biogenous carbon were transferred from biomass to liquid phase pyrolysis oil. Experiments for upgrading of liquid phase pyrolysis oil were investigated in continuous operation mode in lab scale by applying high hydrogen pressure. Thereby, oxygen was removed by forming water, carbon monoxide and carbon dioxide. Various experiments have been performed with a sulfided heterogeneous catalyst, $CoMo/Al_2O_3$, which is commonly used in petroleum refineries. The evaluated parameters include temperature in the range of 250 to 400°C, pressure at 80 and 120 bar, liquid hourly space velocities of 0.5 to 3 h^{-1} and substitution of fossil hydrogen by biogenous synthesis gas. Co-processing of liquid phase pyrolysis oil and petroleum refinery intermediates has been investigated at refinery hydrotreating conditions in order to reduce investment costs and evolve a straightforward process. It was observed that the process is insensitive to temperature in the range of 350 to 400°C and to the liquid hourly space velocity in the range of 0.5 to 1 h^{-1}. With these parameters, a product with a residual water content below 0.05 wt%, a lower heating value of 42 to 43 MJ kg^{-1} and a boiling range between those of gasoline and diesel was obtained. Co-processing of liquid phase pyrolysis oil and heavy gas oil as a petroleum refinery model compound was feasible by applying a two step process, consisting of mild hydrodeoxygenation and thus hydrophobation of liquid phase pyrolysis oil at 300°C and co-processing at 400°C, both at 120 and 80 bar hydrogen pressure. The application of synthesis gas instead of pure hydrogen resulted in comparable product properties with a lowered hydrogen consumption through in situ water-gas shift reaction with the particularly high water portion contained in liquid phase pyrolysis oil. Hydrodeoxygenation of liquid phase pyrolysis oil was shown to be applicable at petroleum refinery conditions of high liquid hourly space velocities in single-step operation due to the low viscosity and buffering of the heat of reaction by water.

KURZFASSUNG

Die Wissenschaft befindet sich in einem Rennen gegen die Zeit, um die globale Erwärmung zu stoppen und den Status quo des Lebensstandards zu erhalten. Dazu gehört unter anderem die Bereitstellung von Energie aus nachhaltigen biogenen statt – wie bisher – hauptsächlich aus fossilen Ressourcen. Im Zuge dieser Doktorarbeit wurde der Ansatz der direkten Biomasseverflüssigung zur Herstellung von flüssigen Energieträgern aus lignocelluloser Biomasse über Flüssigphasenpyrolyse und anschließende Hydrodeoxygenierung von Flüssigphasenpyrolyseöl verfolgt. In der bioCRACK-Pilotanlage zur Flüssigphasenpyrolyse lignocelluloser Biomasse wurden 20 bis 26 m% des biogenen Kohlenstoffs in Flüssigphasenpyrolyseöl transferiert. Dieses wurde im Anschluss im Labormaßstab unter Anwendung von hohem Wasserstoffdruck kontinuierlich hydrodeoxygeniert. Dabei wurde der im Flüssigphasenpyrolyseöl vorhandene Sauerstoff unter Bildung von Wasser, CO und CO_2 entfernt. Es wurden mehrere Versuchsreihen mit einem heterogenen, in der Erdölraffinerie üblichen CoMo/Al_2O_3-Katalysators im Temperaturbereich von 250 bis 400°C, bei 80 sowie 120 bar, bei Raumgeschwindigkeiten von 0,5 bis 3 h^{-1} und mit Substitution von hochreinem, fossilem Wasserstoff durch biogenes Synthesegas durchgeführt. Zusätzlich wurde eine mögliche Integration der Flüssigphasenpyrolyseöl Hydrodeoxygenierung in Erdölraffinarien durch Co-Verarbeitung mit schwerem Gasöl als fossile Modellsubstanz bei raffinerieüblichen Hydrierbedingungen untersucht. Der Temperatureinfluss im Bereich von 350 bis 400°C und der Einfluss der Raumgeschwindigkeit zwischen 0,5 und 1 h^{-1} auf die Produktqualität wurden als gering beobachtet. Bei diesen Bedingungen wurde ein Treibstoff mit einem Wassergehalt von unter 0,5 m% und einem unteren Heizwert von 42 bis 43 MJ kg^{-1} sowie einem Siedebereich entsprechend einem Gemisch aus Benzin und Diesel hergestellt. Die Co-Verarbeitung von Flüssigphasenpyrolyseöl und Erdölraffinationsintermediaten wurde durch einen zweistufigen Prozess ermöglicht. Im ersten Schritt wurde Flüssigphasenpyrolyseöl bei 300°C mild hydrodeoxygeniert und dadurch hydrophobiert. Dieses Zwischenprodukt wurde im zweiten Schritt gemeinsam mit schwerem Gasöl vollständig hydriert. Beide Schritte wurden bei je 120 sowie 80 bar Wasserstoffruck durchgeführt. Die Verwendung von Synthesegas anstelle von Wasserstoff führte zu einer vergleichbaren Produktqualität bei gleichzeitiger Reduzierung des Wasserstoffverbrauchs durch eine in situ durchgeführte Wassergas-Shift-Reaktion mit dem in Flüssigphasenpyrolyseöl vorhandenen Wasser. Es wurde gezeigt, dass die Hydrogeoxygenierung von Flüssigphasenpyrolyseöl durch die niedrige Viskosität und die vom Wasser gepufferte Reaktionswärme bei hohen, in einer Erdölraffinerie üblichen Raumgeschwindigkeiten im einstufigen Betrieb durchgeführt werden kann.

Chapter 1

Framework – Biomass liquefaction with BDI-BioEnergy International GmbH

1. Framework – Biomass liquefaction with BDI-BioEnergy International GmbH

This work was established during the project bioBOOST^{plus} from 2016 to 2018, funded by the Austrian Research Promotion Agency under the scope of Climate and Energy Fund in cooperation with BDI-BioEnergy International GmbH and the Institute of Chemical Engineering and Environmental Technology at Graz University of Technology. It contributes to the continuous upgrading of pyrolysis oil produced by direct biomass liquefaction through liquid phase pyrolysis via hydrodeoxygenation. The project was preceded by several projects of biomass liquefaction via liquid phase pyrolysis and liquid as well as solid product upgrading, starting in 2008. This project was based on the project "bioBOOST" that had engaged in the discontinuous hydrodeoxygenation of liquid phase pyrolysis oil and liquefaction of biochar.

My work on the topic of biomass liquefaction started in 2012 during my bachelor thesis "Liquid phase pyrolysis of beech wood" (Flüssigphasenpyrolyse von Buchenholz). At the same time, the bioCRACK pilot plant started its operation for fuel production via liquid phase pyrolysis. The pilot plant was fully integrated in the OMV refinery in Schwechat/ Vienna, using vacuum gas oil as heat carrier. My research continued during my master thesis, finished in 2016, "Thermal conversion of lignocellulose and petroleum refinery intermediates to biofuels" (Thermische Konversion von Lignocellulose und Erdölraffinationsintermediaten zu Biokraftstoffen).

The work on this doctoral thesis started in 2016. The thesis is divided in 9 chapters. Chapter 1 presents the framework of this thesis. Chapter 2 is an introduction on climate policy and ways to achieve CO_2 neutrality eventually. Chapter 3 gives an overview of direct biomass liquefaction via pyrolysis and liquid product upgrading. Chapter 4, 5, 6 and 8 include peer reviewed publications. Chapter 7 includes a paper that was prepared for publication. Chapter 4 covers liquid phase pyrolysis via the bioCRACK process, chapter 5, 6, 7 and 8 present results from the continuous hydrodeoxygenation of liquid phase pyrolysis oil. Chapter 9 summarises the whole work, followed by the appendix with a listing of all publications and supervised as well as co-supervised theses.

Chapter 2

Introduction

2. Introduction

Since the Kyoto protocol [1] has been published in the mid-90s, climate policy was set in motion. Different protocols, the most common ones being the Paris agreement [2] in 2015 from the United Nations Framework Convention on Climate Change, signed by 196 member states worldwide, and the renewable energy directive [3] (RED) in 2009 by the European Union, have evolved. According to the Paris agreement, global warming is to hold significantly below 2°C above pre-industrial level. Experts are uncertain if this goal is still achievable [4]. The renewable energy directive includes a mandatory renewable energy share of 20 % until 2020. In December 2018, a recast of the renewable energy directive called RES [5] was published, aiming for the reduction of greenhouse gas (GHG) emissions by at least 40 % below 1990 levels until 2030. In all agreements it is stated clearly, that significant reduction of GHG emission has to occur in order to eventually achieve CO_2 neutrality. However, the way to reach this state is not precisely scheduled; simply because it is not yet established.

In the late 10er years of the 21th century, electric vehicles (EV) are on the rise. In a report of Concawe [6], a division of the European Petroleum Refiners Association, two future scenarios for reducing GHG emissions through light duty vehicle propulsions in Europe until 2050 are shown (Figure 1). Those are a high EV scenario on the one hand and a low carbon fuels scenario on the other hand, whereas both scenarios include electrification and use of low carbon fuels. Low carbon fuels include biofuels and eFuels, mainly second-generation biofuels produced by pyrolysis or gasification and subsequent product upgrading (gasoline and diesel), hydrotreated vegetable oils (HVO) and a decreasing portion of first-generation bioethanol and fatty acid methyl esters (FAME). In the high EV scenario, biofuels have an energy share of 25 %, in the low carbon scenario of 100 % by 2050. In both cases, a similar reduction of GHG emissions by about 85 % could be achieved, showing that neither EVs nor biofuels are the sole correct answer for decelerating global warming.

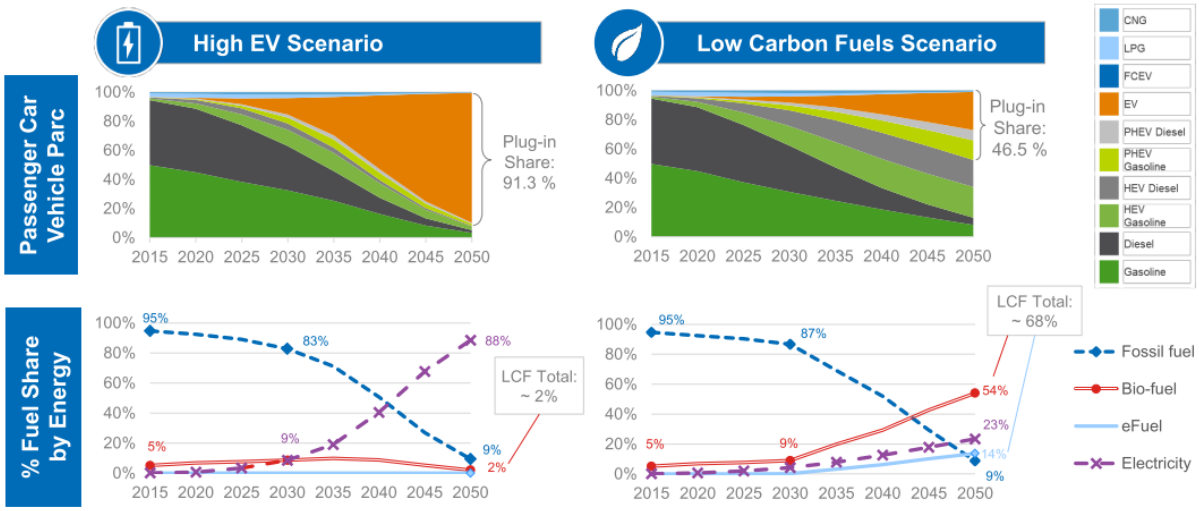

Figure 1: Two scenarios for 2050 from Concawe to reduce GHG emissions. left: High electric vehicles scenario, right: low carbon fuels scenario [6]. © Ricardo plc 2018

It is claimed that some cities have already banned diesel vehicles at least from the inner city, such as Paris, Brussels and Madrid. It is not mentioned, that these bans primarily affect old diesel cars for now, for example since 2019 below Euro-3 norm diesel cars and below Euro-2 Norm gasoline cars in Brussels [7]. The goal to ban all fossil-energy vehicles by 2030 in Paris is ambitious [8]. Concerning air quality in populated areas, equivalent to high particulate matter areas such as Graz, a ban of diesel cars, which are mainly seen to be responsible for particulate matter formation, is essential. The benefit concerning overall CO_2 emissions is questionable. In a sustainability analysis of Casals et al. [9], the impact of EVs on GHG emissions concerning their production and electricity generation was determined. They showed that EVs generally produce less GHG emissions, however, the UK, Germany and the Netherlands, being among the TOP 5 most EV selling countries, still have high pollutant electricity power plant fleets so that the usage of EV does not ensure GHG emission reduction. Despite that, there is still no method for recycling lithium out of batteries. The mining of the precious lithium, which has the highest occurrence in the Atacama Desert in South America, requires two million liters of water per ton Lithium [10], [11].

All these findings imply that there is no all-in-one device that solves the problem of global warming, but a combination of all possible resources: liquid, biogenous fuels or substitute fuels such as FAME, bioethanol, biomethanol and other oxygenated fuel substitutes as well as biomass-to-liquid (BTL) fuels from lignocellulosic biomass or waste materials, biogenous hydrogen, fuel cells, electric vehicles and possible new approaches. To prevent depletion of any resource, research for sustainable energy provision should be done in all directions.

First and foremost, energy is, like everything, subject of a simple balance: If less energy is consumed, less energy has to be provided.

2.1 References

[1] United Nations, *Kyoto Protocol to the United Nations Framework Convention on Climate Change*. United Nations, 1998, p. 20.

[2] UNFCCC, "ADOPTION OF THE PARIS AGREEMENT: Proposal by the President to the United Nations Framework Convention on Climate Change," vol. 21932, no. December, pp. 1–32, 2015.

[3] "Directive 2009/28/EC of the European Parliament and the Council of 23 April 2009 on the promotion of the use of energy from renewable sources and amending and subsequently repealing Directives 2001/77/EC and 2003/30/EC," *Off. J. Eur. Union*, pp. 16–62, 2009.

[4] IPPC, "Climate Change 2014: Synthesis Report. Contribution of Working Groups I, II and III to the Fifth Assessment Report of the Intergovernmental Panel on Climate Change [Core Writing Team, R.K. Pachauri and L.A. Meyer (eds.)]," Geneva, Switzerland, 2014.

[5] "Directive (EU) 2018/2001 of the european parliament and of the council of 11 December 2018 n the promotion of the use of energy from renewable sources (recast)," *Off. J. Eur. Union*, pp. 82–209, 2018.

[6] N. Powell *et al.*, "Impact Analysis of Mass EV Adoption and Low Carbon Intensity Fuels Scenarios – Summary Report," 2018.

[7] H. Crolly and G. Wüpper, "In diesen Städten Europas sind Fahrverbote bereits Realität," *WELT*, 2018. [Online]. Available: https://www.welt.de/wirtschaft/article182744752/Diesel-Fahrverbote-In-diesen-Laendern-Europas-sind-sie-bereits-Realitaet.html. [Accessed: 15-Jan-2019].

[8] B. Love, "Paris plans to banish all petrol and diesel vehicles from city centre by 2030," *The Independent*, 2017. [Online]. Available: https://www.independent.co.uk/environment/paris-petrol-diesel-car-ban-2030-gas-guzzlers-emissions-air-pollution-evs-france-a7996246.html. [Accessed: 29-Jan-2019].

[9] L. Canals Casals, E. Martinez-Laserna, B. Amante García, and N. Nieto, "Sustainability analysis of the electric vehicle use in Europe for CO2 emissions reduction," *J. Clean. Prod.*, vol. 127, pp. 425–437, 2016.

[10] "Lithium," *GLOBAL 2000*. [Online]. Available: https://www.global2000.at/lithium. [Accessed: 29-Jan-2019].

[11] M. Lauerer, "Lithium: Abbau und Gewinnung - Umweltgefahren der Lithiumförderung," *Edison - Handelsblatt GmbH*, 2018. [Online]. Available: https://edison.handelsblatt.com/erklaeren/lithium-abbau-und-gewinnung-umweltgefahren-der-lithiumfoerderung/23140064.html.

Chapter 3

Direct biomass liquefaction

3. Direct biomass liquefaction

Biomass liquefaction concepts can roughly be divided into direct and indirect liquefaction. Indirect liquefaction takes the path of biomass gasification [1], [2] to obtain synthesis gas, which is subsequently processed to hydrocarbons [3] or synthetic chemicals [4]. Direct biomass liquefaction is mostly performed either through pyrolysis [5], solvolysis [6] or hydrothermal liquefaction [7]. Obtained bio-oils from pyrolysis or solvolysis have a high residual oxygen content and a low pH level, due to the high oxygen content of biomass, resulting in negative properties such as high corrosiveness, low stability and a low heating value [8]. Furthermore, the polarity leads to an incompatibility with crude oil processing [9]. This makes it indispensable, to modify them in any way prior to usage. Therefore, direct biomass liquefaction is divided into two steps: liquefaction and subsequent liquid product upgrading. For fuel production, the upgrading step is performed following common refinery processes: fluid catalytic cracker or hydrotreating units. It was shown that upgrading without hydrogen addition, as in a fluid catalytic cracker, leads to high coke and aromatic yields, making hydrotreating of pyrolysis oil a more reasonable process [10].

As the focus of this doctoral thesis, pyrolysis of lignocellulosic biomass (or lignocellulose) and hydrodeoxygenation of bio-oils shall be discussed in detail.

3.1 Structure of lignocellulose

For understanding its liquefaction, the structure of lignocellulose is important. Lignocellulose is built up by its three main polymers cellulose, hemicellulose and lignin. Cellulose and hemicellulose are carbohydrates. Cellulose consists of long strains of D-glucopyranose units that are connected via hydrogen bonds. Hemicellulose is a collective term for all non-cellulose carbohydrates with shorter chain lengths and more branches. The monomers are mostly pentoses, such as D-xylose. Hemicellulose acts as a link between cellulose and lignin. Lignin consists of three phenylpropanoids: paracoumaryl alcohol, coniferyl alcohol and sinapyl alcohol. They are connected via C-C and C-O bonds. Lignin builds up the cell walls and provides strength in biomass. [11], [12]

3.2 Pyrolysis of lignocellulose

Pyrolysis describes the thermal degradation of organic compounds in the absence of oxygen. The degradation follows a homolytic split mechanism, where smaller and bigger molecules as well as unsaturated molecules are formed. [13] Thus, solid, liquid and gaseous products are formed in different proportions. These are mainly dependent on temperature, residence time and heating rate. [14] Below 400°C, biochar is the main product. Liquefaction shows a maximum at about 500°C, above that gasification starts. [8]

The product distribution can be explained by the composition of lignocellulosic biomass. Lignin liquefaction has shown to be more difficult than liquefaction of carbohydrates, as it starts to

decompose at temperatures of about 400°C [15]. Scanning electron microscopy of biochar from liquid phase pyrolysis of spruce wood below 400°C by Schwaiger et al. [16] showed the remaining structure of biochar to be a lignin framework. Corresponding to the pyrolysis temperature and therefore target product, different processes have been developed. To gain biochar as a target product, low temperature of about 290°C is applied. This process is called torrefaction. For high liquid yields, pyrolysis takes place at about 500°C, as it is the case for fast pyrolysis. Gasification takes place at high temperatures of about 750 to 900°C. [17] To reach a high degree of liquefaction, a short residence time and a high heating rate are crucial. Long vapour residence times above 500°C cause secondary cracking reactions and lower temperatures below 400°C lead to condensation reactions and thus formation of low molecular weight components. Therefore, the preferred process of direct biomass liquefaction is fast (or flash) pyrolysis. [5]

3.2.1 Fast Pyrolysis of lignocellulose

Fast (or flash) pyrolysis is performed at about 500°C with very short residence times of about one second and high heating rates of up to 10 000 °C s^{-1} to prevent secondary reactions [5], [17]. Thus, a very small particle size was shown to be necessary to provide a high surface area and enhance heat transfer. Fast pyrolysis processes are mostly performed at atmospheric pressure, yielding in up to 80 wt% liquid yield based on dry biomass feed. [18] [19] Different reactor types have been developed, such as entrained downflow, ablative, bubbling fluidised bed, circulating fluidised bed, moving-grate vacuum and rotating-cone reactors, where the heat is mainly transferred conductively or convectively through sand or a heated fluid as well as hot surfaces such as the reactor wall [5], [20].

The resulting main product is fast pyrolysis oil. Scott and Piskorz [18] described fast pyrolysis oil to be an acidic fluid that appears to be stable and is easy to pour. It contains a few hundred components, mainly levoglucosan, disaccharides, pyrolytic lignin and oligomers of lignin-derived phenolic compounds [21]. It was suggested to deliver a broad spectrum of applications, such as usage as a boiler fuel, in diesel engines, turbines and as a source of different chemicals [19]. An economic assessment by Scott and Piskorz [18] in 1984 showed that production costs of fast pyrolysis oil may compete with conventional fuel oil. Czernik and Bridgwater [9] stated in 2004 that costs of upgraded fast pyrolysis oil are 10 to 100 % higher than that of fossil fuels. The direct use as fuel is troublesome though, as it is not miscible with common fuels.

Benipal et al. [21] investigated fast pyrolysis oil in anion exchange membrane fuel cells which worked well due to the high levoglucosan content of 11.1 wt%, but pure sugar achieved a 1.2 to 3 times higher power density. Chong and Bridgwater 2016 [22] investigated the possible use of fast pyrolysis oil in marine vessels by blending it with biodiesel, marine gas oil and 1-butanol. Due to the polarity and complex composition, blending was not possible without solvent addition. One problem is that even with blending, fast pyrolysis oil does not meet the current fuel specifications. This shows the necessity of pyrolysis oil upgrading, which is still a challenge and not yet economically attractive. In fast pyrolysis, one problem is the low reproducibility of the process and missing standards for product analyses. A round robin study showed clear

differences in pyrolysis oil properties produced by different reactor designs and process configurations [23]. There are no established standards for analyses yet and thus analyses cannot be replicated in other laboratories [20].

An obstacle of fast pyrolysis is the transfer of char and ash particles in the pyrolysis oil fraction, as they cause troubles in storage and further processing through corrosion or blocking of valves [5], [24], [25]. The particles have a high coke forming tendency when exposed to heat [26]. This is why particles have to be removed through hydrodeoxygenation prior to upgrading. There are some approaches to remove these particles, as for example by Javaid et al. [25]. They suggested a microfiltration process with ceramic membranes, removing char particles to sub-micron levels, making fast pyrolysis an even more cost-intensive method. Additionally, different approaches were made to reduce ash content in biomass and thus in the produced pyrolysis oil. Banks et al. [27] pre-treated Miscanthus x giganteus with a surfactant and successfully removed inorganic materials, resulting in a more stable pyrolysis oil. Oudenhoven et al [28] showed that leaching of biomass with organic acids prior to fast pyrolysis increased the organic oil yield and reduced water content as well as residual yield during fast pyrolysis, especially below 500°C.

Fast pyrolysis has developed to a ready for market technology according to the many publications of Bridgwater et al [5], [8], [17], [19]. There are many plants in different scale worldwide to produce fast pyrolysis oil. Lately, research has been more focused on possible catalyst implementation, catalyst design, especially the design of multi-functional catalyst systems, reactor design and biomass pretreatment [17], [19]. Catalytic pyrolysis is performed primarily with different zeolites, often under hydrogen atmosphere, to increase the pyrolysis oil quality, resulting in decreased oxygen content and increased aromatic content, carbon yields are not affected [20], [29]–[31]. Still, biomass is not completely deoxygenated when a catalyst is applied. The produced pyrolysis oil still needs upgrading, but co-processing with petroleum refinery intermediates might be possible without another intermediate step. [10], [32]–[36] Catalytic pyrolysis allows less flexibility, as the temperature has to be high enough for sufficient liquefaction, but also low enough to prevent overheating of the used catalyst. A sophisticated catalyst is required. [20]

3.2.2 Liquid phase pyrolysis of lignocellulose

The term “liquid phase pyrolysis” (LPP) is not clearly defined and has changed in the last decades. Liquid phase pyrolysis was first reported in the early 1970s by Hüttinger [37] and described the degradation of aromatics in molten phase. More or less, it can be compared to coking of different organic material, mainly coal tar pitch, in liquid state. The process was performed at 4 to 50 bar with low heating ramps under inert or hydrogen atmosphere with the target of producing high quality coke. [38], [39]

Later on, “liquid phase pyrolysis” describes pyrolysis, mainly off lignocellulose, in a liquid heat carrier. The heat carrier provides a high heat transfer rate, which is essential for high liquid yields. The process is reported to take place at temperatures between 250 and 400°C under inert gas or reducing hydrogen atmosphere. A catalyst may be used and pressure may be applied to ensure the heat carrier in its liquid state. The process is in general limited by the

boiling range of the heat carrier at the applied pressure. Liquid phase pyrolysis is less common than fast pyrolysis. [16], [40]–[43]

Klaigaew et al. [40] reported about LPP of giant leucaena in hexane as a solvent. They performed experiments between 325 and 400°C in an autoclave reactor with a holding time of 0 to 60 minutes with the usage of a $NiMo/Al_2O_3$ catalyst. Initially, 10 bar nitrogen pressure were applied. They observed a maximum of liquefaction with a yield of 8.67 wt% and a low residual oxygen content of 9.09 wt% at 375°C. Rathanatavorn et al. [41] have performed similar experiments, also with giant leucaena, in decane. The lowest oxygen content of 8.50 wt% was achieved with a $NiMo/Al_2O_3$ catalyst at 400°C with an oil yield of 8.60 wt%. The temperature influence was shown to be significant: increasing temperature facilitated depolymerisation, deoxygenation and cracking reactions. The hydrogen pressure had a minor influence in the observed range. Although in both cases a product with a low oxygen content was produced, the yield of 8.6 to 8.7 wt% is very low. Szabó et al. [42] investigated LPP of wheat straw and poplar in n-hexadecane under inert atmosphere at about 350°C with a maximum pressure of 20 bar. One of the tested parameters was the usage of a catalyst, which was shown to have a negligible influence on the process. They observed a high carbon transfer of 40 to 49 wt% into the carrier oil. The highest yield was found at a residence time of zero minutes, the lowest at a residence time of 120 minutes.

Schwaiger et al.[16], [43] performed liquid phase pyrolysis in a highly hydrogenated mixture of straight long chain alkanes with a boiling range between 410 and 440°C. Thus, the temperature for liquid phase pyrolysis was limited to below this boiling range. Experiments were performed between 350 and 390°C. At 390°C, about 50 wt% were liquefied to pyrolysis oil, consisting of liquid CHO products and water. In fast pyrolysis, residence time should be in the range of a few seconds to prevent secondary reactions of produced vapors for secondary char formation [5]. Liquid phase pyrolysis can be distinguished from fast pyrolysis not only by the heat carrier oil and the applied temperature but also by a higher residence time, as the carrier oil stabilises components that tend to form coke. Additionally, particles are retained by the heat carrier oil, resulting in a pyrolysis oil without particles and thus a low inorganic load. Schwaiger et al. [43] observed that about 3 wt% of the biomass was dissolved in the heat carrier oil. They also observed about 1.4 wt% degradation of the heat carrier itself. An exponentially increasing degradation of the heat carrier oil took place at temperatures above 350°C.

3.2.2.1 Appliance of liquid phase pyrolysis in the bioCRACK process

If a carrier oil of lower value is used, which would need cracking for upgrading either way, as it is the case at petroleum refinery heavy ends, the effect of carrier oil degradation during liquid phase pyrolysis can be turned into a benefit. This led to the development of the bioCRACK process [44], [45]. The bioCRACK process is a refinery integrated process developed by BDI-BioEnergy International GmbH to produce fuels out of lignocellulosic feedstock and petroleum refinery heavy ends. A pilot plant has already been operating with vacuum gas oil as a heat carrier oil. It was fully integrated in the OMV refinery in Schwechat/Vienna. Vacuum gas oil is usually fed into the fluid catalytic cracker to shorten its chain length, as it has a boiling range of

about 365 to 530°C. During liquid phase pyrolysis in vacuum gas oil, biomass as well as vacuum gas oil are decomposed. Biomass was shown to have a supporting influence on cracking of vacuum gas oil. Non-polar biomass constituents are dissolved in the cracked as well as residual vacuum gas oil, polar biomass constituents form liquid phase pyrolysis oil. In the bioCRACK pilot plant, 30 to 39 wt% of the biogenous carbon were transferred into vacuum gas oil fractions, between 20 and 26 wt% into liquid phase pyrolysis oil. The residual biochar as well as inorganic material are retained by the vacuum gas oil, which is why liquid phase pyrolysis oil contains a very low amount of inorganic materials. Through the extraction of non-polar fragments, it also has a high water content and thus a low viscosity. Cracked vacuum gas oil with biogenous content was afterwards upgraded to fuel in a hydrotreating unit, residual vacuum gas oil with biogenous content was treated in a fluid catalytic cracking unit [46]. More about the bioCRACK process can be found in chapter 4: "Diesel production from lignocellulosic feed: the bioCRACK process" [47].

3.2.3 Differentiation of liquid phase pyrolysis to solvolysis

Liquid phase pyrolysis is similar to solvolysis. Both processes take place in liquid phase at elevated temperature. The demarcation lies in the homolytic degradation through heat exposure in liquid phase pyrolysis versus heterolytic degradation through nucleophilic substitution reactions with solvent molecules in solvolysis [13]. In solvolysis, the degradation of biomass occurs in polar liquids, usually water or alcohol, in the presence of an acid or base catalyst, in contrary to liquid phase pyrolysis for which non-polar heat carrier oils are applied [48], [49]. Most common solvents are polyethylene glycol [50], phenol [51], ethylene glycol or propylene glycol [52]–[54]. As acid or base catalyst p-toluenesulfonic acid, H_2SO_4, Na_2CO_3 and KOH are reported [53]–[56]. Biomass is degraded to up to 100 %, resulting in a liquid with a similar elemental composition as biomass and a very high viscosity [55] [54]. Temperature is lower than in liquid phase pyrolysis with 180 [57] to 280°C [56] and residence time is higher with up to 3 hours [57], [58]. Pressure might be applied [51], but solvolysis is also reported at ambient pressure [56]. After solvolysis, the solvent and possibly water has to be removed which increases the viscosity drastically [54]. Therefore, it has to be blended with polar liquids such as alcohols; it is not miscible with non-polar liquids [56], [58]. In comparison, liquid phase pyrolysis oil has a very low viscosity of below 10 mPa·s.

3.2.4 Comparison of bio-oils from fast pyrolysis, liquid phase pyrolysis and solvolysis

The properties of various bio-oils differ considerably, depending on the applied process. In Table 1, the properties and composition of bio-oils produced by fast pyrolysis, liquid phase pyrolysis and solvolysis as well as the process conditions are compared to each other. Whereas fast pyrolysis oil and solvolysed biomass have nearly the same elemental composition, the water content differs drastically, mainly due to the removal of solvent and thus water after solvolysis. This results in an extremely high viscosity of 4000 to 13000 mPa·s at 25°C and makes handling without dilution hardly feasible. From these two bio-oils, liquid phase pyrolysis oil distinguishes

strikingly. Due to a sort of extraction and stabilisation of non-polar biomass constituents by the heat carrier oil, liquid phase pyrolysis oil has a lower organic load and therefore higher water content as well as a significantly lower viscosity. This facilitates handling in subsequent hydrodeoxygenation processes a lot.

Table 1: Typical process conditions of fast pyrolysis, liquid phase pyrolysis and solvolysis as well as comparison of the bio-oil composition

		Fast pyrolysis (Bridgwater et al.) [8]	Liquid phase pyrolysis (bioCRACK)	Solvolysis (Grilc et al.) [6], [59]
LIQUEFACTION PROCESS				
Temperature	[°C]	~500	350-400	180
Pressure	[bar]	ambient	ambient	n.a.
Residence time	[s]	0.5-5	<500	10 800
LIQUID PRODUCT SPECIFICATION				
C	[wt%]	42.3	25.6	46.6
H	[wt%]	7.4	9.4	8.1
O	[wt%]	50.0	64.6	44.2
Water	[wt%]	25	51.9	< 2
Lower heating value	[MJ/kg]	15.4	9.0	19.0
pH		2.5	2.2	<3.5*
Viscosity	[mPa·s]	30-200 (at 40°C)	3.5 (at 20°C)	4000 – 13000 (at 25°C)
Density	[kg/m³]	1200	1090	<1300**

* According to Seljak et al. [58]

** According to Buffi et al. [57]

3.3 Hydrodeoxygenation of bio-oils

Hydrodeoxygenation describes the removal of oxygen with hydrogen through water formation. Simultaneously, cracking, decarbonylation, decarboxylation, hydrocracking, hydrogenation and polymerisation take place. [60] Hydrodeoxygenation is performed at elevated temperatures between 150 and 400°C and high pressure between 80 and 200 bar, whereas partial hydrodeoxygenation is performed at lower temperatures and full hydrodeoxygenation is only achieved at the upper end of the temperature spectrum [26], [61]–[64]. Hydrogen is either introduced as pure hydrogen [26], synthesis gas [65] or through a hydrogen donor [6]. For hydrodeoxygenation, different catalysts are reported. The most common ones are noble metal catalysts [26], [61], [63], [66]–[71] or sulfided metal oxide catalysts on support material [66], [67].

3.3.1 Hydrodeoxygenation of fast pyrolysis oil

Hydrodeoxygenation is mostly applied to fast pyrolysis oil. The focus in research was shifted from liquefaction of lignocellulose through fast pyrolysis to upgrading of fast pyrolysis oil via hydrodeoxygenation. Therefore, many research groups who do not produce their own pyrolysis oil purchase fast pyrolysis oil either from BTG Biomass Technology Group [64], [72]–[75] or VTT Technical Research Centre of Finland Ltd [26], [76]–[78]. Hydrodeoxygenation of fast pyrolysis oil is performed as a two or more step process to prevent coking and thus deactivation of the catalyst, especially at temperatures above 300°C [79]. The high organic load doesn't allow for single-step processing. The first step acts as stabilising step for the most reactive components in pyrolysis oil at lower temperature, such as aldehydes and ketones [80]. The second step includes deep hydrotreatment and hydrocracking at elevated temperature. Hydrodeoxygenation is reported either in batch scale [78], [81]–[85] or continuously with low liquid hourly space velocities of 0.1 to 0.5 h^{-1} [26], [61], [67], [68], [80].

3.3.2 Hydrodeoxygenation of solvolysed biomass

Hydrodeoxygenation of solvolysed biomass is less investigated than that of fast pyrolysis oil. Rezzoug et al. [54], [86] reported about hydrodeoxygenation of liquefied biomass in batch scale. After removal of solvent and water, the obtained bio-oil had an elemental composition of 55-75.3 wt% carbon, 5.9-7.6 wt% hydrogen and 18.1-37.0 wt% oxygen, it was free-flowing above 70°C. As the high viscosity of solvolysed biomass makes blending with solvents necessary, for hydrodeoxygenation often tetralin is used, as it lowers viscosity and serves as hydrogen donor at once. This on the other hand limits hydrodeoxygenation temperature to about 370°C, as tetralin starts to degrade above this temperature. Therefore, it was diluted with tetralin 1:1 and hydrodeoxygenated between 350 and 370°C in batch scale, applying an initial hydrogen pressure of 30 to 90 bar. The products had a lower heating value of 35 to 41.55 MJ kg^{-1}. Grilc et al. [6], [59], [87] also performed hydrodeoxygenation of solvolysed biomass with tetralin, phenol, 2-propanol, pyridine, m-cresol, anthracene, cyclohexanol and xylene at 300°C and 80 bar in batch scale. Prior to solvent addition, the oil had a viscosity of 4000 to 13000 mPa·s at 25°C. They discovered tetralin to have the best hydrogen donor function, stabilising radicals and enhancing hydrogenation and hydrogenolysis reactions.

3.3.3 Hydrodeoxygenation of liquid phase pyrolysis oil

As part of the BiomassPyrolysisRefinery [88], biochar from liquid phase pyrolysis was liquefied using tetralin as hydrogen donor by Feiner et al. [89], [90] and liquid phase pyrolysis oil was hydrotreated in batch scale by Pucher et al. [91], [92]. They applied dehydration of liquid phase pyrolysis oil due to its high water content prior to hydrodeoxygenation. Hydrodeoxygenation was then performed with different noble metal catalysts and a Ni-based catalyst in two steps, the first one at 250°C and 100 bar, the second one at 300°C and 150 bar. Holding time was 2 hours for each step. The final product contained a residual oxygen content of 13 to 19 wt%. Pucher [93] showed the importance of a high heating ramp, as he observed that experiments in batch scale were already completed in the heating up phase of experiments, showing a very short

reaction time. Based on these results, liquid phase pyrolysis oil was upgraded continuously in one step. It was shown, that the high water content of liquid phase pyrolysis oil has a few advantages over fast pyrolysis oil: the water reduces viscosity so that liquid pumping is facilitated, buffers heat of reaction and thus reduces coking and enables processing at high liquid hourly space velocities of up to 3 h^{-1}. Therefore, liquid phase pyrolysis can be used in its native state for continuous hydroprocessing. It is possible to produce a product with fuel properties without residual oxygen content in one step.

Detailed reports of liquid phase pyrolysis oil hydrodeoxygenation are given in chapter 5: "Temperature Dependence of Single Step Hydrodeoxygenation of Liquid Phase Pyrolysis Oil"; chapter 6: "High-throughput continuous hydrodeoxygenation of liquid phase pyrolysis oil"; chapter 7: "Refinery integration of lignocellulose for automotive fuel production" and chapter 8: "Hydrocarbon production by continuous hydrodeoxygenation of liquid phase pyrolysis oil with biogenous hydrogen rich synthesis gas". [52], [94], [95]

3.4 References

[1] H. Hofbauer, "Biomass Gasification for Electricity and Fuels, Large Scale," in *Encyclopedia of Sustainability Science and Technology*, Springer, 2017, pp. 459–478.

[2] A. M. Mauerhofer, F. Benedikt, J. C. Schmid, J. Fuchs, S. Müller, and H. Hofbauer, "Influence of Different Bed Material Mixtures on Dual Fluidized Bed Steam Gasification," *Energy*, vol. 157, pp. 957–968, 2018.

[3] S. Müller *et al.*, "Production of diesel from biomass and wind power – Energy storage by the use of the Fischer-Tropsch process," *Biomass Convers. Biorefinery*, vol. 8, no. 2, pp. 275–282, 2018.

[4] R. Rauch, J. Hrbek, and H. Hofbauer, "Biomass Gasification for Synthesis Gas Production and Applications of the Syngas," *Adv. Bioenergy Sustain. Chall.*, pp. 73–91, 2015.

[5] A. V Bridgwater, "Principles and practice of biomass fast pyrolysis processes for liquids," *J. Anal. Appl. Pyrolysis*, vol. 51, pp. 3–22, 1999.

[6] M. Grilc, B. Likozar, and J. Levec, "Hydrotreatment of solvolytically liquefied lignocellulosic biomass over NiMo/Al2O3catalyst: Reaction mechanism, hydrodeoxygenation kinetics and mass transfer model based on FTIR," *Biomass and Bioenergy*, vol. 63, pp. 300–312, 2014.

[7] D. C. Elliott, P. Biller, A. B. Ross, A. J. Schmidt, and S. B. Jones, "Hydrothermal liquefaction of biomass : Developments from batch to continuous process," *Bioresour. Technol.*, vol. 178, pp. 147–156, 2015.

[8] A. V Bridgwater, D. Meier, and D. Radlein, "An overview of fast pyrolysis of biomass," *Org. Geochem.*, vol. 30, pp. 1479–1493, 1999.

[9] S. Czernik and A. V Bridgwater, "Overview of applications of biomass fast pyrolysis oil," *Energy & Fuels*, vol. 18, no. 2, pp. 590–598, 2004.

[10] L. Gueudré *et al.*, "Coke chemistry under vacuum gasoil/bio-oil FCC co-processing conditions," *Catal. Today*, vol. 257, no. Part 2, pp. 200–212, 2015.

[11] F. Behrendt, Y. Neubauer, K. Schulz-Tönnies, B. Wilmes, and N. Zobel, "Studie zur Bewertung zum Thema Direktverflüssigung von Biomasse – Reaktionsmechanismen und Produktverteilungen," Berlin, 2006.

[12] D. Fengel and G. Wegener, *Wood Chemistry, Ultrastructure Reactions*. München: Kessel, 2003.

[13] K. P. C. Vollhardt and N. E. Shore, *Organische Chemie*, 5th ed. Wiley-VCH Verlag GmbH & Co. KGaA, 2011.

[14] M. Kaltschmitt and W. Streicher, *Energie aus Biomasse*. 2009.

[15] M. Oliet, M. V Alonso, M. A. Gilarranz, and F. Rodr, "Thermal stability and pyrolysis kinetics of organosolv lignins obtained from Eucalyptus globulus," *Ind. Crops Prod.*, vol. 7, pp. 150–156, 2007.

[16] N. Schwaiger *et al.*, "Liquid and Solid Products from Liquid-Phase Pyrolysis of Softwood," *Bioenergy Res.*, vol. 4, no. 4, pp. 294–302, 2011.

[17] A. V Bridgwater, "Review of fast pyrolysis of biomass and product upgrading," *Biomass and Bioenergy*, vol. 38, pp. 68–94, 2011.

[18] D. S. Scott and J. Piskorz, "The continuous flash pyrolysis of biomass," *Can. J. Chem. Eng.*, vol. 62, no. 3, pp. 404–412, 1984.

[19] A. V Bridgwater and G. V. C. Peacocke, "Fast pyrolysis processes for biomass," *Renew. Sustain. energy Rev.*, vol. 4, no. 1, pp. 1–73, 2000.

[20] R. H. Venderbosch and W. Prins, "Fast Pyrolysis," in *Thermochemical Processing of Biomass*, Wiley and Sons, Ltd, 2011, pp. 124–156.

[21] N. Benipal, J. Qi, P. A. Johnston, J. C. Gentile, R. C. Brown, and W. Li, "Direct fast pyrolysis bio-oil fuel cell," *Fuel*, vol. 185, pp. 85–93, 2016.

[22] K. J. Chong and A. V. Bridgwater, "Fast Pyrolysis Oil Fuel Blend for Marine Vessels," *Am. Inst. Chem. Eng.*, vol. 36, no. 3, pp. 677–684, 2016.

[23] D. C. Elliott, D. Meier, A. Oasmaa, B. Van De Beld, A. V. Bridgwater, and M. Marklund,

"Results of the International Energy Agency Round Robin on Fast Pyrolysis Bio-oil Production," *Energy and Fuels*, vol. 31, no. 5, pp. 5111–5119, 2017.
[24] Q. Zhang, J. Chang, T. Wang, and Y. Xu, "Review of biomass pyrolysis oil properties and upgrading research," *Energy Convers. Manag.*, vol. 48, no. 1, pp. 87–92, 2007.
[25] A. Javaid *et al.*, "Removal of char particles from fast pyrolysis bio-oil by microfiltration," *J. Memb. Sci.*, vol. 363, no. 1–2, pp. 120–127, 2010.
[26] M. V. Olarte *et al.*, "Stabilization of Softwood-Derived Pyrolysis Oils for Continuous Bio-oil Hydroprocessing," *Top. Catal.*, vol. 59, no. 1, pp. 55–64, 2016.
[27] S. W. Banks, D. J. Nowakowski, and A. V. Bridgwater, "Fast pyrolysis processing of surfactant washed Miscanthus," *Fuel Process. Technol.*, vol. 128, pp. 94–103, 2014.
[28] S. R. G. Oudenhoven, C. Lievens, R. J. M. Westerhof, and S. R. A. Kersten, "Effect of temperature on the fast pyrolysis of organic-acid leached pinewood; the potential of low temperature pyrolysis," *Biomass and Bioenergy*, vol. 89, pp. 78–90, 2015.
[29] S. Thangalazhy-Gopakumar, S. Adhikari, R. B. Gupta, M. Tu, and S. Taylor, "Production of hydrocarbon fuels from biomass using catalytic pyrolysis under helium and hydrogen environments," *Bioresour. Technol.*, vol. 102, no. 12, pp. 6742–6749, 2011.
[30] S. Thangalazhy-Gopakumar, S. Adhikari, and R. B. Gupta, "Catalytic Pyrolysis of Biomass over H+ZSM-5 under Hydrogen Pressure," *Energy and Fuels*, vol. 26, no. 8, pp. 5300–5306, 2012.
[31] M. Stöcker, "Biofuels and biomass-to-liquid fuels in the biorefinery: Catalytic conversion of lignocellulosic biomass using porous materials," *Angewandte Chemie - International Edition*, vol. 47, no. 48. pp. 9200–9211, 2008.
[32] C. Lindfors, V. Paasikallio, E. Kuoppala, M. Reinikainen, A. Oasmaa, and Y. Solantausta, "Co-processing of dry bio-oil, catalytic pyrolysis oil, and hydrotreated bio-oil in a micro activity test unit," *Energy and Fuels*, vol. 29, no. 6, pp. 3707–3714, 2015.
[33] S. D. Stefanidis, K. G. Kalogiannis, and A. A. Lappas, "Co-processing bio-oil in the refinery for drop-in biofuels via fluid catalytic cracking," *Wiley Interdiscip. Rev. Energy Environ.*, vol. 7, no. 3, pp. 1–18, 2018.
[34] Á. Ibarra, E. Rodríguez, U. Sedran, J. M. Arandes, and J. Bilbao, "Synergy in the Cracking of a Blend of Bio-oil and Vacuum Gasoil under Fluid Catalytic Cracking Conditions," *Ind. Eng. Chem. Res.*, vol. 55, no. 7, pp. 1872–1880, 2016.
[35] N. Thegarid *et al.*, "Second-generation biofuels by co-processing catalytic pyrolysis oil in FCC units," *Appl. Catal. B Environ.*, vol. 145, pp. 161–166, 2014.
[36] Y. Schuurman, G. Fogassy, and C. Mirodatos, "Tomorrow's Biofuels: Hybrid Biogasoline by Co-processing in FCC Units," in *The Role of Catalysis for the Sustainable Production of Bio-Fuels and Bio-Chemicals*, © 2013 Elsevier B.V. All rights reserved., 2013, pp. 321–349.
[37] K. J. Hüttinger, "Bildung graphitischer Kohlenstoffe durch Flüssigphasenpyrolyse," *Chemie Ing. Tech.*, vol. 21, pp. 1145–1188, 1971.
[38] K. J. Hüttinger, "Flüssigphasenpyrolyse von Kohlenwasserstoffen Physikalisch-chemische und reaktionstechnische Grundlagen - Teil I," *Erdöl und Kohle - Erdgas - Petrochemie Ver. mit Brennstoff-Chemie*, vol. 39, no. 11, pp. 495–500, 1986.
[39] R. Hegermann and K. J. Hüttinger, "Flüssigphasenpyrolyse von Kohlenwasserstoffen Physikalisch-chemische und reaktionstechnische Grundlagen - II," *Erdöl und Kohle - Erdgas - Petrochemie Ver. mit Brennstoff-Chemie*, vol. 40, no. 1, pp. 21–27, 1987.
[40] K. Klaigaew *et al.*, "Liquid Phase Pyrolysis of Giant Leucaena Wood to Bio-Oil over NiMo/Al2O3 Catalyst," *Energy Procedia*, vol. 79, pp. 492–499, 2015.
[41] W. Ratanathavorn, C. Borwornwongpitak, C. Samart, and P. Reubroycharoen, "Bio-Oil Production from Liquid-Phase Pyrolysis of Giant Leucaena Wood," *Chem. Technol. Fuels Oils*, vol. 52, no. 4, pp. 360–368, 2016.
[42] B. Szabó, M. Takács, A. Domján, E. Barta-rajnai, and J. Valyon, "Journal of Analytical and Applied Pyrolysis Liquid phase pyrolysis of wheat straw and poplar in hexadecane solvent," *J. Anal. Appl. Pyrolysis*, vol. 137, no. June, pp. 237–245, 2019.
[43] N. Schwaiger *et al.*, "Formation of liquid and solid products from liquid phase pyrolysis,"

Bioresour. Technol., vol. 124, pp. 90–94, 2012.
[44] J. Ritzberger, P. Pucher, and N. Schwaiger, "The BioCRACK Process - A Refinery Integrated Biomass-to-Liquid Concept to Produce Diesel from Biogenic Feedstock," vol. 39, no. 2010, pp. 1189–1194, 2014.
[45] J. Ritzberger, "Flüssigphasenpyrolyse Prozessmodellierung und Scale-Up," Graz University of Technology, 2016.
[46] M. Berchtold, J. Fimberger, A. Reichhold, and P. Pucher, "Upgrading of heat carrier oil derived from liquid-phase pyrolysis via fluid catalytic cracking," *Fuel Process. Technol.*, vol. 142, pp. 92–99, 2016.
[47] K. Treusch, J. Ritzberger, N. Schwaiger, P. Pucher, and M. Siebenhofer, "Diesel production from lignocellulosic feed : the bioCRACK process," *R.Soc.open sci.*, vol. 4, no. 171122, 2017.
[48] Y. Lee and E. Y. Lee, "Thermochemical conversion of red pine wood, Pinus densiflora to biopolyol using biobutanediol-mediated solvolysis for biopolyurethane preparation," *Wood Sci. Technol.*, vol. 52, no. 2, pp. 581–596, 2018.
[49] T. Renders *et al.*, "Synergetic Effects of Alcohol/Water Mixing on the Catalytic Reductive Fractionation of Poplar Wood," *ACS Sustain. Chem. Eng.*, vol. 4, no. 12, pp. 6894–6904, 2016.
[50] E. Takata, T. T. Nge, S. Takahashi, Y. Ohashi, and T. Yamada, "Acidic solvolysis of softwood in recycled polyethylene glycol system," *BioResources*, vol. 11, no. 2, pp. 4446–4458, 2016.
[51] M. Takada, Y. Tanaka, E. Minami, and S. Saka, "Comparative study of the topochemistry on delignification of Japanese beech (Fagus crenata) in subcritical phenol and subcritical water," *Holzforschung*, vol. 70, no. 11, pp. 1047–1053, 2016.
[52] K. Treusch, N. Schwaiger, K. Schlackl, R. Nagl, and P. Pucher, "Temperature Dependence of Single Step Hydrodeoxygenation of Liquid Phase Pyrolysis Oil," *Front. Chem.*, vol. 6:297, no. July, pp. 1–8, 2018.
[53] A. Kržan and E. Žagar, "Microwave driven wood liquefaction with glycols," *Bioresour. Technol.*, vol. 100, no. 12, pp. 3143–3146, 2009.
[54] S.-A. Rezzoug and R. Capart, "Solvolysis and hydrotreatment provide fuel," *Biomass and Bioenergy*, vol. 11, no. 4, pp. 343–352, 1996.
[55] M. Kunaver, E. Jasiukaityte, and N. Čuk, "Ultrasonically assisted liquefaction of lignocellulosic materials," *Bioresour. Technol.*, vol. 103, no. 1, pp. 360–366, 2012.
[56] A. Demirbaş, "Conversion of biomass using glycerin to liquid fuel for blending gasoline as alternative engine fuel," *Energy Convers. Manag.*, vol. 41, no. 16, pp. 1741–1748, 2000.
[57] M. Buffi, A. Cappelletti, T. Seljak, T. Katrašnik, A. Valera-Medina, and D. Chiaramonti, "Emissions and Combustion Performance of a Micro Gas Turbine Powered with Liquefied Wood and its Blends," *Energy Procedia*, vol. 142, pp. 297–302, 2017.
[58] T. Seljak, S. Rodman Oprešnik, M. Kunaver, and T. Katrašnik, "Wood, liquefied in polyhydroxy alcohols as a fuel for gas turbines," *Appl. Energy*, vol. 99, pp. 40–49, 2012.
[59] M. Grilc, B. Likozar, and J. Levec, "Hydrodeoxygenation and hydrocracking of solvolysed lignocellulosic biomass by oxide, reduced and sulphide form of NiMo, Ni, Mo and Pd catalysts," *Appl. Catal. B Environ.*, vol. 150–151, pp. 275–287, 2014.
[60] P. M. Mortensen, J. D. Grunwaldt, P. A. Jensen, K. G. Knudsen, and A. D. Jensen, "A review of catalytic upgrading of bio-oil to engine fuels," *Appl. Catal. A Gen.*, vol. 407, no. 1–2, pp. 1–19, 2011.
[61] D. C. Elliott, T. R. Hart, G. G. Neuenschwander, L. J. Rotness, and A. H. Zacher, "Catalytic hydroprocessing of biomass fast pyrolysis bio-oil to produce hydrocarbon products," *Environ. Prog. Sustain. Energy*, vol. 28, no. 3, pp. 441–449, 2009.
[62] R. S. Weber, M. V. Olarte, and H. Wang, "Modeling the kinetics of deactivation of catalysts during the upgrading of bio-oil," *Energy and Fuels*, vol. 29, no. 1, pp. 273–277, 2015.
[63] M. V. Olarte *et al.*, "Characterization of upgraded fast pyrolysis oak oil distillate fractions

from sulfided and non-sulfided catalytic hydrotreating," *Fuel*, vol. 202, pp. 620–630, 2017.
[64] W. Yin *et al.*, "Catalytic hydrotreatment of fast pyrolysis liquids in batch and continuous set-ups using a bimetallic Ni–Cu catalyst with a high metal content," *Catal. Sci. Technol.*, vol. 6, no. 15, pp. 5899–5915, 2016.
[65] P. H. Steele, S. K. Gajjela, T. E. Mlsna, C. U. Pittman, and F. Yu, "Upgrading of bio-oil using synthesis gas," *Pat. US 2014/0073827 A1*, 2014.
[66] D. Howe *et al.*, "Field-to-fuel performance testing of lignocellulosic feedstocks: An integrated study of the fast pyrolysis-hydrotreating pathway," *Energy and Fuels*, vol. 29, no. 5, pp. 3188–3197, 2015.
[67] P. A. Meyer, L. J. Snowden-Swan, K. G. Rappé, S. B. Jones, T. L. Westover, and K. G. Cafferty, "Field-to-Fuel Performance Testing of Lignocellulosic Feedstocks for Fast Pyrolysis and Upgrading: Techno-economic Analysis and Greenhouse Gas Life Cycle Analysis," *Energy and Fuels*, vol. 30, no. 11, pp. 9427–9439, 2016.
[68] D. Carpenter *et al.*, "Catalytic hydroprocessing of fast pyrolysis oils: Impact of biomass feedstock on process efficiency," *Biomass and Bioenergy*, vol. 96, pp. 142–151, 2017.
[69] G. Kim *et al.*, "Two-step continuous upgrading of sawdust pyrolysis oil to deoxygenated hydrocarbons using hydrotreating and hydrodeoxygenating catalysts," *Catal. Today*, vol. 303, pp. 130–135, 2018.
[70] I. Kim *et al.*, "Upgrading of sawdust pyrolysis oil to hydrocarbon fuels using tungstate-zirconia-supported Ru catalysts with less formation of cokes," *J. Ind. Eng. Chem.*, vol. 56, pp. 74–81, 2017.
[71] K. Routray, K. J. Barnett, and G. W. Huber, "Hydrodeoxygenation of Pyrolysis Oils," *Energy Technol.*, vol. 5, no. 1, pp. 80–93, 2017.
[72] C. Guo *et al.*, "Novel Inexpensive Transition Metal Phosphide Catalysts for Upgrading of Pyrolysis Oil via Hydrodeoxygenation," *AIChE J.*, vol. 62, no. 10, pp. 3364–3372, 2016.
[73] S. Ahmadi, E. Reyhanitash, Z. Yuan, S. Rohani, and C. (Charles) Xu, "Upgrading of fast pyrolysis oil via catalytic hydrodeoxygenation: Effects of type of solvents," *Renew. Energy*, vol. 114, pp. 376–382, 2017.
[74] L. Gueudré *et al.*, "Optimizing the bio-gasoline quantity and quality in fluid catalytic cracking co-refining," *Fuel*, vol. 192, pp. 60–70, 2017.
[75] C. Wang, R. Venderbosch, and Y. Fang, "Co-processing of crude and hydrotreated pyrolysis liquids and VGO in a pilot scale FCC riser setup," *Fuel Process. Technol.*, vol. 181, no. October, pp. 157–165, 2018.
[76] F. de Miguel Mercader, M. J. Groeneveld, S. R. A. Kersten, N. W. J. Way, C. J. Schaverien, and J. A. Hogendoorn, "Production of advanced biofuels: Co-processing of upgraded pyrolysis oil in standard refinery units," *Appl. Catal. B Environ.*, vol. 96, no. 1–2, pp. 57–66, 2010.
[77] F. de Miguel Mercader *et al.*, "Hydrodeoxygenation of pyrolysis oil fractions: process understanding and quality assessment through co-processing in refinery units," *Energy Environ. Sci.*, vol. 4, no. 3, p. 985, 2011.
[78] F. De Miguel Mercader, P. J. J. Koehorst, H. J. Heeres, S. R. A. Kersten, and J. A. Hogendoorn, "Competition Between Hydrotreating and Polymerization Reactions During Pyrolysis Oil Hydrodeoxygenation," *AIChE Journal*, vol. 57, no. 11. pp. 3160–3170, 2011.
[79] D. C. Elliott and E. G. Bager, "United States Patent: Process for Upgrading Biomass Pyrolyzates," 4,795,841, 1989.
[80] D. C. Elliott, "Historical developments in hydroprocessing bio-oils," *Energy and Fuels*, vol. 21, no. 3. pp. 1792–1815, 2007.
[81] S. Oh, H. S. Choi, I.-G. Choi, and J. W. Choi, "Evaluation of hydrodeoxygenation reactivity of pyrolysis bio-oil with various Ni-based catalysts for improvement of fuel properties," *RSC Adv.*, vol. 7, no. 25, pp. 15116–15126, 2017.
[82] S. Cheng, L. Wei, J. Julson, K. Muthukumarappan, P. R. Kharel, and E. Boakye, "Hydrocarbon bio-oil production from pyrolysis bio-oil using non-sulfide Ni-

Zn/Al2O3catalyst," *Fuel Process. Technol.*, vol. 162, pp. 78–86, 2017.
[83] C. Boscagli *et al.*, "Effect of pyrolysis oil components on the activity and selectivity of nickel-based catalysts during hydrotreatment," *Appl. Catal. A Gen.*, vol. 544, pp. 161–172, 2017.
[84] C. Boscagli, K. Raffelt, and J. D. Grunwaldt, "Reactivity of platform molecules in pyrolysis oil and in water during hydrotreatment over nickel and ruthenium catalysts," *Biomass and Bioenergy*, vol. 106, pp. 63–73, 2017.
[85] S. Cheng, L. Wei, J. Julson, and M. Rabnawaz, "Upgrading pyrolysis bio-oil through hydrodeoxygenation (HDO) using non-sulfided Fe-Co/SiO2catalyst," *Energy Convers. Manag.*, vol. 150, no. June, pp. 331–342, 2017.
[86] S. A. Rezzoug and R. Capart, "Liquefaction of wood in two successive steps: Solvolysis in ethylene-glycol and catalytic hydrotreatment," *Appl. Energy*, vol. 72, no. 3–4, pp. 631–644, 2002.
[87] M. Grilc, G. Veryasov, B. Likozar, A. Jesih, and J. Levec, "Hydrodeoxygenation of solvolysed lignocellulosic biomass by unsupported MoS2, MoO2, Mo2C and WS2catalysts," *Appl. Catal. B Environ.*, vol. 163, pp. 467–477, 2015.
[88] N. Schwaiger *et al.*, "BiomassPyrolysisRefinery - Herstellung von nachhaltigen Treibstoffen," *Chemie-Ingenieur-Technik*, vol. 87, no. 6, pp. 803–809, 2015.
[89] R. Feiner, N. Schwaiger, H. Pucher, L. Ellmaier, P. Pucher, and M. Siebenhofer, "Liquefaction of pyrolysis derived biochar: a new step towards biofuel from renewable resources," *RSC Adv.*, vol. 3, no. 39, pp. 17898–17903, 2013.
[90] R. Feiner *et al.*, "Kinetics of Biochar Liquefaction," *Bioenergy Res.*, vol. 7, no. 4, pp. 1343–1350, 2014.
[91] H. Pucher, N. Schwaiger, R. Feiner, P. Pucher, L. Ellmaier, and M. Siebenhofer, "Catalytic hydrodeoxygenation of dehydrated liquid phase pyrolysis oil," *Energy Res.*, vol. 38, no. 15, pp. 1964–1974, 2014.
[92] H. Pucher *et al.*, "Lignocellulosic Biofuels: Phase Separation during Catalytic Hydrodeoxygenation of Liquid Phase Pyrolysis Oil," vol. 50, no. 18, pp. 2914–2919, 2015.
[93] H. Pucher, "Entwicklung, Design und Modellierung eines Upgrading-Prozesses biobasierter flüssiger Energieträger," Graz University of Technology, 2014.
[94] K. Treusch *et al.*, "High-throughput continuous hydrodeoxygenation of liquid phase pyrolysis oil," *React. Chem. Eng.*, vol. 3, pp. 258–266, 2018.
[95] K. Treusch *et al.*, "Hydrocarbon production by continuous hydrodeoxygenation of liquid phase pyrolysis oil with biogenous hydrogen rich synthesis gas," *React. Chem. Eng.*, 2019.

Chapter 4

Diesel production from lignocellulosic feed: the bioCRACK process

ROYAL SOCIETY OPEN SCIENCE

rsos.royalsocietypublishing.org

Research

Cite this article: Treusch K, Ritzberger J, Schwaiger N, Pucher P, Siebenhofer M. 2017 Diesel production from lignocellulosic feed: the bioCRACK process. *R. Soc. open sci.* **4**: 171122. http://dx.doi.org/10.1098/rsos.171122

Received: 11 August 2017
Accepted: 13 October 2017

Subject Category:
Engineering

Subject Areas:
chemical engineering/power and energy systems

Keywords:
bioCRACK, biofuel, liquid phase pyrolysis, refinery integrated

Author for correspondence:
K. Treusch
e-mail: klara.treusch@bdi-bioenergy.com

THE ROYAL SOCIETY PUBLISHING

Diesel production from lignocellulosic feed: the bioCRACK process

K. Treusch[1,2], J. Ritzberger[1], N. Schwaiger[1,2], P. Pucher[1] and M. Siebenhofer[2]

[1]BDI – BioEnergy International AG, Parkring 18, 8074 Raaba-Grambach, Austria
[2]Institute of Chemical Engineering and Environmental Technology, Graz University of Technology, Inffeldgasse 25/C, 8010 Graz, Austria

KT, 0000-0002-3706-4986

The bioCRACK process is a promising technology for the production of second generation biofuels. During this process, biomass is pyrolized in vacuum gas oil and converted into gaseous, liquid and solid products. In cooperation with the Graz University of Technology, the liquid phase pyrolysis process was investigated by BDI – BioEnergy International AG at an industrial pilot plant, fully integrated in the OMV refinery in Vienna/Schwechat. The influence of various biogenous feedstocks and the influence of the temperature on the product distribution in the temperature range of 350°C to 390°C was studied. It was shown that the temperature has a major impact on the product formation. With rising temperature, the fraction of liquid products, namely liquid CHO-products, reaction water and hydrocarbons, increases and the fraction of biochar decreases. At 390°C, 39.8 wt% of biogenous carbon was transferred into a crude hydrocarbon fractions. The type of lignocellulosic feedstock has a minor impact on the process. The biomass liquefaction concept of the bioCRACK process was in pilot scale compatible with oil refinery processes.

1. Introduction

According to the adoption of the Paris Agreement in 2015 the global average temperature increase is to be kept significantly below 2°C above the preindustrial level. This target has to be achieved by reducing greenhouse gas emissions without threatening food production [1]. Second generation biofuels based on lignocellulose will play a sustainable key role for future fuel production from renewable feedstock. Main lignocellulose-conversion technologies are: indirect liquefaction via gasification and methanol synthesis or Fischer–Tropsch synthesis; pyrolysis-based direct liquefaction with subsequent hydrodeoxygenation; upgrading of residues from solvent-based pulping processes and biotechnological treatment of biomass [2]. Gasification methods

such as the Choren technology and the successor Linde Carbo-V® technology [3] require extensive gas treatment in order to remove impurities from crude gas for subsequent processes like Fischer–Tropsch synthesis [4]. Particles have to be removed and sulfur content reduced by gas cleaning concepts, e.g. the low-temperature Rectisol process using methanol as scrubbing agent [5]. Bioethanol from fermentation of cellulose can be admixed to gasoline. However, bioethanol-based biofuels are faced with several unfavourable properties like different density, corrosiveness, low calorific value, low boiling point and miscibility with water, to mention just a few [6]. Pyrolysis of biomass yields in the production of pyrolysis oil, biochar and pyrolysis gas, which can be further upgraded to biofuels [7]. Crude products from dry pyrolysis of lignocellulose need extensive pretreatment for further processing due to coal particle load and the high viscosity of pyrolysis oil. The solids content varies between 0.3% and 3% [8].

Liquid phase pyrolysis (LPP) [9,10], as applied in the bioCRACK process [11], is a promising alternative technology for fuel production from lignocellulosic biomass. The acronym 'bioCRACK' was generated from the words 'biomass' and 'cracking', as the biomass is cracking the carrier oil. BioCRACK is a registered word and design mark. In liquid phase pyrolysis, biomass is thermally treated in a heat carrier oil, e.g. vacuum gas oil (VGO), a side product of crude oil refining. The process is operated in the temperature range between 350°C and 390°C. Due to elevated operation temperature, VGO is partially cracked during pyrolysis, an advantageous side effect of biomass pyrolysis. Biomass is converted into pyrolysis gas, biochar and liquid products. The homolytic degradation process of biomass during pyrolysis is slightly modified by the influence of VGO. Repolymerization reactions are reduced and particles are held back in the heat carrier. The liquid products partially dissolve in vacuum gas oil and may be processed in the refinery without further treatment, achieving a direct transfer of biogenous carbon into VGO. The bioCRACK process was operated in pilot scale (100 kg h^{-1} biomass) at OMV refinery in Vienna/Schwechat [12]. Vacuum gas oil limits the pyrolysis temperature to about 400°C because of its boiling range between 365°C and 530°C [13]. This allows process operation at ambient pressure which simplifies construction and significantly decreases investment costs. Kumar *et al*. [14] have described a related process with a pressure of at least 50 bar and a reaction time of at least 15 min. Nevertheless, the bioCRACK process is the first direct biomass liquefaction process that has already been operated in pilot scale in a petrol refinery. Compared to other biomass liquefaction technologies, the concept is very simple [3–5,7].

1.1. BiomassPyrolysisRefinery

For an economic operation of the bioCRACK pyrolysis process, a high recovery of all product streams is obligatory. The upgrading of the two main side streams biochar and pyrolysis oil is part of the BiomassPyrolysisRefinery concept [15,16,17]. Feiner [18] investigated the liquefaction of biochar, Pucher [19] the hydrodeoxygenation of LPP oil.

Experiments for the liquefaction of biochar [20] were performed in a stirred 450 ml batch reactor between 370°C and 450°C at 180 bar. In order to avoid polymerization reactions [21], hydrogen was provided with tetralin as a hydrogen donor. Biochar conversion of 84 wt% and an oil yield of 72 wt% could be achieved. Hydrodeoxygenation of LPP oil [22] was investigated at 250°C and 100 bar and at 300°C and 150 bar in a batch reactor. Pyrolysis oil from the bioCRACK process has a higher water content than pyrolysis oil from flash pyrolysis [23]. This results in a lower viscosity. In LPP oil, no particles are present, as they are held back together with the biochar by the VGO. This facilitates the handling of pyrolysis oil. An oil yield of up to 56 wt% was observed.

2. Material and methods

Analytical methods, feedstock and process parameters will be discussed in this section.

2.1. Feedstock material

Lignocellulosic feedstock was spruce wood, beech wood, miscanthus and wheat straw. All lignocelluloses were provided in pelletized form. The pellets were milled on-site with a mechanical mill. For temperature study, spruce wood was used as lignocellulosic feed. Spruce wood was provided in ENplus A1 and DINplus accredited pellets from RZ Pellets GmbH in Bad St Leonhard, Austria. Beech wood and wheat straw were provided by FAIR Holz in Leopoldshöhe, Germany. Miscanthus was provided by TD Zorn GmbH in Heidenrod–Zorn, Germany. An elemental analysis of the feedstock is shown in table 1. Lignocellulosic biomass contains up to 50% oxygen [24]. This oxygen has to be

Table 1. Elemental analysis of feedstock material.

	carbon [wt%]	hydrogen [wt%]	nitrogen [wt%]	balance [wt%]
spruce wood	50.1	6.3	0.04	43.5
beech wood	45.3	6.3	0.09	48.3
miscanthus	43.3	6.4	0.14	50.2
wheat straw	45.1	6.0	0.58	48.4
VGO	86.31	12.26	0.55	0.88

removed in order to produce hydrocarbons with fuel quality. The carbon content of the wood samples varies between 43.3 and 50.1%.

Liquid phase pyrolysis product formation is not significantly dependent on the particle size of the biogenous feedstock in the range between 1 mm and 1 cm [9]. The elemental composition of VGO is shown in table 1. Vacuum gas oil has a boiling range between 365°C and 530°C [13]. The VGO used for the bioCRACK had a boiling range between 300°C and 530°C.

2.2. Analytical methods

The elemental analyses of all streams were characterized by a vario MACRO CHN-analyzer from 'Elementar Analysensysteme GmbH'. The water content of pyrolysis oil was determined by a gas chromatograph, type Agilent 7890A, with a TCD detector and a HP-INNOWAX column, 30 m × 0.53 mm × 1 µm. The water content of the oil fraction was determined by Karl-Fischer-titration with a Schott Titro Line KF-Titrator and a Hydranal titration reagent. The boiling range of the oil fractions was determined by a gaschromatograph, type Agilent 7890A, with an FID-detector and the Restek-column MXT-2887, 10 m × 0.53 mm × 2.65 µm. Density and viscosity were measured with a digital viscometer, SVM 3000, of Anton Paar GmbH. The content of biogenous carbon (^{14}C) was determined by the external laboratory Beta Analytic Limited, SO/IEC 17025:2005 accredited, in Miami, FL, via acceleration mass spectrometry.

2.3. The bioCRACK pilot plant

The bioCRACK pilot plant with a nominal biomass capacity of 100 kg h^{-1} and 600 kg h^{-1} VGO was in continuous operation for two years. The mass ratio of VGO to biomass was 6. A scheme of the bioCRACK process is shown in figure 1. Biomass is impregnated with VGO in a first vessel and then fed in reactors 1 and 2 together with additional recycle-VGO. The reaction takes place at 350–400°C and ambient pressure. Biogenous and fossil vapours are condensed and separated in two steps, obtaining the aqueous pyrolysis oil fraction, the non-polar bioCRACK oil fraction and high boiling heat carrier residues. Biochar and heat carrier are separated in a decanter. Figure 2 shows the integration concept of the bioCRACK process in an existing refinery [11], as practised during operation of the pilot plant. Utilities, such as steam, power, cooling water and nitrogen, can be used from the refinery. Gaseous products generate electricity and/or steam. The reaction products can be upgraded in existing refinery facilities.

3. Results and discussion

The mass balance of the liquid phase pyrolysis process at 375°C with the feedstock spruce wood is shown in figure 3. Process operation is 5 days, balance period is about 36 h. The carrier oil feed is composed of the oil from the impregnator and the carrier oil buffer. To minimize the consumption of VGO, the bottom product of the distillation as well as the spent VGO are recycled. The reaction products consist of non-condensible gases (at ambient temperature and pressure), pyrolysis oil, mixed oil, pyrolysis char, spent VGO and the water-content of the biomass. The water formed during LPP and the feed moisture are discharged with the pyrolysis oil. The amount of dry biochar is determined analytically through extraction of VGO residues with hexane in laboratory scale. The composition of these product streams is shown in table 2. The mixed oil is distilled to obtain bioCRACK oil (naphtha, kerosene, diesel) and

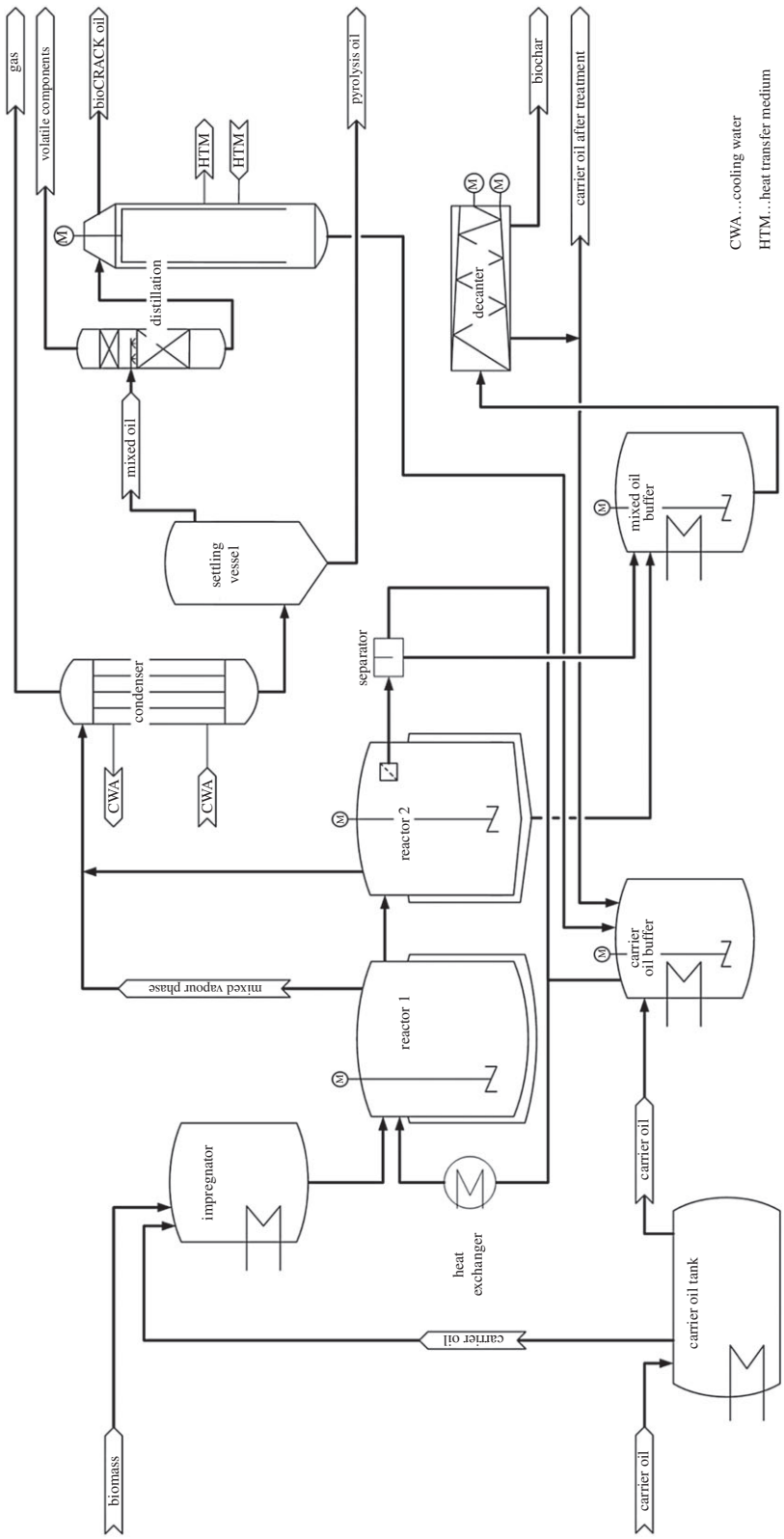

Figure 1. Integration of the bioCRACK process in a refinery [11].

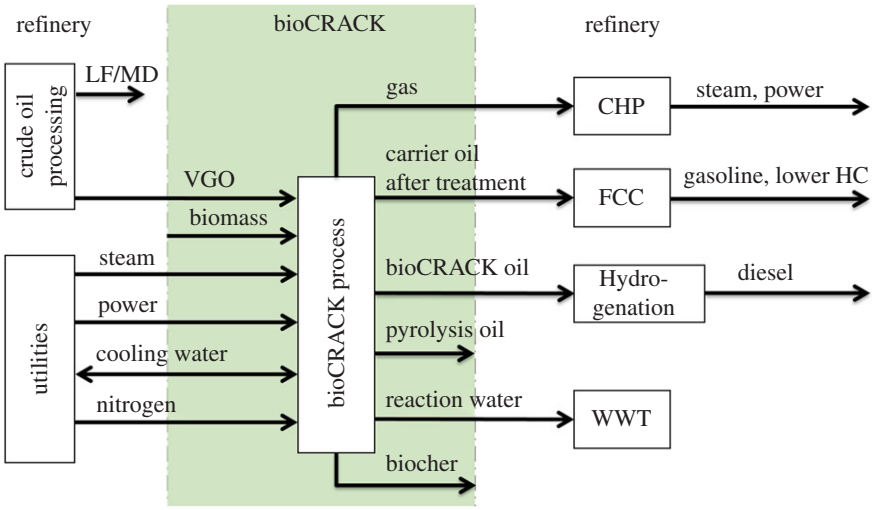

Figure 2. Scheme of the bioCRACK process [16].

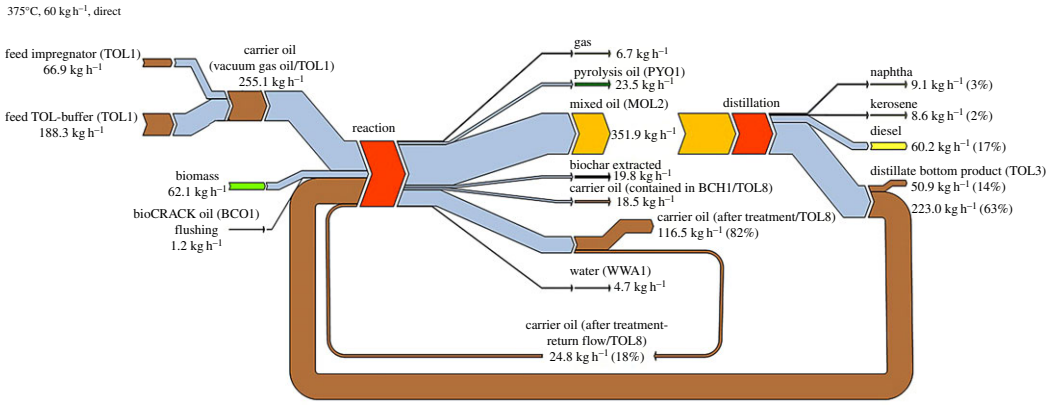

Figure 3. Mass balance of the bioCRACK process (375°C, spruce wood).

a bottom product. The MIX-buffer contains spent VGO and biochar and is fed to the decanter. The bioCRACK oil feed is used for washing purposes between experiments.

3.1. Influence of the reaction temperature

The reaction temperature has a major impact on the product distribution of pyrolysis processes. The higher the temperature, the more gas and the less biochar is produced, whereas liquid products show a maximum at 500°C (fast pyrolysis processes) [25]. As shown in figure 4, lignocellulose is transferred into biochar, hydrocarbons, pyrolysis oil and gaseous products during liquid phase pyrolysis. Elevated temperature leads to a decreasing amount of biochar and rising liquefaction. At temperatures below 385°C, biochar is the main reaction product, and liquid CHO products above 385°C.

The balance of biogenous carbon is in accordance with the mass balance. With increasing temperature, the biochar yield decreases and more liquid products are formed. The transfer of biogenous carbon into the fossil oil fraction rises with increasing temperature. The transfer of biogenous carbon into hydrocarbon fraction increases from 29 wt% at 350°C to about 40 wt% at 390°C. The difference in ^{14}C balance compared to the mass balance is caused by the different carbon content of the individual products. Whereas biochar has a carbon content of 81% and hydrocarbons about 85%, the carbon content of pyrolysis oil amounts to 26%, as shown in the elemental analysis in table 2.

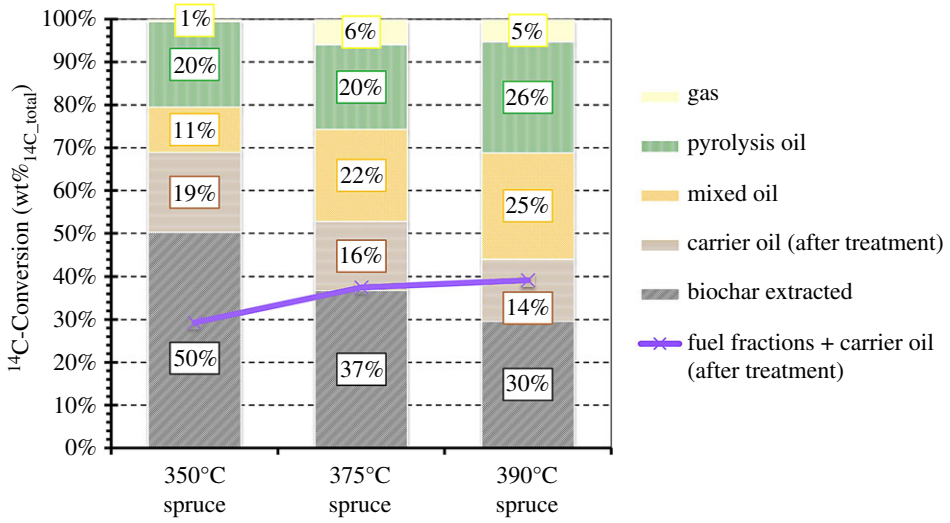

Figure 4. Bio-carbon transfer as a function of the pyrolysis temperature.

Table 2. Product characterization in dependence of the pyrolysis temperature.

[wt%]	biochar			pyrolysis oil			mixed oil			carrier oil after treatment			gas		
reaction temperature [°C]	350	375	390	350	375	390	350	375	390	350	375	390	350	375	390
C [wt%]	77.5	80.9	80.9	25.8	25.6	26.6	85.3	84.9	84.3	86.2	86.6	86.3	—	—	—
H [wt%]	5.3	5.4	5.4	9.2	9.4	9.2	12.3	12.3	12.1	12.2	12.1	11.8	—	—	—
N [wt%]	0.2	0.3	0.3	0.3	0.4	0.4	0.4	0.4	0.5	0.5	0.5	0.6	—	—	—
residue [wt%]	16.9	13.5	13.4	64.7	64.6	63.8	2.0	2.4	3.2	1.2	0.9	1.3	—	—	—
water [wt%]	—	—	—	50.2	51.9	50.2	—	—	—	—	—	—	—	—	—
^{14}C [wt%]	88.9	84.1	79.4	100	100	100	4.9	6.7	3.4	1.7	2.1	1.7	—	—	—
CO [wt%]	—	—	—	—	—	—	—	—	—	—	—	—	33.9	34.4	33.4
CO_2 [wt%]	—	—	—	—	—	—	—	—	—	—	—	—	61.5	55.0	53.4
CH_4 [wt%]	—	—	—	—	—	—	—	—	—	—	—	—	4.6	10.6	13.2

Through simulated distillation, the bioCRACK oil can be analytically separated in diesel, kerosene and naphtha. With increasing temperature, more fuel gets produced due to VGO cracking. The total amount of fuel fraction based on biomass (BM) and VGO as a function of reaction temperature is shown in figure 5. Although the ^{14}C amount of all fractions rises with temperature, the impact on the diesel fraction deviates strongly. The total amount of fuel is about 5–6% at 350°C. It rises up to 14–15% at 386°C.

3.2. Influence of the biomass feedstock

The bioCRACK process is not very sensitive to different lignocellulosic feedstock. The transfer of biogenous carbon into the fuel fraction of beech wood and wheat straw is similar to the data for spruce wood. The transfer of biogenous carbon into the non-condensable gaseous products is higher for the feedstock wheat straw. This results in a lower CHO-content of the pyrolysis oil (about one third compared to 50% for spruce or beech wood). The CHO-content of pyrolysis oil from miscanthus amounts to about 40%. Caused by the higher ash content of miscanthus and wheat straw, more biochar, but with a lower heating value, is formed. There is no significant difference concerning the power consumption.

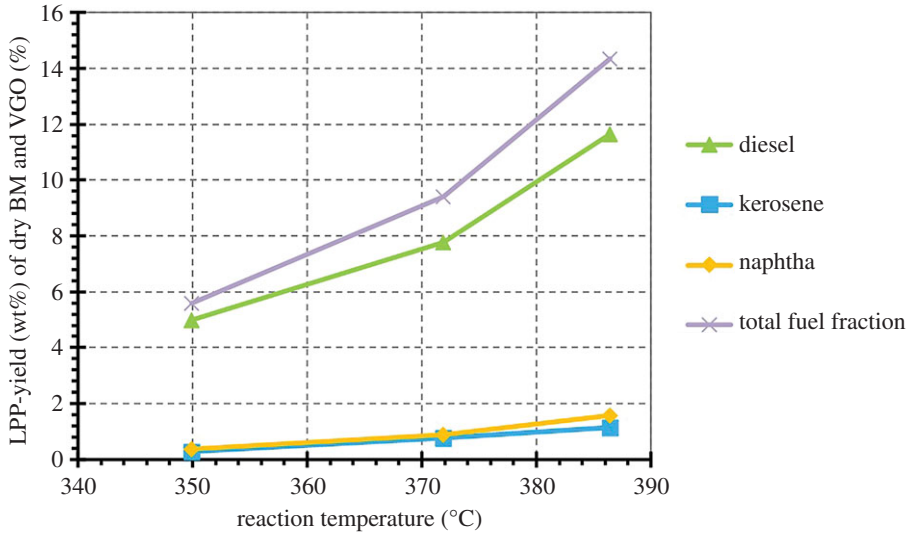

Figure 5. Fuel yield as a function of the pyrolysis temperature.

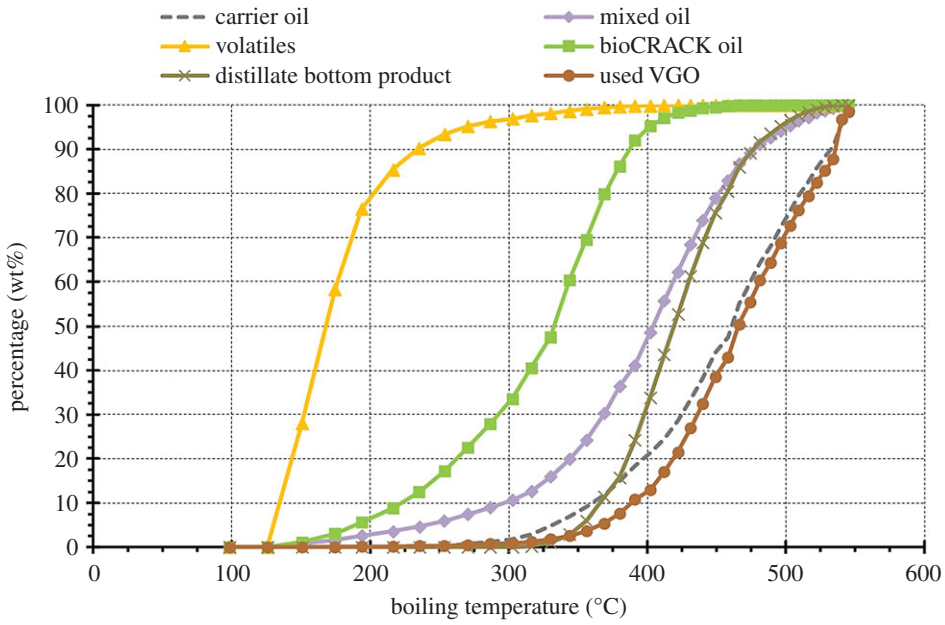

Figure 6. Boiling range of the liquid feed and products (375°C, spruce wood).

3.3. Product characterization

The boiling range of the carrier oil and products is shown in figure 6. The boiling range of spent VGO does not differ from fresh VGO fed to the reactor. The amount of biogenous carbon in the spent VGO is 2–3%. Caused by the small difference in the boiling range, the spent VGO can be fed directly into the refinery FCC. The mixed oil is distilled to yield volatiles, bioCRACK oil and a bottom product. The boiling curve of the bioCRACK oil lies between the bottom product and the volatiles.

The main component of pyrolysis oil is water. It mainly consists of acids, ketones, aldehydes, sugars, phenols and an organic matrix from sugar and lignin derivatives and other substances [22]. A specific extraction is very complex due to the high number and low content of individual components [23]. The composition and characterization of pyrolysis oil is shown in table 3. Caused by the high oxygen content, a direct admixture to fuels is not possible. Pyrolysis oil is very corrosive and therefore needs to undergo further upgrading.

Table 3. Characterization of liquid phase pyrolysis oil.

water content	[wt%]	49.6
heating value	[MJ kg^{-1}]	9.2
density	[kg m^{-3}]	1090
kinetic viscosity	[mm^2 s^{-1}]	3.9
biogenous carbon	[wt%]	100
carbon	[wt%]	25.6
hydrogen	[wt%]	9.2
oxygen	[wt%]	64.9
nitrogen	[wt%]	<1

Table 4. Quality of bioCRACK diesel before and after hydrotreatment compared to EN 590.

parameter	untreated raw diesel	after hydrotreatment	EN 590
density (15°C) [kg m^{-3}]	868	833	820–845
viscosity (40°C) [mm^2 s^{-1}]	2.53	n.a.	2–4.5
Cetan	44	53	>51
C/H/O [wt%]	85/13/2	86/14/0	n.a.
volatile <350°C [wt%]	83	86	>85% (v/v)
sulfur [mg kg^{-1}]	177	3	<10

3.4. Further product processing

The products can be upgraded with existing facilities of oil refineries, where raw fuel and VGO would be processed anyhow. These upgrading facilities are the fluid catalytic cracker (FCC) and hydrogenation reactors for fuel production with a biogenous content [11].

Before hydrogenating in laboratory scale, bioCRACK oil was treated by distillation to produce the fractions light ends (less than 175°C), kerosene (175–225°C), gas oil (225–350°C) and bottom products (more than 350°C). Afterwards, kerosene and gas oil were hydrogenated in a hydrotreater with a feed rate of 65 ml h^{-1} at 41 bar and 360°C. The required hydrogen flow of 200–220 Nm^3 m^{-3} for bioCRACK oil hydrogenation is higher than that for crude raw fuel with about 135 Nm^3 m^{-3}. Also the temperature is higher. This is caused by the higher oxygen content of bioCRACK raw fuel. The density of the hydrogenated gas oil is slightly off the standard for diesel. To achieve the standards, the gas oil has to be fractionated between 200°C and 350°C. After that, the gas oil achieves the quality of diesel according to EN590, as shown in table 4.

The heavy oil fraction is cracked in an FCC. The feed is preheated in a tubular furnace close to boiling, which is approximately between 260°C and 320°C. The feed evaporates instantaneously when getting in contact with the catalyst and is cracked [26].

Berchtold *et al*. [26] investigated four different case studies to survey the influence of different VGO pretreatment and biomass feedstock on the treatment in the FCC. The case studies included: spruce wood and VGO without hydrotreatment, spruce wood and VGO hydrotreated after LPP, spruce wood and VGO hydrotreated prior to LPP, and straw and VGO without hydrotreatment. In case studies without hydrotreatment, more coke was formed. Preceding hydrotreatment reduces coking reactions. The biogenous feedstock straw reduces the yield of fuel due to coking reactions and higher residue. However, the outcome of all case studies did not show significant deviations. It was shown that high conversion efficiency for all performed case studies due to the very low oxygen content of the processed heat carrier oil was achieved. The FCC therefore can be used for cracking of spent VGO with biogenous content from the bioCRACK process without any major modifications of the FCC plant design.

4. Summary and conclusion

In pilot scale operation, up to 40 wt% of the biogenous carbon yielded in hydrocarbon refinery intermediates and fuel fractions. Up to now, the bioCRACK process is the first technology for direct biomass liquefaction integrated in an oil refinery process. However, this process has so far only been practised in pilot scale, the next step would be a demonstration plant. For an economic operation, the bioCRACK process would have to be investigated in industrial scale. The temperature has a major impact on the composition and distribution of LPP products. Higher reaction temperature leads to higher liquid product yield and lower solids yields. The transfer of biogenous carbon into the fuel fraction rises with temperature. The type of lignocellulose has a minor impact on the process. Compared to spruce wood, the main feedstock, beech wood shows no significant difference, while miscanthus and wheat straw lead to lower CHO yield and a higher biochar production with a lower heating value due to the higher ash content. The hydrocarbons can be upgraded in existing refinery facilities with some adaptions. The upgrading of the main side streams, biochar and pyrolysis oil, has been investigated in laboratory scale with promising results.

Ethics. For this work, no ethical assessment was required to be made prior to conducting the research, as no research on humans or animals was included.

Data accessibility. All the performance data are provided in the main text. There are no additional data associated with this submission.

Author's contribution. K.T. participated in laboratory experiments, analytics and data analysis and drafted the manuscript. J.R. worked at the pilot plant for his PhD Thesis, collected field data and was responsible for data analysis. N.S. was responsible for laboratory experiments and data analysis. P.P. was the head of this project in the company BDI – BioEnergy International AG and coordinated the study. He was involved in the conception and design of the pilot plant. M.S. is the director of the Institute of Chemical Engineering and Environmental Technology and helped draft the manuscript. All authors revised the manuscript critically and gave final approval for publication.

Competing interests. The authors have no competing interests.

Funding. This work was funded by the Austrian Research Promotion Agency (FFG) under the scope of the Austrian Climate and Energy Fund.

Acknowledgements. The authors would like to acknowledge their colleagues Lisa Ellmaier and Angela Pieber for their work in the laboratory.

References

1. UNFCCC. 2015 Adoption of the Paris Agreement: Proposal by the President to the United Nations Framework Convention on Climate Change. 21932 (December), 1–32. See: https://unfccc.int/resource/docs/2015/cop21/eng/l09r01.pdf.
2. Stöcker M. 2008 Biofuels and biomass-to-liquid fuels in the biorefinery: catalytic conversion of lignocellulosic biomass using porous materials. *Angew. Chem.– Int. Ed.* **47**, 9200–9211 (doi:10.1002/anie.200801476)
3. Blades T, Rudloff M, Schulze O. 2005 Sustainable SunFuel from CHOREN's Carbo-V ® Process [Internet]. ISAF XV, San Diego. See: http://www.eri.ucr.edu/ISAFXVCD/ISAFXVAF/SSFCCVP.pdf.
4. Fischer F, Tropsch H. 1926 Über die direkte Synthese von Erdöl-Kohlenwasserstoffen bei gewöhnlichem Druck (Erste Mitteilung.). *Chem. Ber.* **59**, 830–831. (doi:10.1002/cber.19260590442)
5. Spath PL, Dayton DC. 2003 *Preliminary screening—technical and economic assessment of synthesis gas to fuels and chemicals with emphasis on the potential for biomass-derived syngas*. National Renewable Energy Laboratory [Internet]. (December): 1–160. Available from: http://www.dtic.mil/cgi-bin/GetTRDoc?AD=ADA436529&Location=U2&doc=GetTRDoc.pdf%5Cn. http://www.osti.gov/servlets/purl/15006100-UpKNFn/native/.
6. Balat M, Balat H, Öz C. 2008 Progress in bioethanol processing. *Prog. Energy Combust. Sci.* **34**, 551–573. (doi:10.1016/j.pecs.2007.11.001)
7. Kaltschmitt M, Streicher W. 2009 Energie aus Biomasse [Internet]. Regenerative Energien in Österreich. 339–532. See: http://dx.doi.org/10.1007/978-3-8348-9327-7_9
8. Bridgwater AV, Peacocke GVC. 2000 Fast pyrolysis processes for biomass. *Renew. Sustain. Energy Rev.* **4**, 1–73. (doi:10.1016/S1364-0321(99)00007-6)
9. Schwaiger N *et al.* 2011 Liquid and solid products from liquid-phase pyrolysis of softwood. *Bioenergy Res.* **4**, 294–302. (doi:10.1007/s12155-011-9132-8)
10. Schwaiger N *et al.* 2012 Formation of liquid and solid products from liquid phase pyrolysis. *Bioresour. Technol.* **124**, 90–94. (doi:10.1016/j.biortech.2012.07.115)
11. Ritzberger J, Pucher P, Schwaiger N, Siebenhofer M. 2014 The BioCRACK process: a refinery integrated biomass-to-liquid concept to produce diesel from biogenic feedstock. *Chem. Eng. Trans.* **39**, 1189–1194.
12. Ritzberger J. 2016 *Flüssigphasenpyrolyse Prozessmodellierung und Scale-Up*. Graz University of Technology.
13. Jones DSJ, Pujadó PR. 2006 *Handbook of petroleum processing*. Berlin, Germany: Springer.
14. Kumar S, Lange JP, Van Rossum G, Kersten SRA. 2015 Liquefaction of lignocellulose in fluid catalytic cracker feed: a process concept study. *ChemSusChem* **8**, 4086–4094. (doi:10.1002/cssc.201500457)
15. Schwaiger N, Feiner R, Pucher H, Ellmaier L. 2015 BiomassPyrolysisRefinery – Herstellung von nachhaltigen Treibstoffen. 1–8.
16. Schwaiger N, Elliott DC, Ritzberger J, Wang H, Pucher P, Siebenhofer M. 2015 Hydrocarbon liquid production via the bioCRACK process and catalytic hydroprocessing of the product oil. *Green Chem.* **17**, 2487–2494. (doi:10.1039/C4GC02344G)
17. Schwaiger N, Treusch K, Siebenhofer M. 2017 Biogene Treibstoffe aus Biomassepyrolyse. *BIOspektrum* **23**, 341–343. (doi:10.1007/s12268-017-0803-7)
18. Feiner R. 2014 *Hydrierende Verflüssigung biogener Einsatzstoffe*. Graz University of Technology.
19. Pucher H. 2014 *Entwicklung, Design und Modellierung eines Upgrading-Prozesses biobasierter flüssiger Energieträger*. Graz University of Technology.
20. Feiner R, Schwaiger N, Pucher H, Ellmaier L, Derntl M, Pucher P, Siebenhofer M. 2014 Chemical loop systems for biochar liquefaction: hydrogenation of naphthalene. *RSC Adv.* **4**, 34955. (doi:10.1039/C4RA03487B)
21. Haenel MW. 2008 Catalysis in direct coal liquefaction. In *Handbook of heterogeneous catalysis* (eds G Ertl, H Knözinger, F Schüth, J Weitkamp), pp. 3023–3036. New York, NY: Wiley.
22. Pucher H, Schwaiger N, Feiner R, Ellmaier L, Pucher P, Chernev BS, Siebenhofer M. 2015 Lignocellulosic biofuels: phase separation during catalytic

hydrodeoxygenation of liquid phase pyrolysis oil lignocellulosic biofuels. *Sep. Sci. Technol.* **50**, 2914–2919.

23. Czernik S, Bridgwater AV. 2004 Overview of applications of biomass fast pyrolysis oil. *Energy Fuels* **18**, 590–598. (doi:10.1021/ef034067u)
24. Fengel D, Wegener G. 2003 *Wood chemistry, ultrastructure reactions*. München, Germany: Kessel.
25. Bridgwater AV, Meier D, Radlein D. 1999 An overview of fast pyrolysis of biomass. *Org. Geochem.* **30**, 1479–1493. (doi:10.1016/S0146-6380(99)00120-5)
26. Berchtold M, Fimberger J, Reichhold A, Pucher P. 2016 Upgrading of heat carrier oil derived from liquid-phase pyrolysis via fluid catalytic cracking. *Fuel Process. Technol.* **142**, 92–99. (doi:10.1016/j.fuproc.2015.09.028)

Chapter 5

Temperature dependence of single step hydrodeoxygenation of liquid phase pyrolysis oil

frontiers in Chemistry

ORIGINAL RESEARCH
published: 19 July 2018
doi: 10.3389/fchem.2018.00297

Temperature Dependence of Single Step Hydrodeoxygenation of Liquid Phase Pyrolysis Oil

Klara Treusch[1,2]*, *Nikolaus Schwaiger*[1,2], *Klaus Schlackl*[2], *Roland Nagl*[2], *Peter Pucher*[1] *and Matthäus Siebenhofer*[2]

[1] BDI – BioEnergy International GmbH, Research and Development, Raaba-Grambach, Austria, [2] Institute of Chemical Engineering and Environmental Technology, Graz University of Technology, Graz, Austria

In this paper, continuous hydrodeoxygenation (HDO) of liquid phase pyrolysis (LPP) oil in lab-scale is discussed. Pyrolysis oil is derived from the bioCRACK pilot plant from BDI - BioEnergy International GmbH at the OMV refinery in Vienna/Schwechat. Three hydrodeoxygenation temperature set points at 350, 375, and 400°C were investigated. Liquid hourly space velocity (LHSV) was 0.5 h^{-1}. Hydrodeoxygenation was performed with an *in situ* sulfided metal oxide catalyst. During HDO, three product phases were collected. A gaseous phase, an aqueous phase and a hydrocarbon phase. Experiment duration was 36 h at 350 and 375°C and 27.5 h at 400°C in steady state operation mode. Water content of the hydrocarbon phase was reduced to below 0.05 wt.%. The water content of the aqueous phase was between 96.9 and 99.9 wt.%, indicating effective hydrodeoxygenation. The most promising results, concerning the rate of hydrodeoxygenation, were achieved at 400°C. After 36/27.5 h of experiment, catalyst deactivation was observed.

Keywords: hydrodeoxygenation, liquid phase pyrolysis, pyrolysis oil, temperature variation, 2nd generation biofuels

OPEN ACCESS

Edited by:
Christophe Len,
University of Technology of Compiègne, France

Reviewed by:
Benjaram M. Reddy,
Indian Institute of Chemical Technology (CSIR), India
Pavel Nikulshin,
Samara State University, Russia
Rafael Luque,
Universidad de Córdoba, Spain

***Correspondence:**
Klara Treusch
klara.treusch@bdi-bioenergy.com

Specialty section:
This article was submitted to Green and Sustainable Chemistry, a section of the journal Frontiers in Chemistry

Received: *15 December 2017*
Accepted: *26 June 2018*
Published: *19 July 2018*

Citation:
Treusch K, Schwaiger N, Schlackl K, Nagl R, Pucher P and Siebenhofer M (2018) Temperature Dependence of Single Step Hydrodeoxygenation of Liquid Phase Pyrolysis Oil. Front. Chem. 6:297. doi: 10.3389/fchem.2018.00297

INTRODUCTION

Biomass pyrolysis is a suitable pathway for the production of second generation biofuels (Demirbas, 2011). During pyrolysis, one of the major products is pyrolysis oil. Due to its high water content, high corrosivity and other negative properties, according to **Table 1**, pyrolysis oil needs intensive upgrading prior to usage as fuel for combustion engines. To achieve fuel quality standards, an upgrading step is necessary. Hydrodeoxygenation (HDO) is a high potential upgrading technology (Pucher et al., 2015). In literature, mainly experiments with fast pyrolysis oil are reported.

One of the biggest issues during HDO of pyrolysis oil in general is catalyst deactivation caused by coke formation. Especially the single-step HDO above 300°C is seen as troublesome, as it leads to coking and plugging (Elliott and Bager, 1989). Therefore, a two-step process is proposed in literature (Elliott, 2007; Elliott et al., 2009; Carpenter et al., 2016; Meyer et al., 2016; Olarte et al., 2016, 2017). In a first step, pyrolysis oil is stabilized (Pucher et al., 2014) through mild hydrotreatment at low temperature. In a second step, the final hydrodeoxygenation, or hydrocracking, takes place. Hydrotreatment temperatures are between 140 and 375°C, at liquid hourly space velocities between 0.28 and 0.5 h^{-1}. The hydrocracking step is performed at temperatures of about 400°C and liquid hourly space velocities of 0.1–0.4 h^{-1} (Elliott et al., 2009; Olarte et al., 2016).

Contrary to these results, in this paper LPP oil is processed continuously in a single-step HDO reactor at 350–400°C. The LHSV was set on the limits of HDO of fast pyrolysis oil with 0.5 h^{-1} (Volume LPP oil/ Volume of empty tube and hour).

LIQUID PHASE PYROLYSIS

In liquid phase pyrolysis, biomass is pyrolyzed in a liquid heat carrier (Schwaiger et al., 2011, 2012). During this conversion, a part of the biomass dissolves in the heat carrier, while a second liquid phase, a polar water containing hydrocarbon phase, is generated (Schwaiger et al., 2015). In the bioCRACK process (Ritzberger et al., 2014; Treusch et al., 2017), LPP was operated with the heat carrier vacuum gas oil to enable integration in an oil refinery. From 2012 to 2014 a pilot plant was operated by BDI – BioEnergy International GmbH at the OMV refinery in Vienna/Schwechat.

MATERIALS AND METHODS

Experiments were carried out in a plug flow reactor with an inner diameter of 3/8 inches and a heated zone of about 30 cm, made by Parr Instrument Company. It was designed for a maximum pressure of 220 bar and a maximum temperature of 550°C. The temperature was detected by an inner thermowell with a thermocouple with three probe points. Heat was provided by a single zone external electric heater. In the temperature range between 350 and 400°C, three operation points were tested: 350, 375, and 400°C. Hydrogen pressure was kept constant at 121.5 bar for all experiments.

Materials

The LPP oil was derived from the bioCRACK pilot plant. It was produced by LPP of spruce wood. The composition of LPP oil is shown in **Table 1**.

HDO was performed with a sulfided $CoMo/Al_2O_3$ catalyst, details are shown in **Table 2**. It was obtained as extrudates with a length of 2–3 mm. The catalyst was chosen as it is cheaper than noble metal catalysts and not susceptible for catalyst poisoning through sulfur, in contrary it gets more active by adding sulfur. For sulfidation, 35 wt.% di-tert-butyldisulfide (DTBDS) in decane was used. To provide enough sulfur during HDO, 150 ppm of sulfur as DTBDS were added to the LPP oil. Hydrogen 5.0 was provided in a 300 bar gas cylinder from AIR LIQUIDE AUSTRIA GmbH.

Analytical Methods

The ultimate analysis of all streams was done by a vario MACRO CHN-analyser from Elementar Analysensysteme GmbH. The oxygen was determined by difference. The water content of the aqueous product phase was determined by a gas-phase chromatograph, type Agilent 7890A, with a TCD-detector and a HP-INNOWAX column, 30 m*0.530 mm*1 μm. For determination of the water content, the GC was calibrated with high-purity water (type I) in THF in the range of 1–8 wt.% water. The boiling range of the hydrocarbon product phase was determined by a gas-phase chromatograph, type Agilent 7890A, with a FID-detector and a Restek-column MXT-2887, 10 m *0.530 mm *2.65 μm, according to ASTM Method D2887. The water content of the oil fraction was determined by Karl-Fischer-titration with a Schott Titro Line KF-Titrator and a Hydranal titration reagent. Density and viscosity were measured by a digital viscosimeter, SVM 3000, of Anton Paar GmbH. The composition of the hydrocarbon product phase was determined by gas chromatography-MS with a quadrupole mass spectrometer (GC-MS), type Schimadzu GCMS QP 2010 Plus, with a VF-1701 MS column, 60 m *0.25 mm *0.25 μm. The GC-MS was calibrated with a multi-component standard, consisting of: pentane, 2-methyl-pentane, hexane, methyl-cyclohexane, ethyl-cyclopentane, octane, toluene, ethyl-cyclohexane, propyl-cyclohexane and decane in THF, in the range of 100–3,000 ppmw each. Additionally, flouranthene was used as internal standard. The gas phase composition was determined by a micro gas-phase chromatograph (micro-GC), type Agilent 3000A, with a TCD-detector, a molecular sieve column and a plot u column. The micro-GC was calibrated with oxygen, nitrogen, hydrogen, methane, ethane, acetylene and carbon dioxide.

TABLE 1 | Properties and composition of LPP oil.

Property	Unit	LPP oil
Water content	[wt.%]	57.0
Lower heating value	[MJ/kg]	7.4
Density	[kg/m^3]	1092
Viscosity	[mPa·s]	3.5
Carbon content	[wt.%]	22.3
Hydrogen content	[wt.%]	9.4
Oxygen content (balance)	[wt.%]	67.8
Nitrogen content	[wt.%]	<1

TABLE 2 | Catalyst details ($CoMo/Al_2O_3$).

Supplier	Alfa Aesar
Cobalt oxide [wt.%]	4.4
Molybdenum oxide [wt.%]	11.9
Surface area [m^2/g]	279
Stock number	45579

Catalyst Preparation

To increase the specific surface area, the catalyst was milled in a centrifugal mill with trapezoidal perforations of 1 mm diameter. The ground material was sieved in a sieving tower of Retsch to obtain the target particle size of 200–600 μm. The reactor was then filled upside down with catalyst. On bottom and top a few cm of catalyst extrudates were applied. The heated zone of the reactor (30 cm) was filled with particles of 200–600 μm size. The catalyst was held in the reactor with a sieve at the bottom.

For each experiment, the reactor was filled with fresh $CoMo/Al_2O_3$ catalyst of Alfa Aesar and inertised with nitrogen. Afterwards the reactor was flushed with hydrogen. Then a hydrogen flow rate of 0.5 l/h was adjusted.

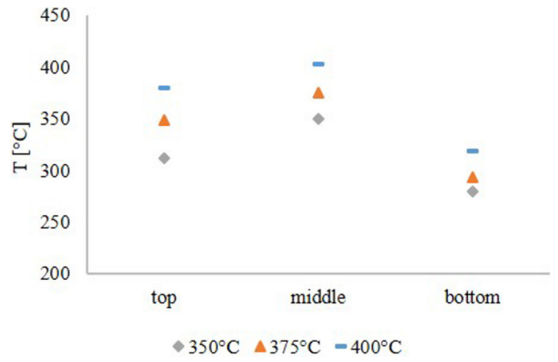

FIGURE 1 | Temperature profile in the reactor.

For the activation of the catalyst, a sulfidation step preceded the HDO experiments. Thus, 35 wt.% di-tert-butyldisulfide (DTBDS) in decane was pumped through the reactor during heating up. Sulfidation was continued for five hours at 400°C. After sulfidation, the temperature was reduced to the requested temperature of HDO procedure.

Experimental Procedure

After sulfidation, 5 h of HDO of LPP oil were performed in the unsteady state operation mode. Afterwards, 36 h of HDO were performed, with liquid product sampling every 12 h for experiments at 350 and 375°C. At 400°C, experiment duration was 27,5 h and sampling periods were 8, 7.5, and 12 h. The gas phase composition was monitored every 4 h. After 36/27.5 h of steady state operation, the reactor was shut down and the catalyst bed was washed with acetone for catalyst analysis. Plugging was not observed.

RESULTS

In this chapter, observations during experiments, mass balance and product characterization are given. Possible pathways of biomass constituents to components in the final product, derived from GC-MS analysis, are discussed.

Temperature Profile in the Reactor

The temperature profile, shown in **Figure 1**, was similar for all experiments. Due to the fact, that the pyrolysis oil was not pre-heated, the feed temperature was lower than the temperature in the middle of the reactor. The temperature maximum was obtained in the middle of the reactor. This temperature was the set point temperature for all HDO experiments. At the exit of the reactor, the temperature dropped significantly due to external cooling effects. From the temperature profile it was concluded, that the exothermal HDO reaction was completed after about 2/3 of the reactor.

TABLE 3 | Mass balance based on LPP oil and H_2 feed.

Temperature	350°C	375°C	400°C
LPP oil [wt.%]	79.13	79.32	80.47
H_2 [wt.%]	20.87	20.68	19.53
Aqueous [wt.%]	59.96	58.94	58.62
Hydrocarbon [wt.%]	7.68	7.76	7.79
Gaseous [wt.%]	26.82	27.55	28.37
Coke [wt.%]	1.34	1.35	1.36

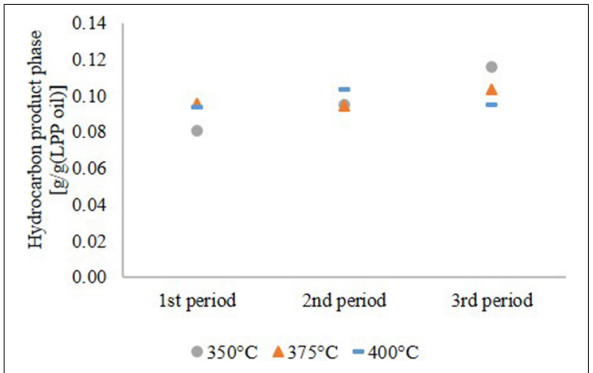

FIGURE 2 | Yield on hydrocarbon product phase based on LPP oil.

Mass Balance and Coke Formation

During HDO, three product phases were formed. A hydrocarbon phase, the target product, an aqueous phase and a gaseous phase. In general, the difference concerning the product distribution between hydrocarbon product and aqueous phase is not depending on temperature in the range of 350–400°C. The differences are more recognizable in the stream compositions. **Table 3** shows that the yield of aqueous phase decreased with temperature, whereas the gas yield increased.

The yield of the hydrocarbon product phase based on the LPP oil in the feed is shown in **Figure 2**. At 350 and 375°C it increased continuously until the end of experiment. The increasing production rate of organic phase at 350 and 375°C is not caused by a higher conversion of LPP oil to fuel, it is rather a consequence of incomplete HDO. This indicates faster catalyst deactivation at lower temperatures. However, at 400°C the hydrocarbon product yield was constant.

Rate of HDO

As shown in **Table 1**, LPP oil contains a high amount of water. Yield, based on the LPP oil feed, was therefore low too. Referring to the carbon content of LPP oil, a carbon transfer into the hydrocarbon product phase, given in **Figure 3**, of up to 45 wt.% was obtained. The rest merged into the gas phase. Scattered carbon transfer was observed at 350°C HDO temperature. After 12 h of operation, it was only about 30 wt.% and increased to 45 wt.% after 36 h. This observation goes along with the

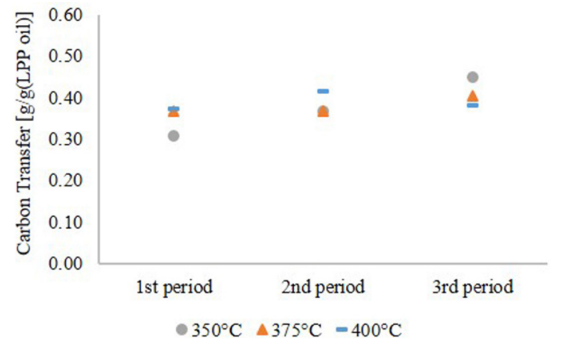

FIGURE 3 | Carbon transfer into the hydrocarbon product phase.

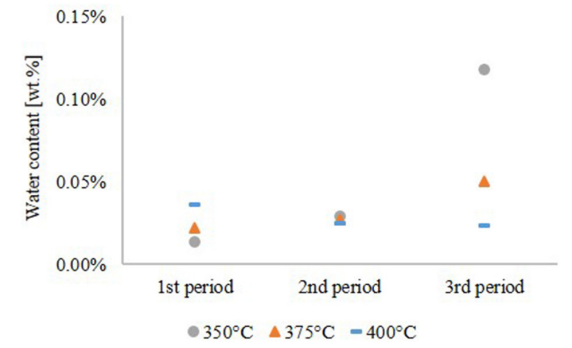

FIGURE 4 | Water content of the hydrocarbon product phase.

TABLE 4 | Oxygen content of the organic product phase (determined by balance of the ultimate analysis).

Oxygen [wt.%]	1st Period	2nd Period	3rd Period
350°C	0.00	0.00	1.11
375°C	0.00	0.00	0.00
400°C	0.00	0.00	0.00

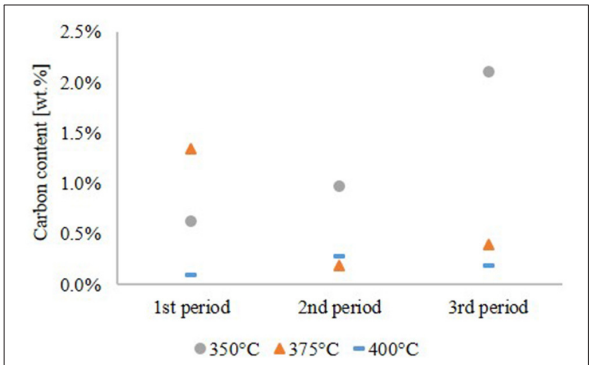

FIGURE 5 | Carbon content of the aqueous phase.

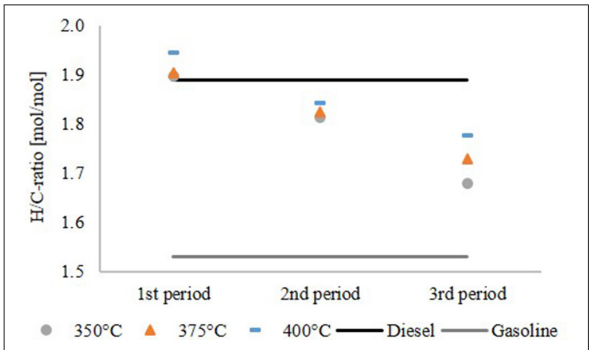

FIGURE 6 | H/C ratio of the hydrocarbon product phase.

yield of hydrocarbon products and is partly caused by a higher oxygen content. This leads to the conclusion, that more polar compounds are dissolved in the hydrocarbon product phase. Due to the lower gas yield one can also assume, that less cracking reactions occurred due to deactivation of the catalyst at low temperature. The carbon transfer increased slightly at 375°C and was nearly constant at 400°C, indicating stable catalyst performance.

The H/C ratio, is a very significant indicator for characterizing the degree of hydrogenation. In combination with the oxygen content, it quantifies the degree of HDO. The oxygen content was derived from the balance of the ultimate analysis. According to **Table 4**, the oxygen content was zero for all experiments over the whole time range except for the experiment at 350°C after 36 h of operation. It is obvious that at this temperature the activity of the catalyst depleted during the experiment. Therefore, the H/C ratio can be considered as main quality criterion for the degree of HDO for all other data points.

As shown in **Figure 4**, the water content of the hydrocarbon product phase correlates with the oxygen content. Except the experiment at 350°C, the water content of the hydrocarbon product phase was 0.02–0.05 wt.%.

The carbon content of the aqueous phase, given in **Figure 5**, is a complementary quality parameter for the HDO performance. A high carbon content of the aqueous phase correlates with a high oxygen content of the hydrocarbon product phase due to incomplete hydrophobation of LPP oil. At 350°C, the carbon content of the aqueous phase increased during the experiment with a maximum of about 2.1 wt.%. The opposite happened at 375°C, where the carbon content was highest in the first period of the experiment. At 400°C the carbon content, indicating carbon loss into the aqueous phase, was below 0.5 wt.% over the whole experiment and didn't show a trend.

The water content of the aqueous phase was between 96.9 and 99.9 wt.% in all cases, as shown in **Table 5**. This result confirms

TABLE 5 | Water content of the aqueous phase.

Water [wt.%]	1st Period	2nd Period	3rd Period
350°C	99.9	99.7	97.8
375°C	97.0	97.6	96.9
400°C	98.5	97.6	98.1

the low carbon loss into the aqueous phase and high effectiveness of HDO.

Figure 6 shows the H/C ratio of the hydrocarbon product phase compared to diesel and gasoline. For comparison, the H/C ratio of diesel with hydrotreated vegetable oil (HVO) additives and gasoline without biogenic additives were used. The H/C ratio decreased over the time span of the experiment and increased with the temperature. The highest H/C ratio was observed at 400°C in the first period of the experiment. Afterwards deactivation of the catalyst became detectable, although the H/C ratio was still in the range of diesel and gasoline. The results of the experiment at 350°C again confirmed a significant oxygen content, indicating insufficient HDO.

Product Characterization

In **Table 6**, the properties of the hydrocarbon product phase, depending on the HDO temperature, are summarized and compared to diesel and gasoline. Water content, lower heating value, density, viscosity and boiling range are between the values for diesel and gasoline, indicating that the product is a mixture of diesel and gasoline and that these fractions can be obtained by distillation. Through the high grade of HDO a high heating value of about 42.7 wt.% was achieved.

The ultimate analysis is compared with gasoline without biogenic additives and diesel with HVO additives. The lower heating value was calculated with the algorithm of Boie (Grote and Feldhusen, 2007 Equation 1).

$$LHV = 35 \cdot c + 94,3 \cdot h - 10,8 \cdot o + 10,4 \cdot s + 6,3 \cdot n - 2,44 \cdot w \quad (1)$$

with, *c, h, o, s, n* and *w* representing the amount of carbon, hydrogen, oxygen, sulfur, nitrogen and water in wt.%, respectively.

Water content, density, viscosity and boiling cut points of diesel and gasoline are derived from the standard of diesel (EN 590, 2004) and gasoline (EN 228, 2004).

By GC-MS analysis, the components in the HDO product phases were determined. The 10 most frequent components are shown in **Figure 7**. Nine of them are alkanes and cycloalkanes, only one of them is an aromatic hydrocarbon, toluene. The components amount between 6.5 and 10 wt.% Together with the high H/C ratio this implies a high grade of saturation in the organic product. In general, the amount of saturated molecules increased with the HDO temperature. This means, that HDO is more effective at higher temperature in the range of 350–400°C. Through the composition of LPP oil, one can assume a few transfer routes from the biomass constituents cellulose, hemicellulose and lignin to the final product after HDO. In LPP oil, the main components were: levoglucosan, 1-(4-hydroxy-3-methoxyphenyl)-2-propanone, 2-hydroxy-3-methyl-2-cyclopentenone, 1-hydroxy-2-butanone, 1-hydroxypropanone, acetic acid and methyl acetate. After fractionation of lignin during pyrolysis, the phenol-alcohols are possibly transformed into cyclohexanes during HDO. This might explain the presence of propyl cyclohexane, as it could be derived from 1-(4-hydroxy-3-methoxyphenyl)-2-propanone, and cyclohexane from guaiacol. Hexane can both be derived from lignin derivatives, such as 2-hydroxy-3-methyl-2-cyclopentenone or levoglucosan, or the cellulose derivative glucose. Pentane is a characteristic hemicellulose fragment, referring to the high amount of pentoses present in hemicellulose (Collard and Blin, 2014).

These suggested pathways are supplemented by many other routes, such as the fractionation from higher molecular structures and formation of C-C bonds, occurring during the pyrolysis of lignocellulosic biomass.

Gas Phase Composition

The main components of the product gas phase, given in **Figure 8**, were alkanes as methane and ethane. No oxygen or nitrogen was detected. Acetylene was measured but only detected in the first few hours of experiments as a startup effect. The rest of the gas phase was assumed to be "C_3 and higher," describing all alkanes and alkenes with 3 or more carbon atoms. Due to the high excess, the gas phase consisted to about 95 mol% of hydrogen and only to about 5 mol% of product gas. Although little differences are visible, no temperature dependency was detected. Cracking reactions start at elevated temperature and are not observable in large amounts at those process conditions.

DISCUSSION

HDO has been performed successfully in a single-step process. The water content of LPP oil could be decreased to below 0.05 wt.%. The carbon loss into the aqueous product phase was very low, with carbon contents of 0.5 wt.% at 400°C. Nine of the 10 most frequent components were alkanes and cycloalkanes, as determined by GC-MS analysis. Decreasing HDO rate at 350°C indicates deactivation of the catalyst. The carbon transfer from LPP oil into the hydrocarbon product phase was highest at 400°C. Also the H/C ratio, an indicator for the degree and effectiveness of HDO, was highest at this temperature. The decreasing H/C ratio even at 400°C indicates catalyst activation loss. This can be caused by coke formation, another potential reason might be sulfur depletion during HDO. Ongoing tests indicate a more stable operation if 1000 ppm of sulfur are added to LPP oil (Treusch et al., 2018).

Coke formation at HDO of LPP oil was very low with about 1.35 wt.% based on LPP oil and H_2 feed and didn't depend on the temperature at the conditions mentioned above. Assuming that the mass growth at the catalyst was 100 wt.% carbon, this still results in a comparable very low carbon transfer from LPP oil to coke of 7.5 wt.%, despite the high LHSV. In comparison, Kim G. et al. proposed a two-step process at an overall LHSV of 0.4 h^{-1}, obtaining 1–17 g coke per g pyrolysis oil in the first step

TABLE 6 | Hydrocarbon product characterization of the 2nd period of experiment compared to diesel and gasoline.

Compound	Unit	HDO 350°C	HDO 375°C	HDO 400°C	Diesel	Gasoline
Water content	[wt.%]	0.03	0.03	0.03	<0.02 EN 590, 2004	n.a.
Lower heating value (Boie; Grote and Feldhusen, 2007)	[MJ/kg]	42.68	42.73	42.72	43.2	41.8
Density	[kg/m^3]	829	823	805	820–845 EN 590, 2004	720-775 EN 228, 2004
Viscosity	[mPa·s]	1.56	1.45	1.07	2.0–4.5 EN 590, 2004	n.a.
Boiling at 150°C	[V.%]	32.6	31.0	20.7	n.a.	≥75 EN 228, 2004
Boiling at 350°C	[V.%]	96.6	97.2	98.5	≥85 EN 590, 2004	n.a.
Carbon transfer	[%]	36.7	36.6	41.5	–	–
Carbon content	[wt.%]	86.37	86.35	86.03	86.3	88.7
Hydrogen content	[wt.%]	13.17	13.24	13.33	13.7	11.4
Balance (oxygen content)	[wt.%]	0.00	0.00	0.00	0.0	0.0
Nitrogen content	[wt.%]	<1	<1	<1	<1	<1

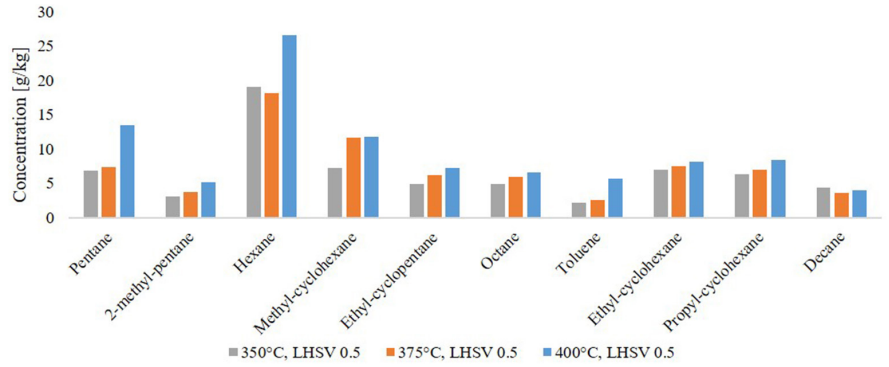

FIGURE 7 | Molecules found in the hydrocarbon product phase by GC-MS analysis.

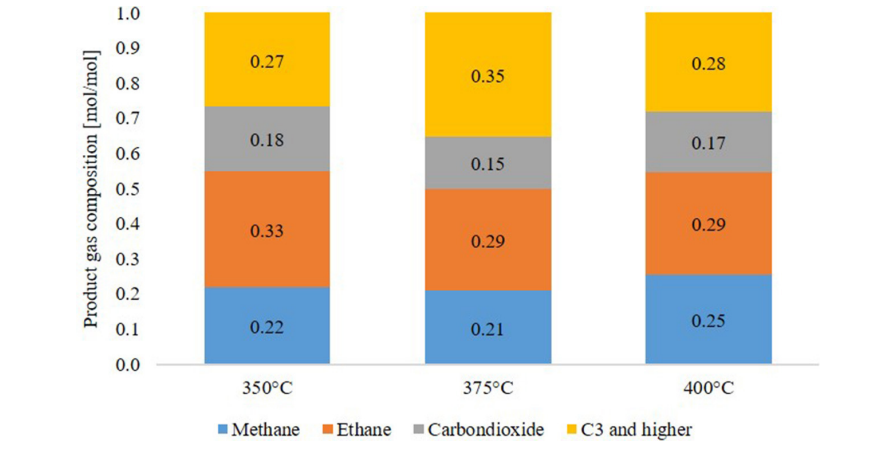

FIGURE 8 | Product gas composition after 12 h of experiment.

at 100–190°C and 1–23 g coke per g pyrolysis oil in the second step at 300–390°C (Kim G. et al., 2017). These results are most likely to be effected by the pyrolysis oil itself. Plugs are typically polymerized bio-oil and inorganic constituents (Olarte et al.,

2016). Additionally, organic condensation products of partially upgraded pyrolysis oil components lead to fouling of the catalyst, inhibiting educts to bind to the catalyst and get hydrogenated, which leads to more coking (De Miguel Mercader et al., 2011; Weber et al., 2015). Another point is coke, that is already contained in pyrolysis oil. Fast pyrolysis oils usually contain between 0.3 and 3 wt.% particles (Bridgwater and Peacocke, 2000). In LPP oil, no particles were detected as they are retained by the heat carrier oil during the liquid phase pyrolysis step. Furthermore, through the high dilution by water, heat of reaction is buffered and coke formation, caused by overheating of the catalyst surface, is lowered. At the relatively high LHSV of 0.5 h^{-1}, the temperature profile in the reactor shows a lower temperature at the top due to the high heat capacity of water. This results in a short preheating zone and might explain the low coke formation, as high heating ramps promote coking (De Miguel Mercader et al., 2011). Water is also described as stabilization agent for instable charged molecules in pyrolysis oil, reducing the activation energy of ketonisation and increasing the driving force for forming ketones, that are afterwards hydrodeoxygenated (De Miguel Mercader et al., 2011). These reactions usually occur at the front end of the reactor, where coke formation is highest (Elliott et al., 2009).

Compared to LPP oil, the water content of fast pyrolysis oils is much lower. HDO reactions are highly exothermic. Therefore, a two-step process is necessary, where the first step acts as a stabilizing step. It reduces the reactivity of functional groups such as aldehydes, ketones and double C-C bonds (Laurent et al., 1992). Routray et al. described the goal of the first, mild HDO step to be the reduction of some more active compounds like alkenes, aromatics and carbonyl groups, as they are most likely responsible for coke formation. They proposed a two-step process with mild hydrotreatment taking place at 130°C using a Ru/C catalyst and deep HDO taking place at 300–400°C using a Pt/ZrP catalyst. Both steps were performed at 140–150 bar. Although they managed to produce a hydrocarbon phase with primarily cyclic alkanes, after 55 h time on stream (TOS), more than 25 wt.% of the carbon contained in the feed pyrolysis oil was transformed into coke. Plugging by coke formation occurred in all experiments after 55–72 h TOS. (Routray et al., 2017) Elliott et al. described coking in single step processes at 340°C after 30–40 h TOS (Elliott et al., 2009). Olarte et al. observed plugging of the reactor in a single-step reference experiment using fast pyrolysis oil after 48 h TOS at a space velocity of 0.1 h^{-1} ($ml_{oil}/ml_{catalyst}$) (Olarte et al., 2016). Kim I. et al. investigated a preceding extraction step to remove particles and most likely lignin components, which are partly responsible for coking. Although experiments were performed at high liquid hourly space velocities of up to 2.3 h^{-1}, they observed rapidly decreasing product quality, beginning at about 3 h TOS, resulting in a product with 6.1 wt.% oxygen after 13.1 h TOS. Due to plugging, experiments had to be stopped after 5.7–14.2 h TOS (Kim I. et al., 2017).

The low coke formation during HDO is significant for LPP oil and distinguishes LPP oil from fast pyrolysis oils. Therefore, a two-step process is not obligatory.

AUTHOR CONTRIBUTIONS

KT was responsible for laboratory experiments, analytics, data analysis and drafted the manuscript. NS was head of this project at Graz, University of Technology, coordinated the study, was responsible for laboratory experiments and was involved in the conception of the laboratory setup. KS and RN participated in laboratory experiments, analytics and data analysis. PP was head of this project on the site of BDI—BioEnergy International GmbH and coordinated the study. MS is the director of the Institute of Chemical Engineering and Environmental Technology and helped draft the manuscript. All authors gave final approval for publication.

FUNDING

This work has been funded by the Austrian Research and Promotion Agency (FFG) under the scope of the Climate and Energy Fund. Grant number: 853577.

ACKNOWLEDGMENTS

The authors want to acknowledge Andrea Rollett, Michael Schadler, Thomas Pichler, Manuel Tandl, Anna Mauerhofer, Manuel Menapace and Dominik Heinrich for their outstanding work in our labs as well as the contribution of COST Action FP1306 in supporting interaction and collaboration.

REFERENCES

Bridgwater, A. V., and Peacocke, G. V. C. (2000). Fast pyrolysis processes for biomass. *Renew. Sustain. Energy Rev.* 4, 1–73. doi: 10.1016/S1364-0321(99)00007-6

Carpenter, D., Westover, T., Howe, D., Deutch, S., Starace, A., Emerson, R., et al. (2016). Catalytic hydroprocessing of fast pyrolysis oils: impact of biomass feedstock on process efficiency. *Biomass Bioenergy* 96, 142–151. doi: 10.1016/j.biombioe.2016.09.012

Collard, F. X., and Blin, J. (2014). A review on pyrolysis of biomass constituents: mechanisms and composition of the products obtained from the conversion of cellulose, hemicelluloses and lignin. *Renew. Sustain. Energy Rev.* 38, 594–608. doi: 10.1016/j.rser.2014.06.013

Demirbas, A. (2011). Competitive liquid biofuels from biomass. *Appl. Energy* 88, 17–28. doi: 10.1016/j.apenergy.2010.07.016

De Miguel Mercader, F., Koehorst, P. J. J., Heeres, H. J., Kersten, S. R. A., and Hogendoorn, J. A. (2011). Competition between hydrotreating and polymerization reactions during pyrolysis oil hydrodeoxygenation. *AIChE J.* 57, 3160–3170. doi: 10.1002/aic.12503

Elliott, D. C. (2007). Historical developments in hydroprocessing bio-oils. *Energy Fuels.* 21: 1792–1815. doi: 10.1021/ef070044u

Elliott, D. C., and Bager, E. C. (1989). *Process for Upgrading Biomass Pyrolyzates. 4,795,841, issued 1989.* Richland, WA.

Elliott, D. C., Hart, T. R., Neuenschwander, G. G., Rotness, L. J., and Zacher, A. H. (2009). Catalytic hydroprocessing of biomass fast pyrolysis bio-oil to

produce hydrocarbon products. *Environ. Prog Sustainable Energy* 28, 441–449. doi: 10.1002/ep.10384

EN 228 (2004). *DIN EN 228:204-03, Automotive Fuels – Unleaded Petrol – Requirements and Test Methods*. German version EN228:2004.

EN 590 (2004). *DIN EN 590:2004-03, Automotive Fuels – Diesel – Requirements and Test Methods*. German version EN 590:2004.

Grote, K. H., and Feldhusen, J. (2007). *Dubbel Taschenbuch Für Maschinenbau*. 22nd Edn. Berlin: Springer.

Kim, G., Seo, J., Choi, W. J., Jae, J., Ha, J. M., Suh, D. J., et al. (2017). Two-step continuous upgrading of sawdust pyrolysis oil to deoxygenated hydrocarbons using hydrotreating and hydrodeoxygenating catalysts. *Catal. Today* 303, 130–135. doi: 10.1016/j.cattod.2017.09.027

Kim, I., Dwiatmoko, A. A., Choi, J. W., Suh, D. J., Jae, J., Ha, J. M., et al. (2017). Upgrading of sawdust pyrolysis oil to hydrocarbon fuels using tungstate-zirconia-supported ru catalysts with less formation of cokes. *J. Industr. Eng. Chem.* 56, 74–81. doi: 10.1016/j.jiec.2017.06.013

Laurent, E., Pierret, C., Grange, P., and Delmon, B. (1992). "Control of the deoxygenation of pyrolytic oils by hydrotreatment," in *Proceedings of the 6th Conference on Biomass for Energy, Industry and Environment*. Vol. 6. (Athens: ECC).

Meyer, P. A., Snowden-Swan, L. J., Rappé, K. G., Jones, S. B., Westover, T. L., and Cafferty, K. G. (2016). Field-to-fuel performance testing of lignocellulosic feedstocks for fast pyrolysis and upgrading: techno-economic analysis and greenhouse gas life cycle analysis. *Energy Fuels* 30, 9427–9439. doi: 10.1021/acs.energyfuels.6b01643

Olarte, M. V., Padmaperuma, A. B., Ferrell, J. R., Christensen, E. D., Hallen, R. T., Lucke, R. B., et al. (2017). characterization of upgraded fast pyrolysis oak oil distillate fractions from sulfided and non-sulfided catalytic hydrotreating. *Fuel. Elsevier Ltd*. 202, 620–630. doi: 10.1016/j.fuel.2017.03.051

Olarte, M. V., Zacher, A. H., Padmaperuma, A. B., Burton, S. D., and Job, H. M., Lemmon, T. L., et al. (2016). Stabilization of softwood-derived pyrolysis oils for continuous bio-oil hydroprocessing. *Topics Catal.* 59, 55–64. doi: 10.1007/s11244-015-0505-7

Ritzberger, J., Pucher, P., and Schwaiger, N. (2014). The BioCRACK Process - a refinery integrated biomass-to-liquid concept to produce diesel from biogenic feedstock. *Chem. Eng. Trans.* 39, 1189–94. doi: 10.3303/CET1439199

Pucher, H., Schwaiger, N., Feiner, R., Ellmaier, L., Pucher, P., Chernev, B. S. et al. (2015). Biofuels from liquid phase pyrolysis oil: a two-step hydrodeoxygenation (HDO) process. *J. Green Chem.* 17, 1291–1298. doi: 10.1039/c4gc01741b

Pucher, H., Schwaiger, N., Feiner, R., Pucher, P., E.llmaier, L., and Siebenhofer, M. (2014). Catalytic hydrodeoxygenation of dehydrated liquid phase pyrolysis oil. *Energy Res.* 31:3205. doi: 10.1002/er.3205

Routray, K., Barnett, K. J., and Huber, G. W. (2017). Hydrodeoxygenation of pyrolysis oils. *Energy Technol.* 5, 80–93. doi: 10.1002/ente.201600084

Schwaiger, N., Feiner, R., Pucher, H., and Ellmaier, L. (2015). BiomassPyrolysisRefinery – Herstellung von Nachhaltigen Treibstoffen *Chemie Ingenieur Technik* 87, 1–8. doi: 10.1002/cite.201400099

Schwaiger, N., Feiner, R., Zahel, K., Pieber, A., Witek, V., Pucher, P., et al. (2011). Liquid and solid products from liquid-phase pyrolysis of softwood. *Bioenergy Res.* 4, 294–302. doi: 10.1007/s12155-011-9132-8

Schwaiger, N., Witek, V., Feiner, R., Pucher, H., Zahel, K., , Pieber, A., et al. (2012). Formation of liquid and solid products from liquid phase pyrolysis. *Bioresour. Technol.* 124. Elsevier Ltd: 90–94. doi: 10.1016/j.biortech.2012.07.115

Treusch, K., Schwaiger, N., Schlackl, K., Nagl, R., Rollett, A., Schadler, M., et al. (2018). High-throughput continuous hydrodeoxygenation of liquid phase pyrolysis oil. *Reaction Chem. Eng. R. Soc. Chem*. 3, 258–266. doi: 10.1039/C8RE00016F

Treusch, K., Ritzberger, J., Schwaiger, N., Pucher, P., and Siebenhofer, M. (2017). Diesel production from lignocellulosic feed : the bioCRACK process. *R. Soc. Open Sci.* 4:171122. doi: 10.1098/rsos.171122

Weber, R. S., Mariefel, V. O., and Huamin, W. (2015). Modeling the kinetics of deactivation of catalysts during the upgrading of bio-oil. *Energy Fuels* 29, 273–277. doi: 10.1021/ef502483t

Conflict of Interest Statement: The authors declare that the research was conducted in the absence of any commercial or financial relationships that could be construed as a potential conflict of interest.

Chapter 6

High-throughput continuous hydrodeoxygenation of liquid phase pyrolysis oil

Showcasing research from the Institute of Chemical Engineering and Environmental Technology at Graz University of Technology in Cooperation with BDI – BioEnergy International GmbH.

High-throughput continuous hydrodeoxygenation of liquid phase pyrolysis oil

Biogenous liquid phase pyrolysis oil from the bioCRACK pilot plant was hydrodeoxygenated at high liquid hourly space velocities to form a product with properties close to those of diesel and gasoline. Image reproduced by permission of BDI – BioEnergy International GmbH.

As featured in:

See N. Schwaiger *et al.*, *React. Chem. Eng.*, 2018, **3**, 258.

Reaction Chemistry & Engineering

PAPER

Cite this: *React. Chem. Eng.*, 2018, **3**, 258

High-throughput continuous hydrodeoxygenation of liquid phase pyrolysis oil

K. Treusch, [ab] N. Schwaiger,*[ab] K. Schlackl,[a] R. Nagl,[a] A. Rollett,[a] M. Schadler,[a] B. Hammerschlag,[a] J. Ausserleitner,[a] A. Huber,[a] P. Pucher[b] and M. Siebenhofer[a]

Received 31st January 2018,
Accepted 10th April 2018

DOI: 10.1039/c8re00016f

rsc.li/reaction-engineering

Hydrodeoxygenation (HDO) of liquid phase pyrolysis oil with high water content was performed continuously in a plug flow reactor on a sulfided $CoMo/Al_2O_3$ catalyst under a hydrogen pressure of 120 bar at 400 °C. The intention of this project was to achieve fuels of diesel, kerosene and gasoline quality from liquid phase pyrolysis oil (LPP oil). The liquid hourly space velocity (LHSV) was altered between 0.5 h^{-1} and 3 h^{-1}. The LHSV was higher than those reported for state-of-the-art HDO processes. The LPP oil was derived from the bioCRACK pilot plant in the OMV refinery in Vienna/Schwechat, which was operated by BDI – BioEnergy International GmbH. After HDO, separation of the upgraded hydrocarbon fraction from the aqueous carrier was achieved. About 50% of the biogenous carbon was transferred into the liquid hydrocarbon product phase, and the residual amount was transferred into the gas phase. Comparably slow catalyst aging by coke formation was attributed to the high water content of LPP oil. During HDO, a fuel of almost gasoline and diesel quality was produced. The H/C ratio was between 1.7 and 2 with a residual oxygen content of 0.0 wt% to 1.2 wt%. The boiling range of the hydrocarbon product phase was between those of gasoline and diesel. In GC-MS analysis, mainly saturated alkanes were found.

Introduction

Transport and therefore fuel demands are continuously increasing, along with increasing CO_2 emissions. According to the adoption of the Paris agreement in 2015,[1] climate change is targeted to be kept significantly below 2 °C. It is therefore of high importance to find alternative ways for the production of fuels out of biogenous feedstock. Lignocellulosic biomass plays a key role in this process because of its availability and sustainability.

Among others, such as indirect liquefaction *via* gasification[2] or hydrolysis,[3] pyrolysis is a promising technology for fuel production. During the pyrolysis of biomass, under ambient conditions liquid, solid and gaseous products are formed.[4] Liquid phase pyrolysis[5] is a basic pyrolysis technology. The liquid heat carrier provides good heat transfer, and additionally to the formation of pyrolysis oil, biochar and gas, a part of the biomass is directly dissolved in the heat carrier during pyrolysis.[6] Liquid phase pyrolysis is applied in the bioCRACK process,[7,8] a refinery integrated process, developed by BDI – Bioenergy International GmbH. The bioCRACK process uses the heat carrier vacuum gas oil (VGO), combining the cracking of VGO with the pyrolysis of biomass.

Due to its properties, pyrolysis oil is not suitable to be used as a fuel. It has a low pH value, a high water and oxygen content and therefore a low calorific value.[9] An upgrading step is necessary. This may be done by hydrodeoxygenation. Hydrogen reacts with the oxygen of pyrolysis oil to form water. For sustainable and cost-efficient application, hydrogen would be produced *via* gasification of biomass.[10–12] HDO is usually performed in batch reactors[13–18] or continuously at low liquid hourly space velocities of 0.1–0.5 h^{-1} in two steps,[19–22] a hydrotreating step for stabilization purposes and a hydrocracking step.[23] In most cases, oxygen cannot be removed completely.[24] A single step process at a LHSV of 0.35 h^{-1} was described by D. Elliott,[20] resulting in a bio-oil containing 3.6 wt% to 5.9 wt% oxygen. Low LHSV for the pyrolysis oil upgrade is a great hindrance to industrial application. Standard hydrocracking is operated at liquid hourly space velocities of up to 2.0 h^{-1}, whereas hydrotreating of gasoil can be performed at liquid hourly space velocities of up to 3.0 h^{-1}.[25] This results in the incompatibility of pyrolysis oil HDO as a co-process of petrol refinery hydrocracking and hydrotreating. To overcome this problem, single step hydrodeoxygenation of LPP oil was investigated in the liquid hourly space velocity range of 0.5 h^{-1} to 3 h^{-1}. The temperature was held constant at 400 °C. A sulfided metal oxide catalyst was used. Experiments were carried out at a hydrogen pressure of 120 bar.

An overview of state-of-the-art continuous HDO processes at various space velocities is shown in Table 1. A summary of

[a] *Institute of Chemical Engineering and Environmental Technology, Graz University of Technology, Austria. E-mail: nikolaus.schwaiger@tugraz.at*
[b] *BDI – BioEnergy International GmbH, Austria*

Table 1 State-of-the-art continuous pyrolysis oil HDO processes

Publication	Institution	Pyrolysis oil	Stage	LHSV [h^{-1}]	Catalyst	T [°C]	P [bar]	C/H/O [wt%] hydrocarbon product phase
Elliott *et al.*[23] 2009	PNNL	Fast pyrolysis oil	1	0.18–1.12 (optimum: 0.28)	Pd/C	310–375	137.9	75.5/9.4/12.3
			2	0.2	Conventional sulfide hydrocracking catalyst	405	103.4	86.6/12.9/0.4
Howe *et al.*[26] 2015	PNNL/INL/NREL	Different fast pyrolysis oils	1	~0.6[a]	Ru/C	220	107	
			2		$CoMo/Al_2O_3$	400	107	85.3–87.52/11.99–12.94/0.66–1.08
Schwaiger *et al.*[27] 2015	Graz, University of Technology/PNNL/ BDI – BioEnergy International GmbH	Liquid phase pyrolysis oil	1	0.2	$CoMo/Al_2O_3$	400	121	83.94–84.41/14.77–15.22/0.68–0.96
		Dewatered liquid phase pyrolysis oil	1	0.2	$CoMo/Al_2O_3$	400	121	85.04–85.41/13.24–13.86/1.08–1.21
Meyer *et al.*[22] 2016[d]	PNNL/INL	Fast pyrolysis oil	1	0.5	Ru-based	140–180	83	n.a.
			2	0.15	Ru-based	180–250	108	
			3		Sulfided Mo-based	350–425	108	Less than 2 wt% oxygen
Yin *et al.*[28] 2016	University of Groningen/BTG	Fast pyrolysis oil	1	0.2–0.3[b]	Ni–Cu/SiO_2–ZrO_2	60–90	200	n.a.
			2			150–200	200	
			3			410	200	3.1–15.9 wt% water
Neumann *et al.*[29] 2016	Fraunhofer UMSICHT	Catalytic pyrolysis oil	1	0.6	$NiMo/Al_2O_3$	230–370	140	86.2/13.0/<0.8
Carpenter *et al.*[21] 2016	NREL/INL/PNNL	Fast pyrolysis oil and blends	1	n.a.	Ru/C	220	107	
			2		$CoMo/Al_2O_3$	400	107	87.7/12.6/1.08
Olarte *et al.*[19] 2016	PNNL	Fast pyrolysis oil	1	0.5[c]	Sulfided Ru/C	140	84	55.3/6.2–6.3/38.1–38.2
			2	0.1[c]	Sulfided Ru/C	170	n.a.	n.a.
			3		Sulfided commercial HDO/HC	402		
G. Kim *et al.*[30] 2017	Korea University, *etc.*	Ether extracted pyrolysis oil	1	0.4	Pd/C	100–190	100	
			2		Ru/WZr	300–390	100	67.7–85.0/11.2–14.0/0.7–18.0
Olarte *et al.*[24] 2017	PNNL/NREL	Fast pyrolysis oil	1	0.5[c]	Ru/C	140	82	56.9/6.7/36.3
			2a	0.27[c]	Ru/C and Pd/C	170–405	135	81.9/12.3/5.9
			2b	0.22[c]	Sulfided Ru/C and commercial HT catalyst	170–400	123	84.9/13.3/1.8
I. Kim *et al.*[31] 2017	Korea Institute of Science and Technology/KIST School Korea, *etc.*	Ether extracted pyrolysis oil	1	0.2–2.3	Various supported noble metal catalysts	300–350	100	83.3/10.2/6.1 after 10.9–13.1 h TOS for Ru/WZr
Routray *et al.*[32] 2017	University of Massachusetts	n.a.	1	~0.15[a]	Ru/C	130	137.9	
			2		Pt/ZrP	300–400		

[a] Calculated out of flow and reactor volume. [b] Weight hourly space velocity (WHSV) [g(oil) per g(cat) h]. [c] [ml(oil) per ml(catalyst)]. [d] Techno-economic analysis.

historical HDO development of pyrolysis oils until 2007 was provided by Douglas C. Elliott.[20] In the literature, the usage of the term liquid hourly space velocity varies and may be based on the volume of the reactor or the volume of the catalyst, where it is not clearly defined whether the bulk volume or the actual volume of the catalyst is meant. Sometimes the weight hourly space velocity (WHSV) is used. In many publications, there is no space velocity given at all, but it has to be calculated out of the reactor volume and the liquid flow rate.[21,26,32] This makes a comparison based on the space velocity difficult.

Often a two-step process is applied[21,23,26,30,32] for pyrolysis oil HDO; in many cases, a 2 zone catalyst bed is applied in the second step.[19,22,24,28] As Olarte *et al.*[19] showed, single-step hydroprocessing of fast pyrolysis oil is very troublesome. They observed plugging with non-pre-treated fast pyrolysis oil after 48 h TOS at a space velocity of 0.1 h^{-1}. This was also observed by Kim *et al.*[31] who performed HDO experiments with a preceding extraction step to remove particles and most likely lignin components from pyrolysis oil. Although they managed to produce a product with a low oxygen content of 1.5 wt% for a 3 wt% Ru/WZr catalyst with a high LHSV of 2.3 h^{-1} after about 3 h TOS, they observed coke formation which led to rapidly decreasing product quality (6.1 wt% oxygen after 13.1 h TOS) and finally to plugging. Experiments at a LHSV of 2.3 h^{-1} had to be stopped after 5.7 to 14.2 h TOS.

Meyer *et al.*[22] performed a techno-economic analysis of the hydrodeoxygenation of pyrolysis oil. They mentioned the high potential of the LHSV to significantly reduce the size of HDO reactors. Doubling the LHSV of the stabilizer from 0.5 to 1 h^{-1} would reduce the minimum fuel selling price by 2%, and increasing the LHSV in the first hydrotreater from 0.15 h^{-1} to 0.5 h^{-1} would decrease the minimum fuel selling price by 4%. This shows the necessity of high liquid hourly space velocities for industrial application.

Liquid phase pyrolysis oil has been examined before at a low liquid hourly space velocity of 0.2 h^{-1}. This is the first time that LPP oil was hydrotreated at high space velocities of up to 3 h^{-1}. Higher space velocities have not been reported yet.

Experimental

The following materials, analytical methods and experimental setup were used.

Experimental setup

The experiments were performed in a plug flow reactor with an inner diameter of 3/8 inches and a heated zone of 12 inches, specified for 200 bar at 550 °C, with a maximum working pressure of 180 bar from Parr Instrument Company. The reactor was heated using a single zone external electric heater. The temperature was detected using an internal thermowell with a thermocouple with three probe points. The temperature could be controlled at four points: the three probe points of the inner thermowell and the heater. The reactor was fed from the top with gaseous and liquid reactants. The gas flow was controlled using a mass flow controller (Bronkhorst High-Tech B.V.) with a bypass valve for flushing the reactor in the start-up phase of experiments. The liquid feed was pumped through the reactor with a HPLC pump (Fink Chem + Tec GmbH). The pressure was regulated with a pressure regulating valve (Swagelok). A scheme of the whole setup is shown in Fig. 1.

Analytical methods

The ultimate analysis of all streams was performed using a vario MACRO CHN-analyzer from "Elementar Analysensysteme GmbH". The water content of the aqueous product phase was determined using a gas-phase chromatograph, Agilent 7890A, with a TCD-detector and a HP-INNOWAX column, 30 m × 0.530 mm × 1 μm. To determine the water content, the GC was calibrated with high-purity water (type I) in THF in the range of 1 wt% to 8 wt% water. The

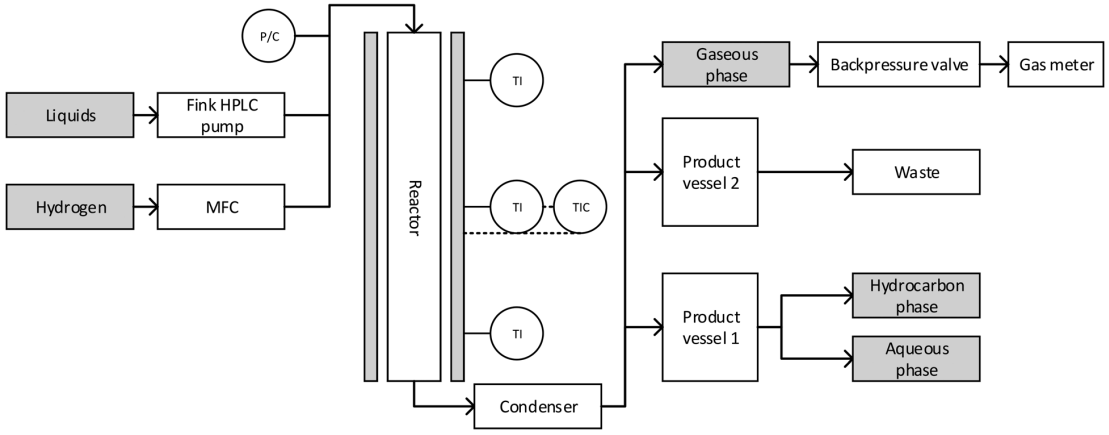

Fig. 1 Scheme of the reactor setup: liquid and gaseous input, reactor, condenser and product vessels.

boiling range of the hydrocarbon product phase was determined using a gas-phase chromatograph, Agilent 7890A, with a FID and a Restek-column MXT-2887, 10 m × 0.530 mm × 2.65 μm, according to ASTM Method D2887. The water content of the hydrocarbon product phase was determined by Karl-Fischer titration with a Schott TitroLine KF titrator and a Hydranal titration reagent. The carbon content of the aqueous phase was determined using a total organic carbon analyser, Shimadzu TOC-L. Density and viscosity were measured with a digital viscosimeter, SVM 3000, Anton Paar GmbH. The composition of the hydrocarbon product phase was determined by gas chromatography-MS with a quadrupole mass spectrometer (GC-MS), Shimadzu GCMS QP 2010 Plus, with a VF-1701 MS column, 60 m × 0.25 mm × 0.25 μm. The GC-MS was calibrated with a multi-component standard, consisting of pentane, 2-methylpentane, hexane, methylcyclohexane, ethylcyclopentane, octane, toluene, ethylcyclohexane, propylcyclohexane and decane, in the range of 100 ppmw to 3000 ppmw each.

The composition of the gas phase was analysed using a micro gas-phase chromatograph, Agilent 3000A, with a TCD, a molecular sieve column and a plot u column. Additionally, a gas sample was analysed by ASG Analytik-Service Gesellschaft mbH according to DIN 5166.

Materials

HDO was performed with a sulfided $CoMo/Al_2O_3$ catalyst, details are shown in Table 2. This catalyst was chosen, as it is cheaper than noble metal catalysts, which are mostly used (Table 1), and not susceptible for catalyst poisoning by sulphur. For sulfidation, 35 wt% di-*tert*-butyldisulfide (DTBDS) in decane was used. Hydrogen 5.0 was provided in a 300 bar gas bomb from Air Liquide Austria GmbH.

LPP oil from spruce wood pyrolysis at 375 °C was provided by the BDI – bioCRACK pilot plant. The LPP oil specification is shown in Table 3. The high water content of LPP oil is a huge advantage, as it lowers the reaction enthalpy and prohibits polymerization and coking reactions. It also allows the operation under refinery exercisable conditions.

Experimental procedure

For each experiment, the reactor was filled with the catalyst in an upside down position. The particle size in the heated zone was 200–600 μm. After installing the reactor, the whole reactor system was inerted with nitrogen and afterwards flushed with hydrogen, until reaching 120 bar. Then the reactor was filled with DTBDS in decane (35 wt%) at a flow rate of 3 ml min^{-1}, and finally the flow rate was adjusted to 0.18 ml min^{-1}. The temperature was increased with a heat ramp from 150 °C to 350 °C in 3 hours. When 400 °C was reached, the sulfidation of the catalyst started. After sulfidation, LPP oil was pumped into the reactor. HDO balance period began after 5 hours of lead time and experiments did then last 36 hours.

Table 2 $CoMo/Al_2O_3$ catalyst details

Supplier	Alfa Aesar
Cobalt oxide [wt%]	4.4
Molybdenum oxide [wt%]	11.9
Surface area [m^2 g^{-1}]	279
Stock number	45 579

Table 3 Properties of the used LPP oil

Property	Unit	LPP oil
Water content	[wt%]	57.0
Lower heating value	[MJ kg^{-1}]	7.4
Density	[kg m^{-3}]	1092
Viscosity	[mPa s]	3.5
Carbon content	[wt%]	22.3
Hydrogen content	[wt%]	9.4
Oxygen content (balance)	[wt%]	67.8
Nitrogen content	[wt%]	<1

The LHSV was varied between 0.5 h^{-1} and 3 h^{-1} with the following operating points: LHSV 0.5 h^{-1}, 1 h^{-1}, 2 h^{-1} and 3 h^{-1}. HDO experiments at LHSVs between 0.5 h^{-1} to 2 h^{-1} were performed without irregularities, while at the LHSV of 3 h^{-1} an unstable operation mode was observed, indicated by pressure irregularities. Nevertheless, the HDO process could still be performed at the LHSV of 3 h^{-1}.

Balancing

The experiment duration and mass balance period were 36 hours in steady state operation mode for LHSVs of 1 h^{-1}, 2 h^{-1} and 3 h^{-1} and 60 hours for the LHSV of 0.5 h^{-1}. Samples were taken every 12 hours. During the HDO of LPP oil, two liquid phases, a hydrocarbon and an aqueous phase, and a gas phase were formed.

The lower heating value was determined using the Boie equation:[33]

$$LHV(MJ\ kg^{-1}) = 35{\cdot}c + 94.3{\cdot}h - 10.8{\cdot}o + 10.4{\cdot}s + 6.3{\cdot}n - 2.44{\cdot}w$$

In this equation c, h, o, s, n and w represent carbon, hydrogen, oxygen, sulphur, nitrogen and water in wt%.

The oxygen content was assumed to be the difference to 100%:

$$O[wt\%] = 1 - C[wt\%] - H[wt\%] - N[wt\%]$$

Results

The impact of the LHSV on the experimental operation, product formation and product quality is discussed. In general, at higher LHSV the residence time is lowered.

Temperature profile in the reactor

The LHSV had a major impact on the temperature profile in the reactor, as shown in Fig. 2. At LHSVs of 0.5 h^{-1} and 1 h^{-1}, the temperature was adjusted to 400 °C at the middle probe

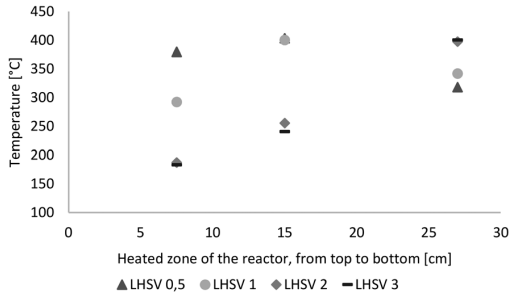

Fig. 2 Temperature profile over the length of the heated zone of the reactor (from top to bottom) dependent on the LHSV [h^{-1}].

Table 4 Mass balance of HDO dependent on LHSV based on LPP oil and H_2

LHSV	0.5 [h^{-1}]	1 [h^{-1}]	2 [h^{-1}]	3 [h^{-1}]
LPP oil [wt%]	79.6	78.3	78.8	78.3
H_2 [wt%]	20.4	21.7	21.2	21.7
Hydrocarbons [wt%]	9.6	9.4	9.7	10.0
Aqueous [wt%]	57.6	56.5	58.5	57.9
Gaseous [wt%]	28.3	29.2	29.4	29.6
Balance inaccuracy [wt%]	4.5	5.0	2.5	2.5

point of the thermowell after 15 cm of the heated zone of the reactor. At LHSVs of 2 h^{-1} and 3 h^{-1}, it wasn't possible to adjust the temperature to 400 °C at the middle probe point without exceeding 400 °C at the end of the reactor. Therefore the controlled probe point was the third one for those cases after 27 cm of the heated zone of the reactor.

Overall mass balance

The overall mass balance is shown in Table 4. Generally, there are no major differences in the mass balances between experiments with different throughputs. The yields of the hydrocarbon product phase and gaseous phase increased slightly with the throughput, whereas the amount of the aqueous phase fluctuated randomly in a small range. The balance inaccuracy was between 2.5 wt% and 5 wt%. 2.5 wt% was achieved at LHSVs of 2 h^{-1} and 3 h^{-1}.

Product characterization

The properties of the HDO product phase are very different compared with those of LPP oil. As shown in Table 5, they correlate well with those of diesel and gasoline. With increasing LHSV, the residence time decreases. This influences the chemical reaction. A lower residence time may result in an incomplete hydrodeoxygenation reaction and less cracking reactions. This is reflected in the H/C ratio and oxygen content of the product phase and the chain length of the cracked molecules. Products with a low H/C ratio and high oxygen content are less stable and have a lower heating value.

The water content of LPP oil was reduced from 57 wt% to below 0.2 wt% for all liquid hourly space velocities. According to the diesel standard, it has to be below 0.02 wt%. This was achieved by one-step HDO for the LHSV of 1 h^{-1} and almost for the LHSV of 0.5 h^{-1}. The lower heating value of all products was increased from 7.4 MJ kg^{-1} (LPP oil) to beyond 40 MJ kg^{-1}. The density of all products was between the standards for gasoline and diesel. It increased with the LHSV. This might be explained by the less cracking reaction occurring due to a lower residence time, resulting in a higher density. The viscosity was even below that of the diesel standard.

The carbon yield indicates the transfer of carbon from LPP oil into the hydrocarbon liquid phase. It was up to 50%. The carbon yield increased with the LHSV. This goes along with more impurities by oxygen-containing compounds, as the residence time was lower and HDO was not complete. In the hydrocarbon liquid phase, no oxygen could be found for LHSVs of 0.5 h^{-1} and 1 h^{-1}.

Simulated distillation

Over a wide range, the boiling ranges of the hydrocarbon product phase were between those of diesel and gasoline, as shown in Fig. 3. Generally, the difference between products at different LHSVs was small. Except at the LHSV of 0.5 h^{-1}, boiling ranges were shifted towards higher boiling points

Table 5 Composition and properties of the hydrocarbon product phases dependent on LHSV compared to diesel and gasoline

		LPP oil	HDO LHSV 0.5 [h^{-1}]	HDO LHSV 1 [h^{-1}]	HDO LHSV 2 [h^{-1}]	HDO LHSV 3 [h^{-1}]	Diesel	Gasoline
Water content	[wt%]	57.0	0.03	0.01	0.11	0.16	<0.02 (ref. 34)	n.a.
Lower heating value (Boie[33])	[MJ kg^{-1}]	7.4	43.2	43.0	41.9	41.3	43.2	41.8
Density	[kg m^{-3}]	1092	798	784	819	839	820–845 (ref. 34)	720–775 (ref. 35)
Viscosity	[mPa s]	3.5	1.0	0.9	1.3	1.6	2.0–4.5 (ref. 34)	n.a.
Carbon yield	[%]	—	43.6	44.2	47.1	49.2	—	—
H/C ratio	[—]	—	1.89	1.92	1.80	1.72	1.89	1.53
Carbon content	[wt%]	22.3	86.5	85.6	85.5	85.1	86.3[a]	88.7[a]
Hydrogen content	[wt%]	9.4	13.7	13.8	12.9	12.3	13.7[a]	11.4[a]
Balance (oxygen content)	[wt%]	67.8	0.0	0.0	1.2	0.9	0.0[a]	0.0[a]
Nitrogen content	[wt%]	<1	<1	<1	<1	<1	<1[a]	<1[a]

[a] Diesel with HVO additives and gasoline without biogenous content.

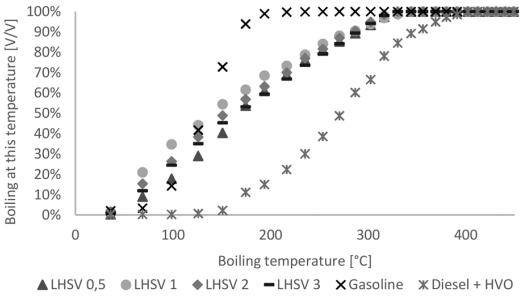

Fig. 3 Boiling range of hydrocarbon product phases compared to diesel with HVO additives and gasoline without biogenous content.

with increasing LHSV, and less cracking reactions seemed to occur.

Rate of hydrodeoxygenation

The H/C ratio is used to characterize the rate of hydrogenation and the quality of fuel, provided that the O/C ratio is zero. As Table 5 shows, the H/C ratios of all HDO products were between 1.7 and 2 and therefore in the range of those of gasoline and diesel. Altogether, the H/C ratio was quite comparable to those at LHSVs of 0.5 h^{-1} to 2 h^{-1} for the first 36 hours; at LHSV 3 h^{-1} it was a bit lower with about 1.75. The highest H/C ratio was achieved at the LHSV of 1 h^{-1}.

The properties of the aqueous phase are used to characterize the effectiveness of hydrodeoxygenation. A low carbon content and therefore low loss of carbon are desirable. The carbon content of the aqueous phase increased with the LHSV and fluctuated over the experiment duration. For the LHSV of 3 h^{-1}, the carbon content was about 1 wt% to 2 wt%, and at lower LHSVs the carbon content was below 1 wt%. In the experiment at the LHSV of 0.5 h^{-1}, no carbon was detected at all. Different to the carbon content of the aqueous phase, the oxygen content of the hydrocarbon product phase shows the effectiveness of the deoxygenation step. Again, the oxygen content increased with the LHSV and fluctuated over the experiment duration. It correlated with the carbon content of the aqueous phase. For LHSVs of 0.5 h^{-1} and 1 h^{-1}, no oxygen was detected. At LHSVs of 2 h^{-1} and 3 h^{-1}, it fluctuated between 0.5 wt% and 1.5 wt%. The components in the HDO products were determined by GC-MS analysis. From GC-MS chromatograms, a shift towards lower boiling saturated molecules was observed. According to Fig. 4, the 10 most frequent components were mainly alkanes and cycloalkanes, amounting to about 10 wt% of the product phase. About 2.5 to 5 g kg^{-1} were allotted to toluene.

GC-MS analysis also gives an insight into the reactions occurring during cracking and hydrogenation. Due to their structure, the reference molecules can be assigned to the 3 principal constituents lignin, cellulose and hemicellulose. In pyrolysis oil, the main components were: levoglucosan, 1-(4-hydroxy-3-methoxyphenyl)-2-propanone, 2-hydroxy-3-methyl-2-cyclopentenone, 1-hydroxy-2-butanone, 1-hydroxypropanone, acetic acid and methyl acetate. Cyclohexanes, such as methylcyclohexane, ethylcyclohexane and propylcyclohexane, are most likely to be derived from lignin derivatives, fractionated from the phenols–alcohols of lignin. Hexane can either be a hydrogenated lignin (phenols) or cellulose (glucose) derivative. pentane is a characteristic hemicellulose fragment, referring to the high amount of pentoses present in hemicellulose. 1-(4-Hydroxy-3-methoxyphenyl)-2-propanone might be the precursor for propyl cyclohexane, and guaiacol for cyclohexane. 2-Hydroxy-3-methyl-2-cyclopentenone and levoglucosan may seemingly convert to hexane. Alkanes of molar mass less than that of pentane were transferred into the gas phase (Fig. 5 and 6). Methane, ethane and carbon dioxide from decarboxylation reactions were

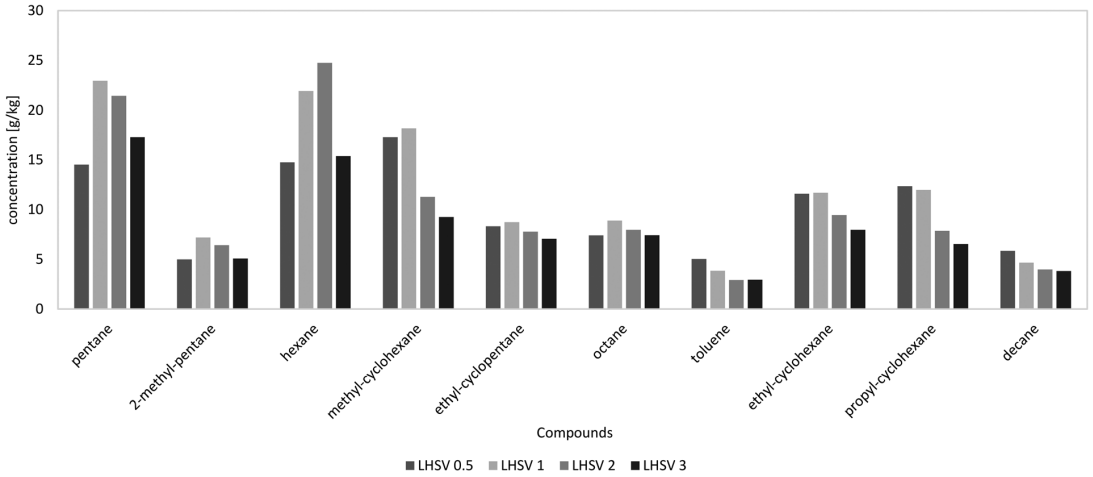

Fig. 4 10 most frequent components in the hydrocarbon product phases dependent on LHSV [h^{-1}] after 36 hours of experiment according to GC-MS analysis.

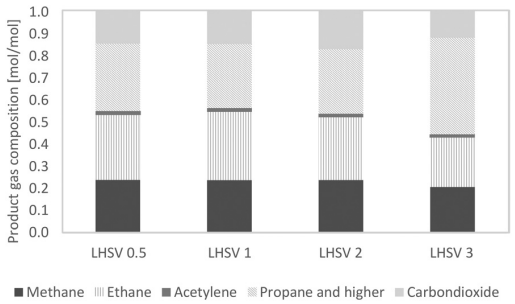

Fig. 5 Composition of gaseous products dependent on LHSV [h^{-1}] after 36 h of experiment.

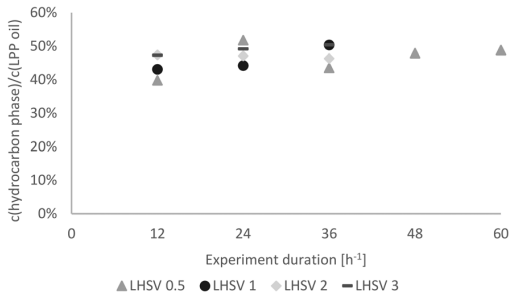

Fig. 7 Carbon yield in the hydrocarbon product phase over the experiment duration dependent on the LHSV [h^{-1}].

partly generated by HDO of methyl acetate and acetic acid. 1-Hydroxypropanone and 1-hydroxy-2-butanone are likely to be converted into propane and butane, respectively.[36–38]

Despite these transfer routes, the fragments can be derived from higher molecular structures in wood, fractionated by cracking reactions during liquid phase pyrolysis. This also leads to the formation of C–C bonds during pyrolysis and molecules larger than the basic molecules present in wood.

Gas phase analysis

The gaseous products mainly contained the alkanes methane ethane, and higher alkanes. A small amount of acetylene was detected, and after 36 hours of experiment, the acetylene amount was close to zero. Up to 20% of the gas phase consisted of carbon dioxide, caused by decarboxylation reactions. Between LHSVs of 0.5 h^{-1} and 2 h^{-1}, there is evidence of a trend towards less alkanes and more carbon dioxide, and at the LHSV of 3 h^{-1} less low-molecular mass alkanes (methane and ethane) and more alkanes, higher than ethane, were present. This indicates less cracking reactions.

Due to the high excess of hydrogen, the gaseous phase was composed of about 95% hydrogen and 5% product gas. Through external analysis by ASG Analytik-Service GmbH, alkanes higher than ethane could be detected. These were mainly propane and *n*-butane, but the amount of each was much less than that of the smaller alkanes, as shown in Fig. 6. It was therefore assumed that the undefined residues of the gas phase are from the alkane fraction of propane and higher alkanes. The results of the two measurement modes didn't differ. The produced gas can be fed into cracking furnaces in petroleum refineries for the production of ethylene, *e.g.* with the PyroCrack®[39] technology by Selas-Linde AG.

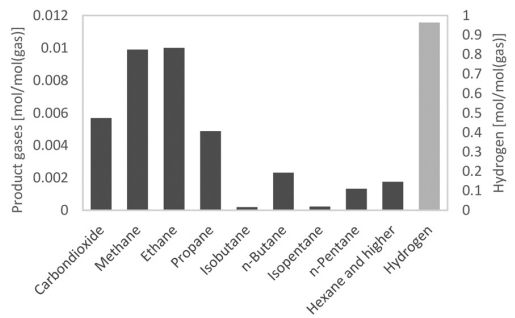

Fig. 6 Gas analysis according to DIN 5166, for the experiment at the LHSV of 0.5 h^{-1}.

Product properties depending on catalyst stability over time

As already mentioned, the experiments were subdivided into 3 periods of 12 h for LHSVs of 1 h^{-1}, 2 h^{-1} and 3 h^{-1} and 5 periods of 12 h for the LHSV of 0.5 h^{-1}, as the sampling interval was 12 hours. Hence, trends over the experiment duration could be observed.

In Fig. 7, the carbon yield over the experiment duration is shown. At the LHSV of 0.5 h^{-1}, the carbon yield fluctuated slightly, whereas it increased at the LHSV of 1 h^{-1} and seemed to reach a plateau at LHSVs of 2 h^{-1} and 3 h^{-1} after 24 hours of experiment. This indicates a stable operation state.

The same trend was observed concerning density (Fig. 8). While it increased at LHSVs of 0.5 h^{-1} and 1 h^{-1}, a kind of plateau state was reached at higher LHSVs after 24 hours of experiment. Overall, the density was between the density of the gasoline and diesel standards.

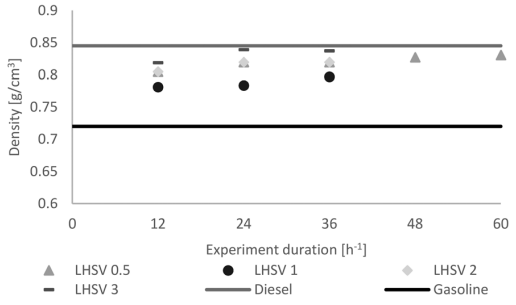

Fig. 8 Distribution of the density of the hydrocarbon product phase dependent on the LHSV [h^{-1}] compared to the minimum of gasoline and the maximum of diesel, according to EN228 (ref. 35) and EN590.[34]

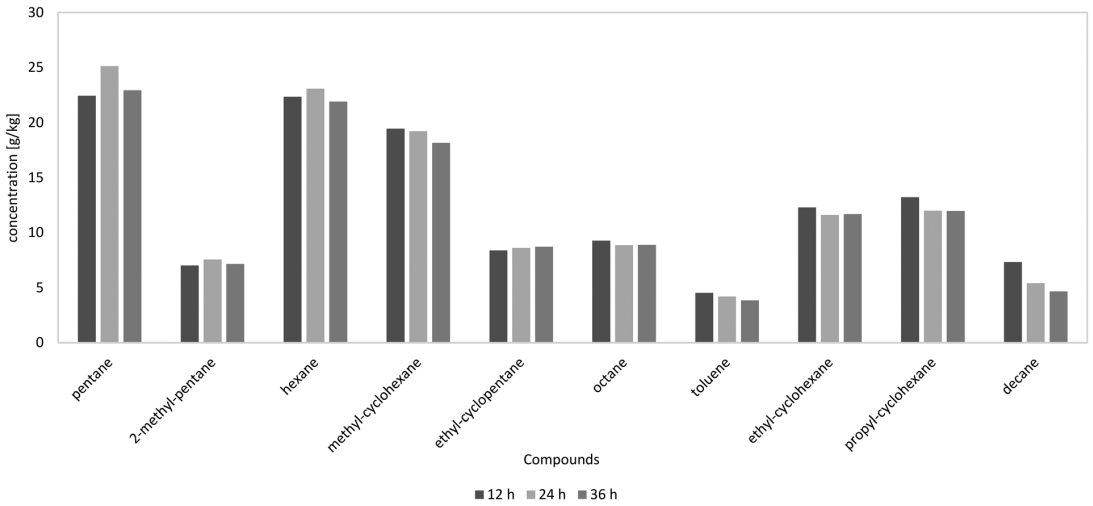

Fig. 9 10 most frequent components in the HDO products depending on the experiment duration at the LHSV of 1 h^{-1}, according to GC-MS analysis.

In Fig. 9, the components of the product phase over the experiment duration at the LHSV of 1 h^{-1} are shown. It can be seen that the experiment duration had no influence on product distribution. A similar product distribution over time led to the conclusion that catalyst deactivation was negligible in the observed time span. A very stable operation mode was achieved.

The slow catalyst aging, only detectable as start-up effects at low liquid hourly space velocities, may be described by the LPP oil itself. In comparison with fast pyrolysis oils, usually used for hydrodeoxygenation processes,[19–24,28,40] LPP oil has a very high water content, as many non-polar components were already extracted by VGO during the LPP step. As HDO is highly exothermic, the water may buffer the heat of reaction and inhibit catalyst overheating. Oh *et al.* investigated mild HDO of fast pyrolysis oil from *Miscanthus sinensis* with ethanol as a solvent in a stirred tank reactor at 250 °C to 350 °C. In experiments without ethanol, they observed a one phase product with a tar-like deposit on the catalyst. In experiments with ethanol, it served as a co-reactant, converting the acid in bio-oil into esters and enhancing acidity and stability.[41] Feng *et al.* investigated the influence of different solvents such as water, alcohols, acetone, ethyl acetate, and tetrahydrofuran and hexane as a hydrocarbon representative on the hydrodeoxygenation of phenol. One interesting result was the high conversion of phenol into cyclohexanol of even 100% at 250 °C in water or hexane. They assumed a few positive effects of water on the HDO. Water may affect the absorption of phenol on the catalyst surface. Phenol itself is soluble in water, but the intermediate product cyclohexanone is not, so it cannot be easily dissolved in the solvent but is further hydrogenated to cyclohexanol, which is finally soluble in water. They also suggest that the binding energy between phenol and the metal surface is decreased due to the formation of hydrogen bonds between phenol and water.[42] After the reaction to cyclohexanol, dissorption may occur. From these results, one can assume that coke formation is supressed in high water diluted HDO reaction systems, which leads to the fact that higher liquid hourly space velocities are feasible process parameters for LPP oil HDO.

Summary

HDO of LPP oil was operated continuously on a lab scale with liquid hourly space velocities of up to 3 h^{-1}. The carbon yield was up to 50%. The rate of HDO was the highest at LHSVs of 0.5 h^{-1} and 1 h^{-1}, resulting in an oxygen content of 0.0 wt% and a high H/C ratio close to 2. Diesel and gasoline qualities were achieved. All products correspond in terms of quality to a mixture of gasoline and diesel, concerning the density, which is between 720 kg m^{-3} (lower limit of gasoline) and 845 kg m^{-3} (upper limit of diesel), and boiling ranges. The hydrocarbon liquid products have high lower heating values of 41 MJ kg^{-1} to 43 MJ kg^{-1}. At LHSVs of 2 h^{-1} and 3 h^{-1}, a plateau of the H/C ratio was reached after 24 h of experiment. A steady state operation mode was achieved specifically at higher liquid hourly space velocities than reported in state-of-the-art HDO processes quoted in Table 1. At the LHSV of 3 h^{-1}, unstable operation was observed, indicated by pressure irregularities. The higher the LHSV, the less cracking reactions occur, resulting in "long-chain" alkanes in the gas phase and higher boiling ranges. The GC-MS analysis showed a stable product yield which is dependent on the LHSV. Catalyst deactivation was very low, visible in almost constant product properties and composition. Thus, a positive influence of water in LPP oil on the coke deposition was stated.

Conflicts of interest

There are no conflicts to declare.

Acknowledgements

This work was funded by the Austrian Research Promotion Agency (FFG) under the scope of the Austrian Climate and Energy Fund. We want to acknowledge Thomas Pichler, Manuel Tandl, Anna Mauerhofer, Manuel Menapace, Dominik Heinrich, Elisabeth Dirninger, Thomas Sterniczky and Martin Dalvai Ragnoli for their outstanding work in our labs.

Notes and references

1 UNFCCC, *Adoption of the Paris Agreement: Proposal by the President to the United Nations Framwork Convention on Climate Change*, 2015, 21932, pp. 1–32.
2 P. L. Spath and D. C. Dayton, *Preliminary Screening – Technical and Economic Assessment of Synthesis Gas to Fuels and Chemicals with Emphasis on the Potential for Biomass-Derived Syngas*, Natl. Renew. Energy Lab., 2003, pp. 1–160.
3 S. Brethauer and C. E. Wyman, *Bioresour. Technol.*, 2010, **101**, 4862–4874.
4 M. Kaltschmitt and W. Streicher, *Energie aus Biomasse*, 2009.
5 N. Schwaiger, V. Witek, R. Feiner, H. Pucher, K. Zahel, A. Pieber, P. Pucher, E. Ahn, B. Chernev, H. Schroettner, P. Wilhelm and M. Siebenhofer, *Bioresour. Technol.*, 2012, **124**, 90–94.
6 N. Schwaiger, R. Feiner, K. Zahel, A. Pieber, V. Witek, P. Pucher, E. Ahn, P. Wilhelm, B. Chernev, H. Schröttner and M. Siebenhofer, *BioEnergy Res.*, 2011, **4**, 294–302.
7 K. Treusch, J. Ritzberger, N. Schwaiger, P. Pucher and M. Siebenhofer, *R. Soc. Open Sci.*, 2017, **4**(11), DOI: 10.1098/rsos.171122.
8 J. Ritzberger, P. Pucher and N. Schwaiger, *Chem. Eng. Trans.*, 2014, **39**, 1189–1194.
9 Q. Zhang, J. Chang, T. Wang and Y. Xu, *Energy Convers. Manage.*, 2007, **48**, 87–92.
10 S. Müller, M. Stidl, T. Pröll, R. Rauch and H. Hofbauer, *Biomass Convers. Biorefin.*, 2011, 55–61.
11 R. Toonssen, N. Woudstra and A. H. M. Verkooijen, *Int. J. Hydrogen Energy*, 2008, **33**(15), 4074–4082.
12 Y. Kalinci, A. Hepbasli and I. Dincer, *Int. J. Hydrogen Energy*, 2012, **37**(19), 14026–14039.
13 S. Oh, H. S. Choi, I.-G. Choi and J. W. Choi, *RSC Adv.*, 2017, **7**, 15116–15126.
14 S. Cheng, L. Wei, J. Julson, K. Muthukumarappan, P. R. Kharel and E. Boakye, *Fuel Process. Technol.*, 2017, **162**, 78–86.
15 F. De Miguel Mercader, P. J. J. Koehorst, H. J. Heeres, S. R. A. Kersten and J. A. Hogendoorn, *AIChE J.*, 2011, **57**, 3160–3170.
16 C. Boscagli, C. Yang, A. Welle, W. Wang, S. Behrens, K. Raffelt and J. D. Grunwaldt, *Appl. Catal., A*, 2017, **544**, 161–172.
17 C. Boscagli, K. Raffelt and J. D. Grunwaldt, *Biomass Bioenergy*, 2017, **106**, 63–73.
18 S. Cheng, L. Wei, J. Julson and M. Rabnawaz, *Energy Convers. Manage.*, 2017, **150**, 331–342.
19 M. V. Olarte, A. H. Zacher, A. B. Padmaperuma, S. D. Burton, H. M. Job, T. L. Lemmon, M. S. Swita, L. J. Rotness, G. N. Neuenschwander, J. G. Frye and D. C. Elliott, *Top. Catal.*, 2016, **59**, 55–64.
20 D. C. Elliott, *Energy Fuels*, 2007, **21**, 1792–1815.
21 D. Carpenter, T. Westover, D. Howe, S. Deutch, A. Starace, R. Emerson, S. Hernandez, D. Santosa, C. Lukins and I. Kutnyakov, *Biomass Bioenergy*, 2016, **96**, 142–151.
22 P. A. Meyer, L. J. Snowden-Swan, K. G. Rappé, S. B. Jones, T. L. Westover and K. G. Cafferty, *Energy Fuels*, 2016, **30**, 9427–9439.
23 D. C. Elliott, T. R. Hart, G. G. Neuenschwander, L. J. Rotness and A. H. Zacher, *Environ. Prog. Sustainable Energy*, 2009, **28**, 441–449.
24 M. V. Olarte, A. B. Padmaperuma, J. R. Ferrell, E. D. Christensen, R. T. Hallen, R. B. Lucke, S. D. Burton, T. L. Lemmon, M. S. Swita, G. Fioroni, D. C. Elliott and C. Drennan, *Fuel*, 2017, 620–630.
25 M. A. Fahim, T. A. Alsahhaf and A. Elkilani, in *Fundamentals of Petroleum Refining*, 2010, pp. 153–198.
26 D. Howe, T. Westover, D. Carpenter, D. Santosa, R. Emerson, S. Deutch, A. Starace, I. Kutnyakov and C. Lukins, *Energy Fuels*, 2015, **29**, 3188–3197.
27 N. Schwaiger, D. C. Elliott, J. Ritzberger, H. Wang, P. Pucher and M. Siebenhofer, *Green Chem.*, 2015, **17**, 2487–2494.
28 W. Yin, A. Kloekhorst, R. H. Venderbosch, M. V. Bykova, S. A. Khromova, V. A. Yakovlev and H. J. Heeres, *Catal. Sci. Technol.*, 2016, **6**, 5899–5915.
29 J. Neumann, N. Jäger, A. Apfelbacher, R. Daschner, S. Binder and A. Hornung, *Biomass Bioenergy*, 2016, **89**, 91–97.
30 G. Kim, J. Seo, J. W. Choi, J. Jae, J. M. Ha, D. J. Suh, K. Y. Lee, J. K. Jeon and J. K. Kim, *Catal. Today*, 2017, 0–1.
31 I. Kim, A. A. Dwiatmoko, J. W. Choi, D. J. Suh, J. Jae, J. M. Ha and J. K. Kim, *J. Ind. Eng. Chem.*, 2017, **56**, 74–81.
32 K. Routray, K. J. Barnett and G. W. Huber, *Energy Technol.*, 2017, **5**, 80–93.
33 K.-H. Grote and J. Feldhusen, *Dubbel Taschenbuch für Maschinenbau*, Springer, 22nd edn, 2007.
34 *EN590*, 2004.
35 *EN228*, 2004.
36 F. X. Collard and J. Blin, *Renewable Sustainable Energy Rev.*, 2014, **38**, 594–608.
37 T. Lin, E. Goos and U. Riedel, *Fuel Process. Technol.*, 2013, **115**, 246–253.
38 Y. Le, L. Jia, S. Cissé, G. Mauviel, N. Brosse and A. Dufour, *J. Anal. Appl. Pyrolysis*, 2016, **117**, 334–346.
39 http://www.linde-engineering.com/en/process_plants/furnaces_fired_heaters_incinerators_and_t-thermal/cracking_furnaces_for_ethylene_production/index.html, 2017.
40 D. C. Elliott and E. G. Baker, Process for upgrading Biomass pyrolyzates, *U.S. Pat.*, 4795841, 1989, p. 7.
41 S. Oh, H. Hwang, H. S. Choi and J. W. Choi, *Fuel*, 2015, **153**, 535–543.
42 G. Feng, Z. Liu, P. Chen and H. Lou, *RSC Adv.*, 2014, **4**, 49924–49929.

Chapter 7

Refinery integration of lignocellulose for automotive fuel production

Refinery integration of lignocellulose for automotive fuel production

Klara Treusch[a,b], Nikolaus Schwaiger[b], Anna Huber[b], Samir Reiter[b], Mario Lukasch[b], Berndt Hammerschlag[b], Julia Außerleitner[b], Peter Pucher[a], Matthäus Siebenhofer[b]

[a]*BDI-BioEnergy International GmbH*
[b]*Institute of Chemical Engineering and Environmental Technology, Graz University of Technology*

ABSTRACT: This paper contributes to the integration of pyrolysis oil in standard refinery hydrotreating units for biogenous fuel production by co-processing. A two-step hydrodeoxygenation (HDO) process was performed at 80 and 120 bar hydrogen pressure. Liquid phase pyrolysis (LPP) oil was hydrodeoxygenated in a first step between 250 and 350°C. An optimum between sufficient hydrophobation and high carbon yield in the product phase was determined at 300°C. Co-processing was performed at 400°C with 10 wt% of the mildly hydrotreated LPP oil in heavy gas oil (HGO). During the co-processing step, a stable operation mode and constant product quality without pressure dependency in the range of 80 to 120 bar was observed. The experimental operability as well as the product quality and carbon yield was the same as with reference experiments without admixture of pre-treated LPP oil. The products contained no residual oxygen and showed a high H/C ratio, equal to that of HGO.

1. Introduction

To cover the increasing energy demand in transportation, various concepts have been developed. They are divided in techniques for the production of fuels or substitute fuels, applicable in conventional combustion engines and completely new approaches like electric engines [1], fuel cells [2] or hydrogen combustion engines [3]. When talking about electricity as an energy carrier, one has to consider the source of electricity. In 2016, only one quarter of the electricity in the European Union was generated from renewable resources, the rest was produced from fossil fuels and nuclear power plants [4]. Especially in freight and air transport, conventional combustion engines are not expected to be replaceable in the near future. This led to the development of fuels and substitute fuels out of biogenous feedstock through indirect liquefaction via gasification and Fischer-Tropsch-Synthesis [5], biotechnological biomass fermentation [6] or direct liquefaction concepts like pyrolysis and subsequent upgrading of pyrolysis oil [7]. A well-known approach for upgrading pyrolysis oil is hydrodeoxygenation (HDO). HDO has mostly been reported for fast pyrolysis oil [8]–[13]. Additionally, HDO of catalytic pyrolysis oil [14] and ether extracted pyrolysis oil [15], [16] have been researched.

1.1 Liquid phase pyrolysis

In liquid phase pyrolysis (LPP) [17], biomass is pyrolysed in a liquid heat carrier oil to assure a good heat transfer. Through the contact of biomass with the heat carrier oil, non-polar biomass fragments are not transferred into pyrolysis oil, but directly into the non-polar heat carrier oil. This leads to an accumulation of biogenous compounds in the heat carrier oil that can further

be upgraded in existing refinery plants. LPP is applied in the bioCRACK process [18], [19]. From 2012 to 2014, a pilot plant was operated in the OMV refinery in Schwechat/ Vienna by BDI-BioEnergy International GmbH. In the pilot plant, vacuum gas oil (VGO) was used as heat carrier oil. As an advantageous effect, LPP also led to the cracking of VGO in this step. The bioCRACK process was operated at mild conditions below 400°C and atmospheric pressure. LPP and subsequent product upgrading is part of the BiomassPyrolysisRefinery concept [20]. In the pilot plant, up to 40 wt% of the biogenous carbon were directly transferred into hydrocarbon fractions of VGO, 30 to 50 wt% were left in the residual biochar and about 20 to 26 wt% were found in the LPP oil fraction [19]. VGO fractions were upgraded in existing refinery units. To obtain more products with fuel quality, biochar liquefaction and LPP oil hydrodeoxygenation have been investigated. Biochar liquefaction was performed discontinuously by Feiner et al. [21]–[23], using tetralin as a hydrogen donor, achieving high oil yields of up to 72 wt%. Based on the work of Pucher et al. [24], [25], who focused on the discontinuous HDO of LPP oil, LPP oil has been hydrodeoxygenated continuously in lab scale. Continuous single step HDO of LPP oil has already been performed successfully in the temperature range between 350 and 400°C [26] and at liquid hourly space velocities (LHSV) of 0.5 h^{-1} to 3 h^{-1} [27]. As for a sustainable biofuel production also hydrogen has to be of biogenous origin, HDO of LPP oil with biogenous hydrogen rich synthesis gas from TU Wien has been investigated, combining direct and indirect biomass liquefaction [28]. The bioCRACK pilot plant was fully integrated in a petroleum refinery. For integration of the whole process as a cost efficient advanced biofuel production approach, upgrading of LPP oil, as shown in this paper, was performed together with refinery intermediates.

1.2 Continuous co-processing of pyrolysis oil and petroleum refinery intermediates

Different attempts for introducing pyrolysis oil into common petroleum refinery units via co-processing with petroleum refinery streams have been researched. Reason for that is a cost efficient possibility for pyrolysis oil upgrading. An overview of published research about co-processing is shown in Table 1. Fast pyrolysis oil is mostly undertaken an upgrading procedure including pre-treatment such as water or organic solvent addition and HDO in one or more steps prior to co-processing [29]–[38], direct co-feed of pyrolysis oil is rather unusual [29], [31], [39]–[42]. Catalytic pyrolysis oil is directly co-processed with fossil feeds. Only small differences between the operation with catalytic and hydrotreated fast pyrolysis oil have been observed. Co-processing of pyrolysis oil with refinery streams is almost exclusively performed in FCC units [29]–[33], [35]–[43], usually in lab scale. Few research groups reported about co-processing of model compounds in a hydrodesulphurisation (HDS)/ HDO unit [44]–[46]. Co-processing of real pyrolysis oil in HDS/ HDO units has so far only been reported by de Miguel Mercader et al. [34]. Prior to co-processing, fast pyrolysis oil was pre-treated intensively by adding 2 wt.% of isopropanol for separation of a top layer, which accounted for 10.6 wt% of the pyrolysis oil and contained a large number of extractives. This layer was rejected. Then water in the proportion of 1:2 was added to the bottom layer to achieve phase separation. The oil fraction contained 32 wt%, the aqueous fraction contained 69 wt% of the organics. The two obtained fractions were then hydrotreated at different temperatures in the range of 220 to 310°C at 190 bar with 5 wt.%

of a Ru/Cu catalyst in an autoclave reactor. The hydrodeoxygenated fractions contained 13.6 to 24.0 wt% residual oxygen, the overall carbon yield from extracted pyrolysis oil into the hydrocarbon phases of the hydrodeoxygenated oil and aqueous fractions was between 42 and 59 wt%.

Table 1: Published research of co-processing pyrolysis oil in crude oil refinery units

Publication	Biogenous feed	Co-feed	Refinery unit	Reactor type
Stefanidis et al.[29] 2018 (Review article)	FPO, CPO, HDO	VGO	Different units	Different reactor types
Gueudré et al. [30] 2017	HDO (10 wt%)	VGO	FCC	MAT unit
Pinho et al. [39] 2017	FPO (10 wt%)	VGO	FCC	Demonstration scale FCC unit
Ibarra et al. [40] 2016	FPO, CPO (20 wt%)	VGO	FCC	Riser simulator reactor
Lindfors et al. [31] 2015	Dry FPO, CPO, HDO	VGO	FCC	MAT unit
Pinho et al. [41] 2015	FPO	VGO	FCC	Demonstration scale FCC unit
Gueudré et al. [32] 2015	HDO, CPO	VGO	FCC	MAT unit
Thegarid et al. [33] 2014	HDO, CPO	VGO	FCC	Fixed bed reactor
Schuurman et al. [42] 2014	FPO, CPO	VGO	FCC	Fixed bed reactor
Sepúlveda et al. [44] 2012	Guaiacol	4,6-dimethyldi-benzothiophene	Combined HDO and HDS	Stirred slurry tank reactor
De Miguel Mercader et al. [34] 2011	HDO	SRGO	HDS	Trickle bed reactor
		Long residue fossil feed	FCC	MAT unit
Fogassy et al. [35] 2010	HDO (20 wt%)	VGO	FCC	Fixed bed reactor
De Miguel Mercader et al. [36] 2010	HDO	Long residue fossil feed	FCC	MAT unit
Pinheiro et al. [45] 2009	2-propanol, cyclopentanone, anisole, guaiacol, propanoic acid, ethyldecanoate	SRGO	HDO+HDS	Down flow pilot scale fixed bed reactor system
Lappas et al. [37] 2009	HDO	VGO	FCC	Small scale pilot plant
Bui et al. [46] 2009	Guaiacol	SRGO	HDS	Trickle bed reactor
Corma et al. [43] 2007	Glycerol, sorbitol with water (1/1)	VGO	FCC	MAT unit
Samolada et al. [38] 1998	HDO	LCO	FCC	Fixed bed reactor

FPO = fast pyrolysis oil
CPO = catalytic pyrolysis oil
HDO = hydrodeoxygenated fast pyrolysis oil
MAT unit = micro activity test unit
SRGO = straight run gas oil
LCO = light cycle oil

Each obtained oil fraction was afterwards diluted with isopropanol, as the viscosity was otherwise too high, and co-processed via HDS. Co-processing was performed together with straight run gas oil (SRGO) at 380°C using a sulphided CoMo catalyst in a trickle bed reactor. During co-processing, no plugging but decreasing desulphurisation was observed. The products had a similar molecular weight distribution to the processed pure SRGO but contained phenolic components. There is no information given on the duration of experiments or product composition. The intention of the research of de Miguel Mercader et al. was to provide a better understanding of pyrolysis oil HDO and possible application of HDS co-processing. It is therefore, due to its complexity, high pressure and batch scale operation of HDO, far away of economic application.

1.3 Co-processing of pyrolysis oil in a FCC

The biggest obstacles when co-processing pyrolysis oil in FCC units are higher coke formation [31], [32], [35], residual oxygen [36], [39], [41] and higher aromatic outcome [35], [43] compared to processing fossil feed only [32], [39], [41], especially if pyrolysis oil is not pre-treated [31] or pre-treated under less severe hydrotreatment conditions [30]. It is clearly stated that direct co-processing without any of the described pre-treatment methods is not advisable. Guedré et al [32] investigated the influence of pyrolysis oil on coke formation during the co-processing with VGO in a lab-scale Micro Activity Test (MAT) type reactor to simulate a FCC unit. It can be seen clearly, that oxygen contained in pyrolysis oil has a high influence on coke formation. Not only the coke from pyrolysis oil itself was increased, but the oxygen also lead to coking of VGO. Pinho et al. [39], [41] indicated, that at larger scale less coking reactions and higher carbon yields of about 30 wt% can be achieved. They suggested injecting pyrolysis oil in the riser at different heights of the reactor. Many research groups suggest further catalyst development to reduce coking reactions. Although this factor has to be taken into account, the conditions of the recent work have to be differed from the results obtained in the FCC. High hydrogen access should suppress coking reactions to a minimum. For an economic and sustainable application, the usage of synthesis gas for pre-treatment of LPP oil is a promising alternative [28]. Not only pure hydrogen from the gas feed has to be considered, but also the higher hydrogen donation capacity of HGO, as de Miguel Mercader et al. [34] observed with straight run gas oil. During hydrotreatment, the synergic effect of HDO and HDS can be used, as crude oils usually contain high amounts of sulphur, which is often needed for catalyst sulphidation to increase the catalyst activity for HDO. It is not clear whether HDO reactions inhibit [44], [45] HDS reactions or not [46].

The results from processing pyrolysis oil in FCC units clearly show that co-processing is possible, but goes along with higher coke yields due to a hydrogen gap, especially when using VGO and not a highly hydrogenated fuel fraction as in the case of this paper. This again leads to high regeneration temperatures and overheating of the catalyst [32]. All these results lead to the conclusion, that co-processing of pyrolysis oil with refinery intermediates in refinery units without added hydrogen will always lead to uncontrolled coke deposition. Therefore, co-processing will only succeed with hydrogen-supplemented technologies.

2. Experimental

2.1 Analytical methods

The ultimate analysis of all streams was performed by a vario MACRO CHN-analyser from "Elementar Analysensysteme GmbH". The water content of the aqueous product phase was determined by a gas-phase chromatograph, type Agilent 7890A, with a TCD-detector and a HP-INNOWAX column, 30m*0.530mm*1μm. For determining the water content, the GC was calibrated with high-purity water (type I) in THF in the range of 1 wt% to 8 wt% water. The boiling range of the hydrocarbon product phase was determined by a gas-phase chromatograph, type Agilent 7890A, with a FID-detector and a Restek-column MXT-2887, 10m*0.53mm*2.65μm, according to ASTM Method D2887. The water content of the oil fraction was determined by Karl-Fischer-titration with a Schott Titro Line KF-Titrator and a Hydranal titration reagent. Density and viscosity were measured by a digital viscosimeter, SVM 3000, Anton Paar GmbH. The composition of the hydrocarbon product phase was determined by gas chromatography-MS with a quadrupole mass spectrometer (GC-MS), type Schimadzu GCMS QP 2010 Plus, with a VF-1701 MS column, 60m*0,25mm*0,25μm. For balancing, the composition of the gas phase was analysed by a micro gas-phase chromatograph, type Agilent 3000A, with a TCD-detector, a molecular sieve column and a plot u column.

Sulphur content, micro carbon residue, H-NMR, metal screening and surface area of catalysts were determined externally by the "Centralni ispitni laboratorij" of INA industrija nafte d.d. Sulphur content was determined according to ASTM D 2622:2016, micro carbon residue according to HRN EN ISO 10370:2014, catalyst surface area according to ASTM D 3663 modified: 2015 and metal screening was performed as a semi-quantitative analysis by wave dispersive X-Ray. The biogenous carbon content was determined by Beta Analytic Inc. via accelerator mass spectrometry according to ISO/IEC 17025:2005.

2.2 Materials

LPP oil was derived from the bioCRACK pilot plant in the OMV refinery in Schwechat/ Vienna in 2014 during LPP of spruce wood at 375°C.

Table 2: Composition and properties of the used LPP oil from the bioCRACK pilot plant

Property	Unit	LPP Oil
Water content	[wt%]	58.9
Lower heating value	[MJ/kg]	6.6
Density	[kg/m^3]	1092
Viscosity	[mPa·s]	3.5
Carbon content	[wt%]	20.8
Hydrogen content	[wt%]	9.4
Oxygen content (balance)	[wt%]	69.4
Nitrogen content	[wt%]	<1

It's properties are shown in Table 2. The co-feed HGO was purchased from ASG Analytic-Service GmbH. HGO is a highly hydrogenated heavy diesel fraction with an H/C ratio of 2.05 mol/mol, the boiling range is shown in Figure 7. For sulphidation, 35 wt% di-tert-butyldisulphide (DTBDS) in HGO was used. Hydrogen 5.0 was provided in a 300 bar gas bomb from AIR LIQUIDE AUSTRIA GmbH.

2.3 Experimental Setup

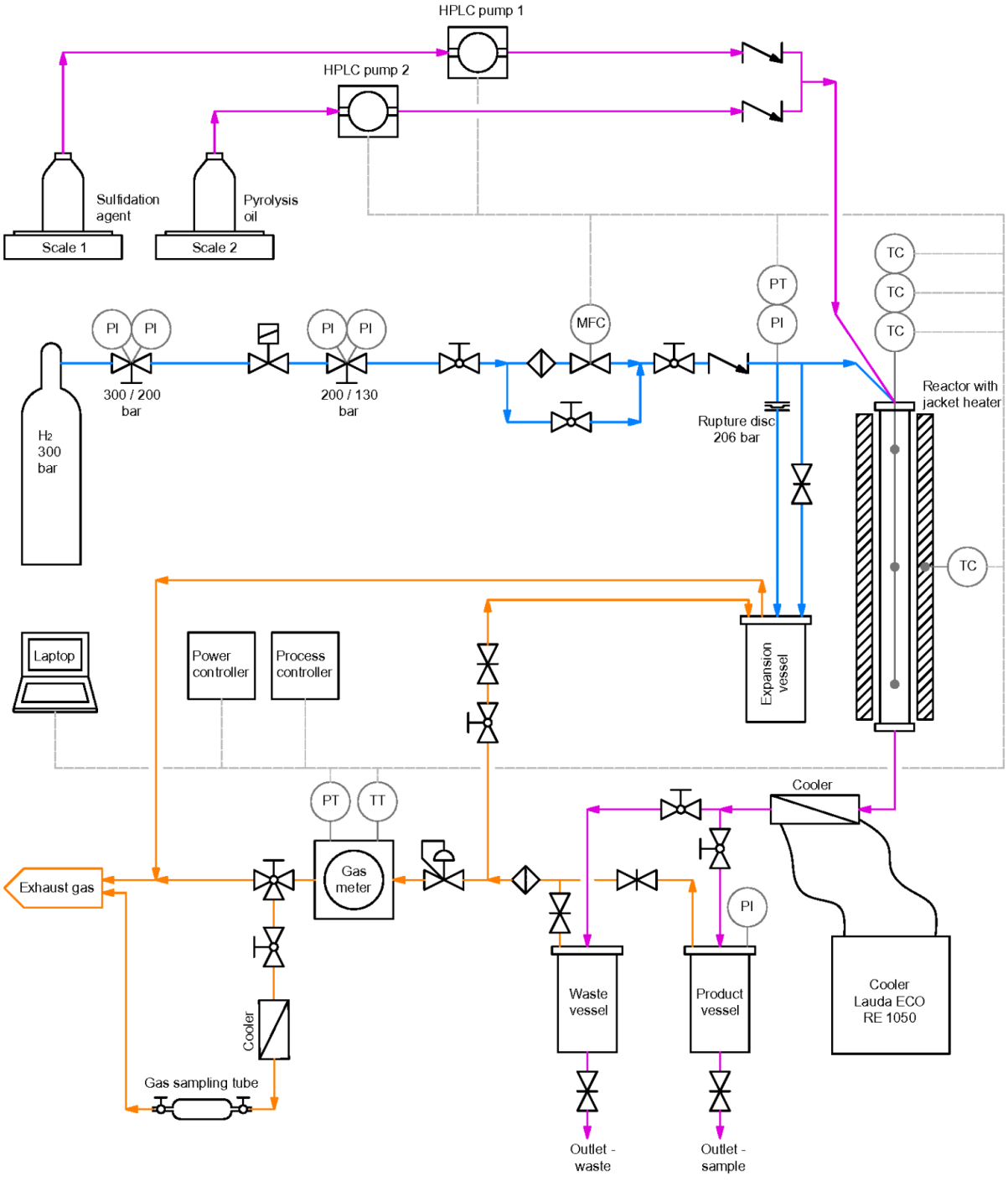

Figure 1: Scheme of the plug flow reactor setup used for mild HDO and co-processing

For mild HDO and co-processing, a plug flow reactor of Parr instrument company with an inner diameter of 3/8 inch and a heated zone of 12 inch was used. The reactor was designed for a maximum pressure of 207 bar and a maximum temperature of 550°C. Temperature was detected by an inner thermowell with a thermocouple consisting of 3 probe points on the top, middle and bottom of the reactor. The temperature of 300 or 400°C was measured in the middle of the reactor as the maximum temperature. Liquids were provided by a HPLC pump of Fink Chem + Tec GmbH. Hydrogen was provided by a mass flow controller of Bronkhorst high – tech B.V. The system pressure was regulated by a pressure regulating valve of Swagelok. The whole reactor setup can be seen in Figure 1.

2.4 Experimental procedure

Before each experiment, the reactor system was inertised with nitrogen and afterwards flushed with hydrogen until the working pressure of 80 or 120 bar was built up. The sulphidation agent (35 wt% DTBDS in HGO) was pumped into the reactor with a flow rate of 0.18 mL min^{-1}, for heating up and sulphidation LHSV was about 0.4 h^{-1}. Between 150°C and 350°C the temperature was increased within 3 h. Sulphidation started, as soon as 400°C were detected in the middle of the reactor. Sulphidation took 2.5 and 3 h for 80 and 120 bar, respectively, afterwards the respective feed was pumped through the reactor with a lead time of 5 h. Experiments took 36 h and were subdivided in 3 time periods à 12 h. The experiments included the direct co-processing of LPP oil and HGO, the mild hydrotreatment of LPP oil with a subsequent co-processing step at each 80 and 120 bar, as well as hydrotreatment of heavy gas oil at 80 and 120 bar for comparison.

2.5 HDO of LPP oil and HGO

Various experiments for the direct co-processing of LPP oil and HGO have been performed. Sulphur content, temperature, sulphidation time and LPP oil to HGO ratio have been varied with the result of plugging after 8 to 12 h. Sulphur content was varied between 250 and 400 ppm, temperature between 350 and 400°C, sufphidation time between 3 and 5 h and LPP admixture between 10 and 25 w%. Although the product quality was good judging on first observations, as it was a clear liquid without a colour and the odour of a mixture of gasoline and diesel, experiments couldn't be proceeded due to plugging of the reactor after maximum 12 h. Unstable components of pyrolysis oil, such as aldehydes, ketones and sugars have a high coking tendency [12]. Still, this doesn't explain the high pressure drop during co-processing, as HDO of pure LPP oil was feasible at different experimental parameters before [26], [27]. Gueudrè et al. [32] observed higher coke yields not only from pyrolysis oil but also of fossil origin through the addition of oxygenated pyrolysis oil components. The reason of the high coke formation in co-processing mode can most likely be found in the non-miscibility of LPP oil and HGO, as this might lead to competing reactions on the catalyst surface. The non-polar HGO might block the polar pyrolysis oil components from binding to the catalyst, which would immediately lead to coking reactions of instable biomass constituents. Even small amounts of formed coke lead to a

high pressure drop and to an immediate abortion of the experiment. According to Pinho et al. [39], [41], coking is a minor issue in large scale operation. It was therefore concluded, that direct co-processing of non-polar components with LPP oil is not operable.

In a second series of experiments, the ideal temperature of the mild HDO step was studied. Therefore, experiments were performed at 250, 300 and 350°C at 120 as well as 80 bar. For co-processing purposes, the product of HDO at 300°C was used. Co-processing was then performed at 400°C, with the feed consisting of 10 wt% mild hydrotreated LPP oil in HGO. Additionally, HGO was solely hydrodeoxgygenated at co-processing conditions for reference. A detailed list of experiments for two-step co-processing can be found in Table 3.

Table 3: Experimental matrix for the 2-step co-processing of LPP oil and HGO at 120 and 80 bar

	Experiment	Feed	T [°C]	p [bar]	LHSV [h^{-1}]
HGO (REFERENCE EXPERIMENT)	HGO 120 bar	HGO	400	120	1
	HGO 80 bar	HGO	400	80	1
HDO 1 (PRE-TREATMENT OF LPP OIL)	HDO 1 120 bar	LPP oil	300	120	1
	HDO 1 80 bar	LPP oil	300	80	0.5
HDO 2 (CO-PROCESSING)	HDO 2 120 bar	10 wt% hydrotreated LPP oil + 90 wt% HGO	400	120	1
	HDO 2 80 bar	10 wt% hydrotreated LPP oil + 90 wt% HGO	400	80	0.5

3. Determination of LPP oil pre-treatment parameters

Pre-treatment of LPP oil has been performed in the temperature range between 250 and 350°C with the objective of sufficient hydrophobation for product solvation in HGO. The goal was to find an optimum between carbon yield and oxygen removal without full hydrodeoxygenation. It was found, that both at 120 and 80 bar, the maximum carbon transfer into the hydrocarbon product phase was achieved at 300°C. Below that temperature, the main part of carbon was transferred into the aqueous phase, showing insufficient HDO. Above, cracking and gaseous product formation started at the expense of liquid hydrocarbon product formation. Having a look at the product composition in Figure 2, one can see that carbon and hydrogen content increased with the temperature, while the oxygen content decreased, as expected. This means that at 250°C a still polar product was gained, also observed at a poorly constructed phase boundary to the aqueous phase, while at 350°C the product was close to be fully hydrodeoxygenated. As reported in a previous publication [26], catalyst stability is poor in one step HDO at 350°C. Mixing of the product from mild HDO at 300°C with HGO led to the formation a homogenous liquid.

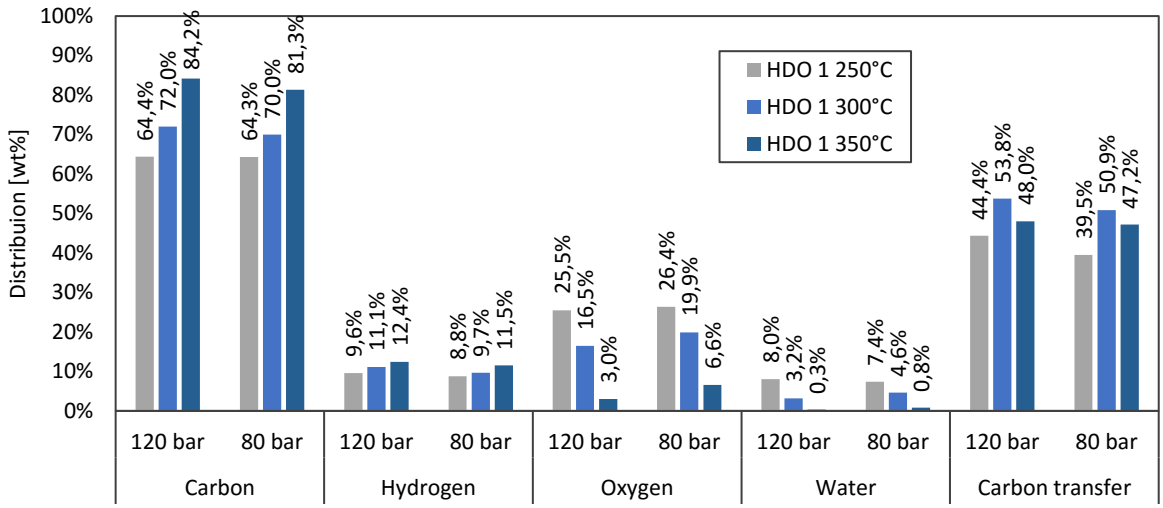

Figure 2: Composition and carbon transfer of the hydrocarbon product phase after mild HDO at 120 and 80 bar as well as 250, 300 and 350°C

Mild HDO at 300°C will further be referred to as "HDO 1" with the epithet "120" for 120 bar and "80" for 80 bar.

According to Elliott et al. [7], the HDO of different oxygenated compounds occur at different temperatures. At 150°C, at first olefins are saturated. When the temperature is increased, next aldehydes and ketones are hydrodeoxygenated to alcohols. According to Yin et al. [10], this should even happen at lower temperature of 80 to 180°C. At about 250°C, aliphatic ethers are hydrodeoxygenated and aliphatic alcohols are transferred into olefins through thermal dehydration. At 300°C, carboxylic groups are hydrodeoxygenated. Above 300°C, phenolic ethers are hydrodeoxygenated, at this temperature also hydrocracking starts, which explains the rapidly increasing formation of gaseous products at HDO 1 at 350°C. At 350°C, phenols react, afterwards di-phenyl ether and at 400°C finally dibenzofuran.

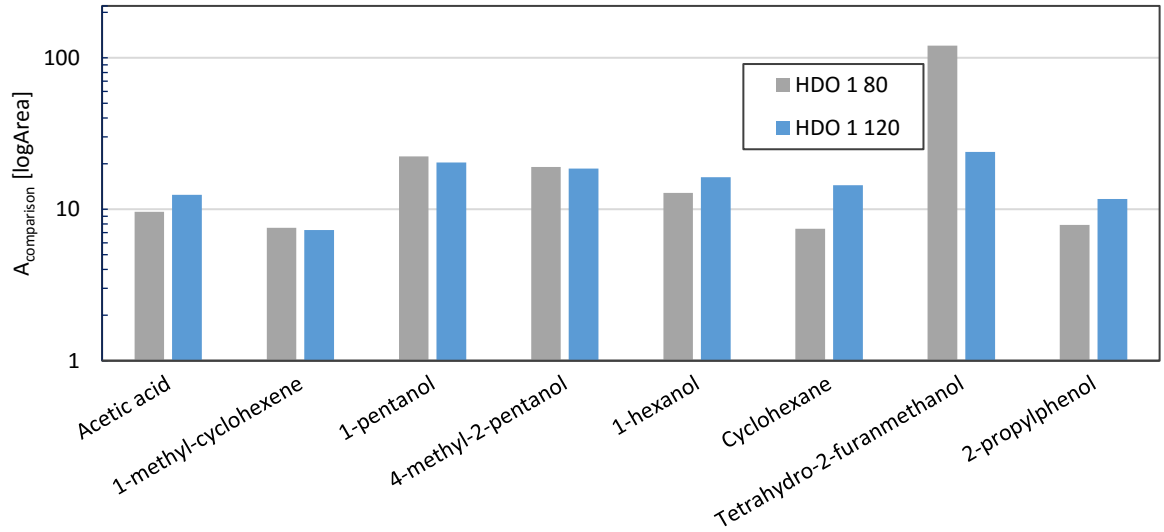

Figure 3: Semi-quantitative GC-MS analysis of the hydrocarbon product phase after mild HDO at 120 and 80 bar as well as 300°C

Through GC-MS analysis, the most frequent components of the hydrocarbon product phase of HDO 1 were determined semi-quantitatively. They are shown in Figure 3. In the products, mainly alcohols were found. They indicate that instable molecules as aldehydes and ketones have expectedly been hydrodeoxygenated partly, so that polarity decreased. Interestingly, also aliphatic alcohols were found. These should have been degraded between 250 and 300°C. The occurrence of 2-propylphenol fits with the observations of Elliot et al. and Yin et al. Although the experiments were performed with different residence times, LHSV was 1 h^{-1} for experiments at 120 bar and 0.5 h^{-1} for experiments at 80 bar, differences in the LPP oil degradation are neglect able.

4. Co-processing results

For co-processing, 10 wt% of pretreated LPP oil from the experiment at 300°C were mixed with 90 wt% HGO. The homogenous mixture was then fully hydrodeoxygenated at 400°C. The mass balances of HDO 1 and HDO 2 are given in Table 4. During HDO 1, the main product was an aqueous phase, as LPP oil contains mostly water and oxygen containing components. After HDO 2, the main fraction was the liquid hydrocarbon phase, not in both cases a water fraction was even formed. At 120 bar, small drops of water were found as a bottom phase in the product. At 80 bar, no water was found at all. Coking, which is defined as the solid layer on the catalyst, was very low at HDO 2, amounting only 0.03 wt% with respect to LPP oil and hydrogen at 80 bar. The coke formation seems to be dependent on three parameters: pressure, hydrogen amount and oxygen content of the feed. The higher the pressure and the hydrogen amount and the lower the oxygen content of the feed, the lower the coke formation.

Table 4: Mass balance of HDO 1 and HDO 2 at 120 as well as 80 bar

	HDO 1 120	HDO 1 80	HDO 2 120	HDO 2 80
LPP oil [wt%]	78.78	78.70	85.58	74.98
H2 [wt%]	21.22	21.30	14.42	25.02
hydrocarbon product [wt%]	11.56	9.50	81.55	67.37
aqueous product [wt%]	64.47	61.74	0.84	0.00
Gaseous product [wt%]	19.92	22.67	18.00	24.31
Coking [wt%]	0.73	1.25	0.37	0.03
balance inaccuracy [wt%]	3.31	4.85	-0.76	8.28

4.1 Catalyst stability

To observe the catalyst activity and potential coke deposition, the surface area was determined by BET analysis; the results are shown in Figure 4. The fresh catalyst has a surface are of 239 $m^2\ g^{-1}$. After HDO 1, catalyst area was decreased to 134 $m^2\ g^{-1}$ at 80 bar and to 137 $m^2\ g^{-1}$ at 120 bar. After HDO 2, surface area was merely deacreased to 183 $m^2\ g^{-1}$ at 80 bar and 194 $m^2\ g^{-1}$ at 120 bar.

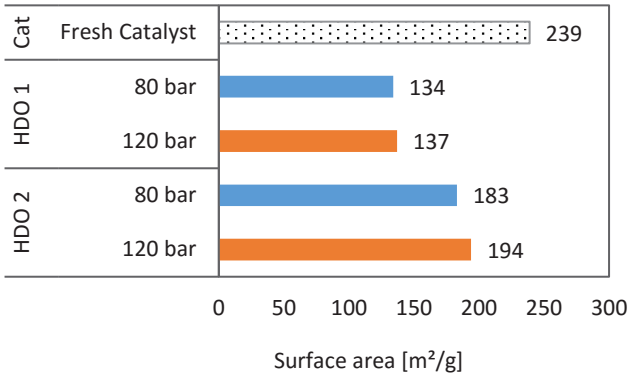

Figure 4: Catalyst surface area after HDO 1 and HDO 2 at 120 and 80 bar compared to fresh $CoMo/Al_2O_3$ catalyst

Each HDO step was comparable and not dependent on the pressure in the observed range. The feed on the other hand hade a high impact on the surface area. The instable components, which tend to coke formation, blocked the catalyst. This also explains decreasing product quality at HDO 1. Through the stabilisation, pre-treated LPP oil ensures, mixed with HGO, a longer catalyst stability due to less coke formation.

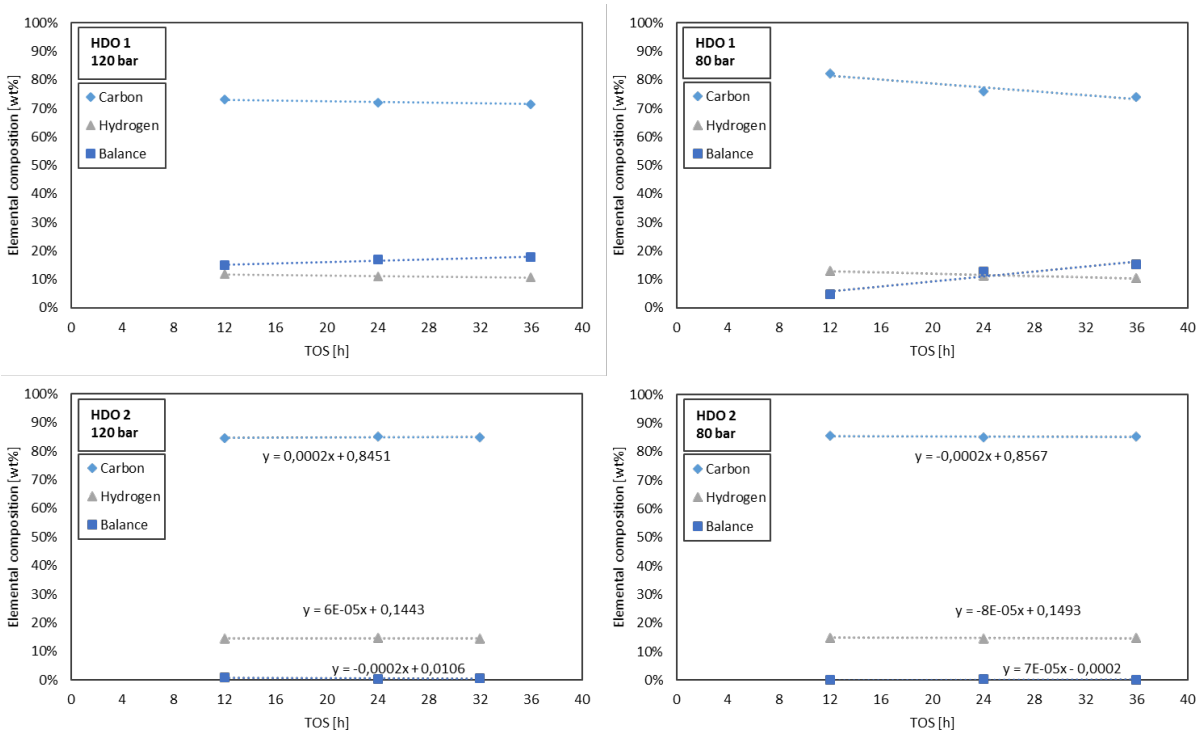

Figure 5: Elemental composition of the hydrocarbon product phases after HDO 1 and HDO 2 at 120 and 80 bar in dependence on time on stream (TOS)

During co-processing, a stable operation without pressure drops was possible. This reflects in the product quality. In comparison to HDO 1, during HDO 2 constant product quality was achieved, as shown in Figure 5. High coke yield was named as one of the biggest challenges during co-processing of crude oils with pyrolysis oil [32]. Whereas during mild pre-treatment of LPP oil coke formation was an issue, it was shown that by addition of hydrogen, admixture of pre-treated LPP oil for co-processing did not yield in higher coke formation. The elemental composition of the hydrocarbon product phase after HDO 2 changed with a slope in the order

of magnitude of 10^{-5} to 10^{-4} wt% h^{-1}, which can be seen as constant. Although after HDO 1 product quality seemed to be higher after the first period of experiments when 80 bar were applied, it changed more rapidly than at 120 bar. This indicates that the better quality, namely the higher H/C ratio and lower oxygen content, in the beginning resulted from the lower liquid hourly space velocity of 0.5 h^{-1} compared to 1 h^{-1}.

After HDO 2, water content of the hydrocarbon product phase was below 0.025 wt%. There was no difference to the reference experiments with pure HGO. Moreover, no dependence on the pressure or experiment time was visible, as shown in Figure 6. The admixture of pre-treated LPP oil had no influence on the water content. This shows that a very stable operation mode was achieved and coke tendency was not increased by the co-processing of HGO with LPP oil.

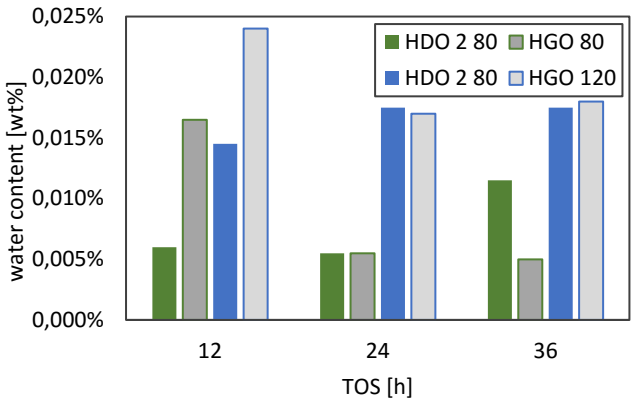

Figure 6: Water content of the hydrocarbon product phase after HDO 2 and after the reference experiments HGO at 120 and 80 bar in dependence on TOS

4.2 Product quality

The composition of all hydrocarbon product phases, the carbon transfer into these fractions as well as important fuel parameters are shown in Table 5. Hydrotreatment of pure HGO, which was performed as reference experiment at 120 as well as 80 bar, showed only a slight influence on the elemental composition, but on the boiling range, as shown in Figure 7. HGO had a very sharp boiling range between 250 and 350°C. When hydrotreated, the chain length of the alkanes was shortened due to cracking reactions. At 120 bar, about 17 vol% boiled before 250°C, at 80 bar the percentage was higher with about 30 vol%. In both cases, about 50 to 55 vol% were boiling at 300°C. This means that under the usage of a sulphided $CoMo/Al_2O_3$ catalyst at conditions of 400°C in the pressure range of 80 to 120 bar the reactor acts as a hydrocracker. This reflects in density and viscosity, as they decreased after HDO. Compared to these results, the products of the co-processing experiments showed the same elemental composition and fuel parameters with negligible deviations, but contained 8 to 9 wt% of biogenous carbon, with respect to the total carbon content. Also, the carbon transfer was not affected by the admixture of pre-treated LPP oil, as it was 96 to 97 wt% at 120 bar and 90 to 93 wt% at 80 bar. The lower carbon yield is related to a generally higher balance inaccuracy at 80 bar.

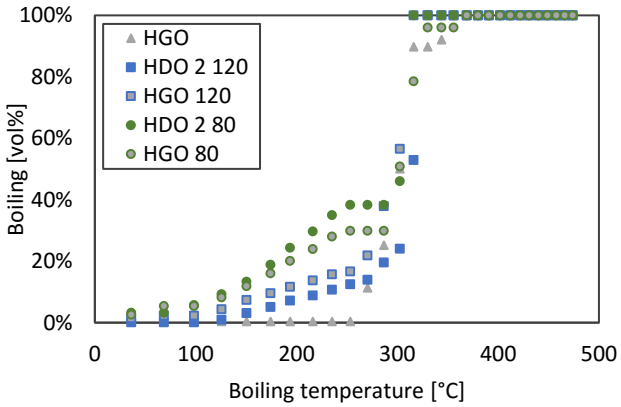

Figure 7: Boiling range of the co-processing products at 120 and 80 bar compared to the reference experiments without LPP oil and to untreated HGO.

After HDO 1, the oxygen content was reduced from 68 wt% to 16.5 and 12.5 wt% at 120 and 80 bar, respectively. The products of HDO 2 contained no detectable residual oxygen and a water content below 0.02 wt%. The sulphur content was low when considering that sulphur was used for catalyst activation. It amounted 5.7 mg/kg after HDO 2 at 80 bar and 11.2 mg/kg after HDO 2 at 120 bar. Thus, also desulphurisation took place.

Table 5: Carbon transfer into the hydrocarbon product phase as well as elemental composition, biogenous carbon content and fuel parameters of the hydrocarbon product phase of HDO 1, HDO 2 and HGO at 120 and 80 bar

		LPP oil	HGO	HGO 120	HDO 1 120	HDO 2 120	HGO 80	HDO 1 80	HDO 2 80
C-Transfer	[wt%]	-	-	96.9	51.0	96.4	92.6	44.3	90.3
ELEMENTAL COMPOSITION									
C	[wt%]	20.8	84.8	84.8	72.0	85.1	84.9	75.6	85.0
H	[wt%]	9.4	14.6	14.7	11.1	14.6	14.7	11.5	14.6
N	[wt%]	<1	<1	<1	<1	<1	<1	<1	<1
S	[mg/kg]	34.6	<5	n.a.	n.a.	11.2	n.a.	n.a.	5.7
O (by difference)	[wt%]	69.4	0.0	0.0	16.5	0.0	0.0	12.5	0.0
Biogenous carbon (C/C)	[wt%]	100	0	0	100	8.1	0	100	9.0
FUEL PARAMETER									
Water content	[wt%]	58.9	0.0	0.02	3.1	0.017	0.006	2.1	0.006
Lower heating value (equation of Boie[47])	[MJ/kg]	6.6	43.6	43.6	33.8	43.6	43.7	35.9	43.7
Density	[kg/m³]	1092	808	791	914	793	776	903	780
Viscosity	[mPa·s]	3.5	13.6	6.0	6.1	4.5	n.a.	n.a.	n.a
TAN	[mg/g]	80.8	0	0	0	0	0	19.4	0
Micro carbon residue	[wt%]	n.a.	n.a.	n.a.	0.12	<0.01	n.a.	n.a.	<0.01
Metal content	[wt%]	Ni: 0.006	Ni: 0.033	n.a.	n.d.	n.d.	n.a.	n.a.	n.d.

n.a. = not available; n.d. = not detected

The products contained no metals and a micro carbon residue below 0.01 wt%, which is an important parameter in petroleum processing as it shows coking tendency. In comparison, the Diesel Norm EN 590 [48] allows for up to 0.3 wt%. Interestingly, although the degree of HDO seemed to be higher after HDO 1 at 80 bar, mainly due to the lower LHSV, residual acid, identified by a TAN of 19.4 mg g^{-1} compared to zero after HDO 1 at 120 bar, was found in the product.

The aromatic content was determined by H-NMR analysis. Over 99 wt% of the hydrogen in the products amounted aliphatic hydrogen, the rest was mostly aromatic hydrogen, as to be seen in Table 6. This means that the biogenous components again didn't influence the HDO of HGO.

Table 6: H-NMR analysis of the HDO 2 hydrocarbon product phase at 120 and 80 bar

[wt%]	H aromatic	H aliphatic	H phenolic	H aldehyde, ketone, acid
HDO 2_{120}	0.65	99.26	0.00	0.09
HDO 2_{80}	0.26	99.73	0.01	0.01

5. Conclusions

In two-step operation mode, co-processing of LPP oil and HGO as a representative for petroleum refinery intermediates was feasible at 120 bar as well as at more common refinery conditions of 80 bar. Therefore, LPP oil was hydrodeoxygenated mildly in a first step between 250 and 350°C. An optimum between sufficient hydrophobation and high carbon yield in the hydrocarbon product phase was observed at 300°C, both for 120 and 80 bar. Co-processing was performed at 400°C with 10 wt% of mildly hydrotreated LPP oil in HGO. Admixture of a higher portion of mildly hydrotreated LPP oil is thinkable. The necessity of hydrogen for LPP oil integrating processes was discussed. During the co-processing step, a stable operation mode and constant product quality without pressure dependency in the range of 80 to 120 bar were observed. The experimental operability as well as the product quality and carbon yield were the same as at reference experiments without admixture of pre-treated LPP oil, but in contrary the products contained 8 to 9 wt% of biogenous carbon. During mild hydrotreatment, product quality decreased rapidly, especially at 80 bar. For mild HDO therefore a higher pressure is necessary. This still did not lead to a constant catalyst stability, which would be necessary for industrial scale operation. Mild HDO of LPP oil might be performed by applying synthesis gas instead of pure hydrogen. For the co-processing step with pre-treated LPP oil and refinery intermediates though 80 bar, which is mostly common in petroleum refineries, is sufficient.

6. References

[1] E. Sokolov, "Comparative Study of Electric Car Traction Motors," *15-th Int. Conf. Electr. Mach. Drives Power Syst.*, pp. 348–353, 2017.

[2] C. Wang and M. H. Nehrir, "Distributed Generation Applications of Fuel Cells," in *Power Systems Conference 2006: Advanced Metering, Protection, Control, Communication and Distributed Resources*, 2006.

[3] J. Michl, J. Neumann, H. Rottengruber, and M. Wensing, "Derivation and validation of a heat transfer model in a hydrogen combustion engine," *Appl. Therm. Eng.*, vol. 98, pp. 502–512, 2016.

[4] "Electricity production, consumption and market overview," *eurostat, Statistics Explained*, 2018. [Online]. Available: https://ec.europa.eu/eurostat/statistics-explained/index.php/Electricity_production,_consumption_and_market_overview#Electricity_generation. [Accessed: 14-Feb-2019].

[5] F. Fischer and H. Tropsch, "Über die direkte Synthese von Erdöl-Kohlenwasserstoffen bei gewöhnlichem Druck (Erste Mitteilung.)," *Chem Ber*, vol. 59, no. November 1925, pp. 830–831, 1926.

[6] M. Balat, H. Balat, and C. Öz, "Progress in bioethanol processing," *Prog. Energy Combust. Sci.*, vol. 34, no. 5, pp. 551–573, 2008.

[7] D. C. Elliott, "Historical developments in hydroprocessing bio-oils," *Energy and Fuels*, vol. 21, no. 3. pp. 1792–1815, 2007.

[8] D. C. Elliott, T. R. Hart, G. G. Neuenschwander, L. J. Rotness, and A. H. Zacher, "Catalytic hydroprocessing of biomass fast pyrolysis bio-oil to produce hydrocarbon products," *Environ. Prog. Sustain. Energy*, vol. 28, no. 3, pp. 441–449, 2009.

[9] P. A. Meyer, L. J. Snowden-Swan, K. G. Rappé, S. B. Jones, T. L. Westover, and K. G. Cafferty, "Field-to-Fuel Performance Testing of Lignocellulosic Feedstocks for Fast Pyrolysis and Upgrading: Techno-economic Analysis and Greenhouse Gas Life Cycle Analysis," *Energy and Fuels*, vol. 30, no. 11, pp. 9427–9439, 2016.

[10] W. Yin *et al.*, "Catalytic hydrotreatment of fast pyrolysis liquids in batch and continuous set-ups using a bimetallic Ni–Cu catalyst with a high metal content," *Catal. Sci. Technol.*, vol. 6, no. 15, pp. 5899–5915, 2016.

[11] D. Carpenter *et al.*, "Catalytic hydroprocessing of fast pyrolysis oils: Impact of biomass feedstock on process efficiency," *Biomass and Bioenergy*, vol. 96, pp. 142–151, 2017.

[12] M. V. Olarte *et al.*, "Stabilization of Softwood-Derived Pyrolysis Oils for Continuous Bio-oil Hydroprocessing," *Top. Catal.*, vol. 59, no. 1, pp. 55–64, 2016.

[13] M. V. Olarte *et al.*, "Characterization of upgraded fast pyrolysis oak oil distillate fractions from sulfided and non-sulfided catalytic hydrotreating," *Fuel*, vol. 202, pp. 620–630, 2017.

[14] J. Neumann, N. Jäger, A. Apfelbacher, R. Daschner, S. Binder, and A. Hornung, "Upgraded biofuel from residue biomass by Thermo-Catalytic Reforming and hydrodeoxygenation," *Biomass and Bioenergy*, vol. 89, pp. 91–97, 2016.

[15] G. Kim *et al.*, "Two-step continuous upgrading of sawdust pyrolysis oil to deoxygenated hydrocarbons using hydrotreating and hydrodeoxygenating catalysts," *Catal. Today*, vol. 303, pp. 130–135, 2018.

[16] I. Kim *et al.*, "Upgrading of sawdust pyrolysis oil to hydrocarbon fuels using tungstate-zirconia-supported Ru catalysts with less formation of cokes," *J. Ind. Eng. Chem.*, vol. 56, pp. 74–81, 2017.

[17] N. Schwaiger *et al.*, "Liquid and Solid Products from Liquid-Phase Pyrolysis of Softwood," *Bioenergy Res.*, vol. 4, no. 4, pp. 294–302, 2011.

[18] J. Ritzberger, P. Pucher, N. Schwaiger, and M. Siebenhofer, "The BioCRACK Process-A Refinery Integrated Biomass-to-Liquid Concept to Produce Diesel from Biogenic Feedstock," *Chem. Eng. Trans.*, vol. 39, no. 2010, pp. 1189–1194, 2014.

[19] K. Treusch, J. Ritzberger, N. Schwaiger, P. Pucher, and M. Siebenhofer, "Diesel

production from lignocellulosic feed : the bioCRACK process," *R.Soc.open sci.*, vol. 4, no. 171122, 2017.
[20] N. Schwaiger *et al.*, "BiomassPyrolysisRefinery - Herstellung von nachhaltigen Treibstoffen," *Chemie-Ingenieur-Technik*, vol. 87, no. 6, pp. 803–809, 2015.
[21] R. Feiner, N. Schwaiger, H. Pucher, L. Ellmaier, P. Pucher, and M. Siebenhofer, "Liquefaction of pyrolysis derived biochar: a new step towards biofuel from renewable resources," *RSC Adv.*, vol. 3, no. 39, pp. 17898–17903, 2013.
[22] R. Feiner *et al.*, "Chemical loop systems for biochar liquefaction: hydrogenation of Naphthalene," *RSC Adv.*, vol. 4, p. 34955, 2014.
[23] R. Feiner *et al.*, "Kinetics of Biochar Liquefaction," *Bioenergy Res.*, vol. 7, no. 4, pp. 1343–1350, 2014.
[24] H. Pucher, N. Schwaiger, R. Feiner, P. Pucher, L. Ellmaier, and M. Siebenhofer, "Catalytic hydrodeoxygenation of dehydrated liquid phase pyrolysis oil," *Energy Res.*, vol. 31, no. April 2014, p. 3205, 2014.
[25] H. Pucher *et al.*, "Lignocellulosic Biofuels: Phase Separation during Catalytic Hydrodeoxygenation of Liquid Phase Pyrolysis Oil," vol. 50, no. 18, pp. 2914–2919, 2015.
[26] K. Treusch, N. Schwaiger, K. Schlackl, R. Nagl, and P. Pucher, "Temperature Dependence of Single Step Hydrodeoxygenation of Liquid Phase Pyrolysis Oil," *Front. Chem.*, vol. 6:297, no. July, pp. 1–8, 2018.
[27] K. Treusch *et al.*, "High-throughput continuous hydrodeoxygenation of liquid phase pyrolysis oil," *React. Chem. Eng.*, 2018.
[28] K. Treusch *et al.*, "Hydrocarbon production by continuous hydrodeoxygenation of liquid phase pyrolysis oil with biogenous hydrogen rich synthesis gas," *React. Chem. Eng.*, 2019.
[29] S. D. Stefanidis, K. G. Kalogiannis, and A. A. Lappas, "Co-processing bio-oil in the refinery for drop-in biofuels via fluid catalytic cracking," *Wiley Interdiscip. Rev. Energy Environ.*, vol. 7, no. 3, pp. 1–18, 2018.
[30] L. Gueudré *et al.*, "Optimizing the bio-gasoline quantity and quality in fluid catalytic cracking co-refining," *Fuel*, vol. 192, pp. 60–70, 2017.
[31] C. Lindfors, V. Paasikallio, E. Kuoppala, M. Reinikainen, A. Oasmaa, and Y. Solantausta, "Co-processing of dry bio-oil, catalytic pyrolysis oil, and hydrotreated bio-oil in a micro activity test unit," *Energy and Fuels*, vol. 29, no. 6, pp. 3707–3714, 2015.
[32] L. Gueudré *et al.*, "Coke chemistry under vacuum gasoil/bio-oil FCC co-processing conditions," *Catal. Today*, vol. 257, no. Part 2, pp. 200–212, 2015.
[33] N. Thegarid *et al.*, "Second-generation biofuels by co-processing catalytic pyrolysis oil in FCC units," *Appl. Catal. B Environ.*, vol. 145, pp. 161–166, 2014.
[34] F. de Miguel Mercader *et al.*, "Hydrodeoxygenation of pyrolysis oil fractions: process understanding and quality assessment through co-processing in refinery units," *Energy Environ. Sci.*, vol. 4, no. 3, p. 985, 2011.
[35] G. Fogassy, N. Thegarid, G. Toussaint, A. C. van Veen, Y. Schuurman, and C. Mirodatos, "Biomass derived feedstock co-processing with vacuum gas oil for second-generation fuel production in FCC units," *Appl. Catal. B Environ.*, vol. 96, no. 3–4, pp. 476–485, 2010.
[36] F. de Miguel Mercader, M. J. Groeneveld, S. R. A. Kersten, N. W. J. Way, C. J. Schaverien, and J. A. Hogendoorn, "Production of advanced biofuels: Co-processing of upgraded pyrolysis oil in standard refinery units," *Appl. Catal. B Environ.*, vol. 96, no. 1–2, pp. 57–66, 2010.
[37] A. A. Lappas, S. Bezergianni, and I. A. Vasalos, "Production of biofuels via co-processing in conventional refining processes," *Catal. Today*, vol. 145, no. 1–2, pp. 55–62, 2009.
[38] M. C. Samolada, W. Baldauf, and I. A. Vasalos, "Production of a bio-gasoline by upgrading biomass flash pyrolysis liquids via hydrogen processing and catalytic cracking," *Fuel*, vol. 77, no. 14, pp. 1667–1675, 1998.
[39] A. de R. Pinho *et al.*, "Fast pyrolysis oil from pinewood chips co-processing with vacuum gas oil in an FCC unit for second generation fuel production," *Fuel*, vol. 188, pp. 462–

473, 2017.
[40] Á. Ibarra, E. Rodríguez, U. Sedran, J. M. Arandes, and J. Bilbao, "Synergy in the Cracking of a Blend of Bio-oil and Vacuum Gasoil under Fluid Catalytic Cracking Conditions," *Ind. Eng. Chem. Res.*, vol. 55, no. 7, pp. 1872–1880, 2016.
[41] A. D. R. Pinho, M. B. B. De Almeida, F. L. Mendes, V. L. Ximenes, and L. C. Casavechia, "Co-processing raw bio-oil and gasoil in an FCC Unit," *Fuel Process. Technol.*, vol. 131, pp. 159–166, 2015.
[42] Y. Schuurman, G. Fogassy, and C. Mirodatos, *Tomorrow's Biofuels: Hybrid Biogasoline by Co-processing in FCC Units*. © 2013 Elsevier B.V. All rights reserved., 2013.
[43] A. Corma, G. W. Huber, L. Sauvanaud, and P. O'Connor, "Processing biomass-derived oxygenates in the oil refinery: Catalytic cracking (FCC) reaction pathways and role of catalyst," *J. Catal.*, vol. 247, no. 2, pp. 307–327, 2007.
[44] C. Sepúlveda, N. Escalona, R. García, D. Laurenti, and M. Vrinat, "Hydrodeoxygenation and hydrodesulfurization co-processing over ReS 2 supported catalysts," *Catal. Today*, vol. 195, no. 1, pp. 101–105, 2012.
[45] A. Pinheiro, D. Hudebine, N. Dupassieux, and C. Geantet, "Impact of oxygenated compounds from lignocellulosic biomass pyrolysis oils on gas oil hydrotreatment," *Energy and Fuels*, vol. 23, no. 2, pp. 1007–1014, 2009.
[46] V. N. Bui, G. Toussaint, D. Laurenti, C. Mirodatos, and C. Geantet, "Co-processing of pyrolisis bio oils and gas oil for new generation of bio-fuels: Hydrodeoxygenation of guaïacol and SRGO mixed feed," *Catal. Today*, vol. 143, no. 1–2, pp. 172–178, 2009.
[47] K.-H. Grote and J. Feldhusen, *Dubbel Taschenbuch für Maschinenbau*, 22nd ed. Springer, 2007.
[48] "EN 590:2004." .

Chapter 8

Hydrocarbon production by continuous hydrodeoxygenation of liquid phase pyrolysis oil with biogenous hydrogen rich synthesis gas

Reaction Chemistry & Engineering

PAPER

View Article Online
View Journal

Cite this: DOI: 10.1039/c9re00031c

Hydrocarbon production by continuous hydrodeoxygenation of liquid phase pyrolysis oil with biogenous hydrogen rich synthesis gas

Klara Treusch, [ab] Anna Magdalena Mauerhofer,[c] Nikolaus Schwaiger, *[a] Peter Pucher,[b] Stefan Müller, [c] Daniela Painer, [a] Hermann Hofbauer [c] and Matthäus Siebenhofer [a]

Received 21st January 2019,
Accepted 7th February 2019

DOI: 10.1039/c9re00031c

rsc.li/reaction-engineering

This paper presents a beneficial combination of biomass gasification and pyrolysis oil hydrodeoxygenation for advanced biofuel production. Hydrogen for hydrodeoxygenation (HDO) of liquid phase pyrolysis oil (LPP oil) was generated by gasification of softwood. The process merges dual fluidized bed (DFB) steam gasification, which produces a hydrogen rich product gas and the HDO of LPP oil. Synthesis gas was used directly without further cleaning and upgrading, by making use of the water gas-shift (WGS) reaction. The water needed for the water gas-shift reaction was provided by LPP oil. HDO was successfully performed in a lab scale over 36 h time on stream (TOS). Competing reactions like the Boudouard reaction and Sabatier reaction were not observed. Product quality was close to Diesel fuel specification according to EN 590, with a carbon content of 85.4 w% and a residual water content of 0.28 w%. The water-gas shift reaction was confirmed by CO/CO_2-balance, high water consumption and 28% less hydrogen consumption during HDO.

Introduction

In the mid-1990s, the first climate agreement was published in the Kyoto protocol,[1] initiating several actions in climate policy. In 2015, the Paris agreement[2] from the United Nations Framework Convention on Climate Change was a big step forward to support renewable energy intentions. The main target of this agreement is to hold climate change significantly below 2 °C above the pre-industrial level; it was signed by 196 member states worldwide. In parallel, the European Union developed different directives, the most important one being the renewable energy directive 2009/28/EC[3] (RED) in 2009, followed by a recast, directive (EU) 2018/2001 called RES,[4] in December 2018. These are just the most important directives. All agreements target a common objective: to mitigate climate change by reducing greenhouse gas emissions. This ambitious goal can only be achieved if all feasible sources for renewable energy production are exploited. From this point of view, the concept of biofuel production *via* the bioCRACK process and subsequent hydrodeoxygenation of liquid phase pyrolysis (LPP) oil with synthesis gas (syngas) from renewable feed has been developed. It combines two major pathways for biomass liquefaction: indirect liquefaction through gasification[5] with subsequent synthesis and direct liquefaction through pyrolysis[6] and hydrodeoxygenation.

Liquid phase pyrolysis

LPP is less common than flash or fast pyrolysis.[6–10] As the name implies, a liquid heat carrier is used for heat transfer during the pyrolysis process. The process may be performed with or without a catalyst, under inert gas or hydrogen atmosphere and under atmospheric or elevated pressure, depending on the boiling point of the heat carrier to assure its liquid state. Klaigaew *et al.*[11] performed LPP of Giant Leucaena in hexane with an initial nitrogen pressure of 10 bar in the presence of a metal oxide catalyst in the temperature range of 325 to 400 °C with different holding times. Ratanathavorn *et al.*[12] used decane as a heat carrier with an initial hydrogen pressure of 5 to 30 bar, also in the presence of different heterogeneous catalysts in the temperature range of 250 to 400 °C. Szabó *et al.*[13] performed LPP of wheat straw and poplar in *n*-hexadecane under inert atmosphere at about 350 °C and a maximum pressure of 20 bar. They observed a negligible effect of different catalysts. Schwaiger *et al.*[14,15] performed various experiments with spruce wood in a mixture of n-alkanes with a boiling range of 410 to 440 °C without a catalyst under nitrogen atmosphere at ambient pressure. He observed a partial degradation of the heat carrier oil as an

[a] *Institute of Chemical Engineering and Environmental Technology, Graz University of Technology, Austria. E-mail: nikolaus.schwaiger@tugraz.at*
[b] *BDI-BioEnergy International GmbH, Austria. E-mail: klara.treusch@bdi-bioenergy.com*
[c] *Institute of Chemical, Environmental and Bioscience Engineering, TU Wien, Austria*

unwanted effect. This effect can be used when the cracking of less valuable streams of crude refining is combined with LPP of biomass.

Based on that, the bioCRACK process was developed by BDI-BioEnergy International GmbH. In this process, biomass is pyrolysed in a heavy oil fraction from crude oil refining. Different to other pyrolysis technologies like fast pyrolysis, non-polar biomass constituents, which are formed during the cracking step, are then dissolved in this heavy oil fraction. The extraction of nonpolar cracking products from biomass into the cracked and residual heavy oil fractions produces a pyrolysis oil of low organic load and high water content, which is called liquid phase pyrolysis oil (LPP oil). A detailed discussion of the bioCRACK process can be found in the publications of Ritzberger *et al.*,[16] Schwaiger *et al.*[17] and Treusch *et al.*[18]

Dual fluidized bed steam gasification

The dual fluidized bed (DFB) steam gasification is a thermochemical conversion process for the production of a hydrogen-rich gas from solid fuels like biomass. Based on the conventional DFB steam gasification process,[5,19–22] the Sorption Enhanced Reforming (SER) process with reduced gasification temperatures of 600–700 °C was developed. The SER process aims to generate a product gas with high hydrogen contents of up to 75 w% db (dry basis) and *in situ* carbon dioxide transfer from the product gas into the flue gas.[23] The DFB reactor system combines a gasification reactor (GR) and a combustion reactor (CR), which are connected *via* a loop seal. Through the loop seal, unconverted fuel from the GR, so called char, is transported to the CR, which is fluidized with air. In the CR, char is burnt and provides heat energy, which is transferred to the GR with the bed material, so that the overall endothermic gasification reactions take place. Fig. 1 displays the fundamental principle of SER with sorption active bed material for the transfer of CO_2 from the GR to the CR.

For the SER process, limestone ($CaCO_3$) is used as bed material. Due to the high temperatures in the CR (800–900 °C), calcination of $CaCO_3$ to calcium oxide (CaO), shown in eqn (1), takes place, and CO_2 is released. The release of CO_2 during calcination reaction in the CR results in a CO_2-enriched flue gas.

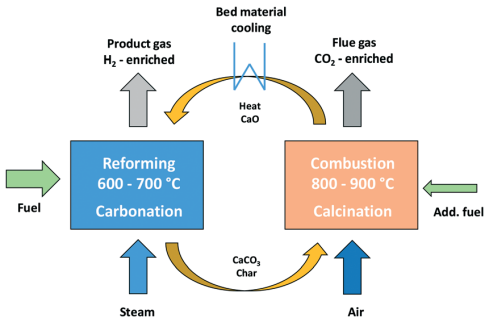

Fig. 1 Fundamental principle of the sorption enhanced reforming process.[22]

$$CaCO_3 \leftrightarrow CaO + CO_2 \quad (1)$$

$$CaO + CO_2 \leftrightarrow CaCO_3 \quad (2)$$

The temperature level in the GR allows carbonation and CO_2 is adsorbed from the product gas to react with CaO, according to eqn (2). Further information about sorption enhanced reforming can be found in literature.[22,24]

Hydrodeoxygenation of pyrolysis oil

Hydrodeoxygenation is a technology for pyrolysis oil upgrading. The technology is not yet established on an industrial scale. During hydrodeoxygenation, oxygen is removed from pyrolysis oil with hydrogen by the formation of water and hydrocarbons. HDO, especially of fast pyrolysis oil, is well investigated und published.[25–34] Usually, a two-step process is applied, whereas the first step is used to stabilize the most reactive components in pyrolysis oil, especially aldehydes and ketones,[30] in order to prevent coking, whereas in the second step it is fully hydrodeoxygenated.[32–38] The process is reported either in batch[27,28,39–41] or in continuous[29,30,32,34–38,42–45] operation mode. Not only hydrodeoxygenation of pyrolysis oil is reported, but also of differently liquefied biomass, such as solvolysed biomass, as reported by Rezzoug and Capart,[46] Kunaver *et al.*[47] and Grilc *et al.*[48–50] The latter ones liquefied biomass through solvolysis and acidolysis in glycerol, diethylene glycol and *p*-toluenesulfonic acid. The resulting liquefied biomass has a composition close to fast pyrolysis oils, with a comparably high carbon content and therefore high gross calorific value of over 20 MJ kg^{-1}. HDO of several bio oils with different biomass origin has been established, the hydrogen source is usually not mentioned, suggesting that the hydrogen is not of biogenous origin.

HDO of LPP oil may be performed at a high liquid hourly space velocity (LHSV), making integration in oil refinery processes feasible. The influence of the LHSV on HDO performance between 0.5 to 3 h^{-1} was investigated.[51] The highest HDO rate was achieved at LHSV 0.5 and 1 h^{-1} with an oxygen content of nearly 0 w% and a H/C ratio of nearly 2. The influence of the temperature was studied in the range of 350 to 400 °C.[52] It was observed, that in this temperature range the difference in product quality is minor. HDO fuel fractions contained less than 0.15 w% water and showed similar properties for different operation temperature. At LHSV between 0.5 and 1 h^{-1}, the influence of the temperature between 350 and 400 °C on product quality can be neglected.

Hydrodeoxygenation with synthesis gas

The application of synthesis gas for hydrodeoxygenation of pyrolysis oil is until now a poorly explored field of research. The underlying basis is an *in situ* water-gas shift (WGS)

reaction[53] according to eqn (3), with water contained in pyrolysis oil. LPP oil contains about 60 w% water. The reaction is exothermic. Reaction starts above 200 °C. A pressure of 25 to 30 bar is typically applied.

$$CO + H_2O \leftrightarrow CO_2 + H_2 \quad (3)$$

In 2014, Steele *et al.*[54] from the Mississippi State University registered a patent application describing the upgrading of bio-oil with synthesis gas. A pressure range between 20 and 83 bar as well as a temperature range between 200 and 350 °C was suggested. Tanneru and Steele[55] as well as Luo *et al.*[56] described the hydrodeoxygenation of oxidized flash pyrolysis oil, following this patent. Both groups performed the experiments discontinuously in two steps, whereas synthesis gas was only used in the first step. Tanneru and Steele used a mixture of H_2 and CO in different proportions at a pressure of 68.9 bar in both steps. The temperature was 340 °C in the first step, 400 °C in the second step. Nickel on different support materials was used as catalyst. Residence time was 90 min in the first and 150 min in the second step. Luo *et al.* hydrodeoxygenated a fractionated oxidized flash pyrolysis oil with a syngas composed of 18 vol% H_2, 22 vol% CO, 11 vol% CO_2, 2 vol% CH_4 and 47 vol% N_2 in the first step. The partially upgraded pyrolysis oil was then fully hydrogenated with pure hydrogen in a second step. They applied 55 bar and 360 °C in the first step and 96 bar and 425 °C in the second step. Residence time was 120 min in each step. Wijayapala *et al.*,[57] also from Mississippi State University, investigated the HDO of two model compounds, guaiacol and furfural, in a batch reactor with a residence time of 240 min. Experiments were performed with two different synthesis gas mixtures, 50/50 synthesis gas and bio synthesis gas consisting of 18 vol% H_2, 23 vol% CO and 46 vol% N_2, at 40 bar and different temperatures.

So far, only batch experiments with oxidized flash pyrolysis oil or model compounds have been performed.[55–57] Until now, only one research group has investigated this topic. They concluded that HDO with synthesis gas could only be successfully performed with oxidized bio-oil. In this paper, the continuous hydrodeoxygenation of untreated liquid phase pyrolysis oil with synthesis gas from biomass gasification is investigated. The application of LPP oil is especially auspicious due to the surpassingly high water content of about 60 w%. As water cannot simply be added to pyrolysis oil, this makes the usage of LPP oil unique.

Combined biofuel production

The combined biofuel production route was composed of three processes carried out by Graz University of Technology in cooperation with BDI-Bioenergy International GmbH and TU Wien. TU Graz and BDI-BioEnergy International GmbH carried out the pyrolysis and the hydrodeoxygenation step, TU Wien provided the H_2-rich product gas for the hydrodeoxygenation step from a SER experiment carried out in the 100 kW_{th} DFB steam gasification pilot plant at TU Wien. In Fig. 2, a flow sheet of the combined processes, the so-called "biofuel production route", is shown. Thus, a 100% biogenous liquid fuel can be produced.

Dual fluidized bed steam gasification

The H_2-rich product gas was produced through the sorption enhanced reforming process. The SER test run was carried out in the 100 kW_{th} pilot plant at TU Wien with softwood as fuel and limestone as bed material. A scheme is shown in Fig. 3. In the lower gasification reactor (bubbling bed), temperatures of about 630 °C were applied, in the upper gasification reactor (counter-current column), temperature was about 670 °C. The steam to fuel ratio was set to 0.8 kg per kg_{daf}. More information about the test run can be found elsewhere.[24]

Validation of process data

Based on the process data, which were recorded during the test campaign, mass and energy balances were calculated with the process simulation tool IPSEpro. For the validation of measured data with IPSEpro, a model library, which was developed at TU Wien, was used.[58,59] For the evaluation of the presented test campaign, the following key figures were selected. The steam to fuel ratio φ_{SF} expresses the mass of steam used as fluidization agent and the mass of water in the fuel, it is related to the mass of dry and ash-free fuel (see eqn (4)). In eqn (5), the steam-related water conversion X_{H_2O} is given. X_{H_2O} describes the amount of water consumed for *e.g.* CO and H_2 formation, it is related to the sum of water, which is fed to the gasification reactor. The product gas yield PGY (see eqn (6)) is defined as the ratio of dry product gas to dry and ash-free fuel fed to the gasification reactor. The cold gas efficiency η_{CG} displayed in eqn (7) presents the chemical energy content of gaseous components in the tar-

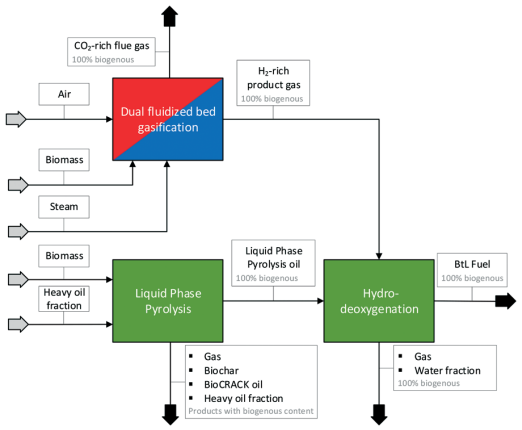

Fig. 2 Combined biofuel production route of TU Wien and TU Graz; dual fluidized bed gasification, liquid phase pyrolysis and hydrodeoxygenation.

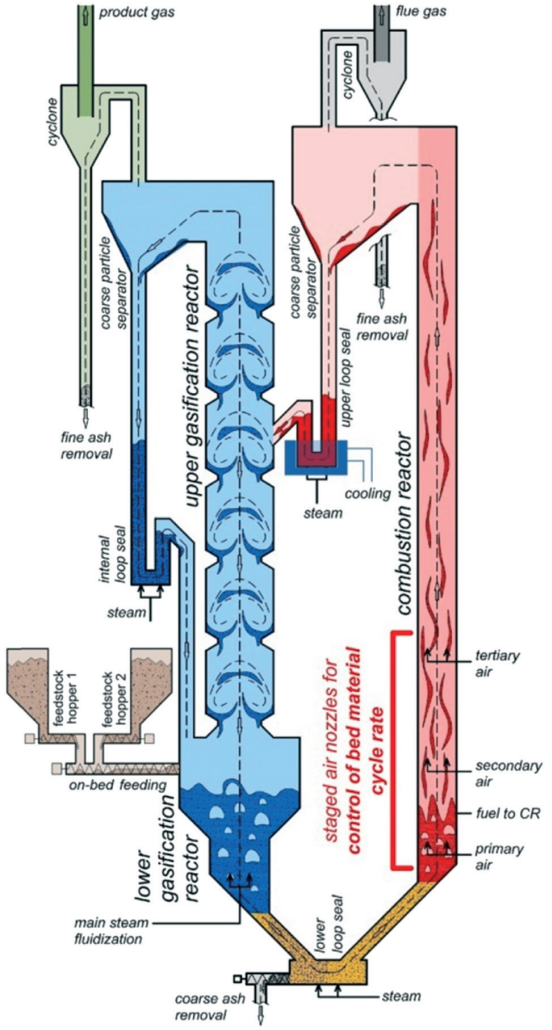

Fig. 3 Schematic plant concept of the 100 kW_{th} dual fluidized bed steam gasification pilot plant.[22]

and char-free product gas to the chemical energy in the fuel fed to the gasification reactor. All values are based on the lower heating value. eqn (8) displays the overall cold gas efficiency $\eta_{CG,o}$. It describes the amount of chemical energy in the product gas related to the fuel fed to the gasification and additional fuel fed to the combustion reactor minus apparent heat losses.

$$\varphi_{SF} = \frac{\dot{m}_{steam} + x_{H_2O,fuel} \cdot \dot{m}_{fuel}}{\left(1 - x_{H_2O,fuel} - x_{ash,fuel}\right) \cdot \dot{m}_{fuel}} \quad (4)$$

$\dot{m}_{steam}$ = mass flow of steam fed to GR in kg s^{-1}.
$\dot{m}_{fuel}$ = mass flow of fuel introduced into GR in kg s^{-1}.
$X_{H_2O,fuel}$ = weight percent of water in the fuel in w%.
$X_{ash,fuel}$ = weight percent of ash in the fuel in w%.

$$X_{H_2O} = \frac{\dot{m}_{steam} + x_{H_2O,fuel} \cdot \dot{m}_{fuel} - x_{H_2O,PG} \cdot \dot{m}_{PG}}{\dot{m}_{steam} + x_{H_2O,fuel} \cdot \dot{m}_{fuel}} \quad (5)$$

$\dot{m}_{PG}$ = mass flow product gas kg s^{-1}.
$X_{H_2O,PG}$ = weight percent of water in the product gas in w%.

$$PGY = \frac{\dot{V}_{PG}}{\dot{m}_{GR,fuel,daf}} \quad (6)$$

$\dot{V}_{PG}$ = dry volumetric product gas flow in m^3 s_{stp}^{-1}.
$\dot{m}_{GR,fuel,daf}$ = mass flow dry an ash-free fuel fed to GR in kg s^{-1}.

$$\eta_{CG} = \frac{\dot{V}_{PG} \cdot LHV_{PG}}{\dot{m}_{fuel} \cdot LHV_{fuel}} \times 100 \quad (7)$$

LHV_{PG} = Lower heating value of product gas in MJ kg_{db}^{-1}.
LHV_{fuel} = Lower heating value of fuel in MJ kg_{db}^{-1}.

$$\eta_{CG,o} = \frac{\dot{V}_{PG} \cdot LHV_{PG}}{\dot{m}_{GR,fuel} \cdot LHV_{GR,fuel} + \dot{m}_{CR,fuel} \cdot LHV_{CR,fuel} - \dot{Q}_{loss}} \times 100 \quad (8)$$

$\dot{m}_{GR,fuel}$ = mass flow fuel fed to GR in kg s^{-1}.
$\dot{m}_{CR,fuel}$ = mass flow fuel fed to CR in kg s^{-1}.
$\dot{Q}_{loss}$ = heat loss in kW.

Materials

For the DFB steam gasification experiment, softwood pellets with an ash content of 0.2 w% and a diameter of 6 mm according to the Austrian standard ÖNORM M 7135 were used as fuel. The proximate and ultimate analysis of softwood pellets can be seen in Table 1. Limestone was used as bed material in the DFB steam gasification experiment. The composition and further properties of limestone can be found in Table 2.

Analytical methods

During gasification experiments, the pilot plant operation control was ensured with a programmable logic controller

Table 1 Proximate and ultimate analysis of softwood pellets used for gasification *via* the SER process

Parameter	Unit	Softwood pellets
Ash content	[$w\%_{db}$]	0.2
Carbon (C)	[$w\%_{db}$]	50.7
Hydrogen (H)	[$w\%_{db}$]	5.9
Nitrogen (N)	[$w\%_{db}$]	0.2
Sulphur (S)	[$w\%_{db}$]	0.005
Chloride (Cl)	[$w\%_{db}$]	0.005
Oxygen (O)	[$w\%_{db}$]	43.0
Volatiles	[$w\%_{db}$]	85.4
Fixed C	[$w\%_{db}$]	14.6
Water content	[w%]	7.2
LHV (dry)	[MJ kg_{db}^{-1}]	18.9
LHV (moist)	[MJ kg^{-1}]	17.4

Table 2 Composition of limestone used for gasification *via* the SER process

Parameter	Unit	Limestone
Al_2O_3	[w%]	—
$CaCO_3$	[w%]	95–97
Fe_2O_3	[w%]	—
K_2O	[w%]	—
$MgCO_3$	[w%]	1.5–4.0
Na_2O	[w%]	—
SiO_2	[w%]	0.4–0.6
Trace elements (<0.4 per element)	[w%]	≤ 3.1
Hardness	[Mohs]	3
Sauter mean diameter	[mm]	0.382
Particle density	[kg m^{-3}]	2650, 1500[a]

[a] Particle density after full calcination.

(PLC). Data of all flow rates, temperatures, pressures and gas compositions were measured and recorded continuously. The main gas components H_2, CO, CO_2 and CH_4 were recorded online with a Rosemount NGA2000 measuring device. C_2H_4 was determined with a Perkin Elmer ARNEL – Clarus 500 gas chromatograph every 12 to 15 min. Before analysis, the product gas had to be cleaned to protect the measurement equipment from contaminants. For this purpose, it was filtered with a glass wool filter and washed with rapeseed methyl ester (RME) to eliminate condensable components like water and tar. A more detailed explanation of the measurement, equipment and procedure is given by Kolbitsch *et al.*[60]

Dual fluidized bed gasification results

The product gas composition as well as relevant process indicating key figures of the SER test run at TU Wien are displayed in Table 3. During the test run, the steam to fuel ratio was set to 0.8 kg kg_{daf}^{-1}. It was possible to generate a product gas with 70 w% hydrogen. The water conversion rate X_{H_2O} as well as the product gas yield PGY lie in a good range compared to other SER test runs (see literature[22]). Cold gas efficiencies of about 70–73% could be reached, which are typical values for this DFB gasification system.[61] Based on these results, a test gas bomb from Air Liquide was transferred to TU Graz with the gas composition given in Table 4.

Table 3 Product gas composition of the SER process

Product gas composition		SER test run
H_2	[$vol\%_{db}$]	70.3
CO	[$vol\%_{db}$]	8.2
CO_2	[$vol\%_{db}$]	5.3
CH_4	[$vol\%_{db}$]	14.0
C_2H_4	[$vol\%_{db}$]	1.14
C_2H_6	[$vol\%_{db}$]	1.14
Performance indicating key parameters		**SER test run**
X_{H_2O}	[kg_{H_2O}/kg_{H_2O}]	0.29
PGY	[$m^3_{stp,db}$ $kg_{fuel,daf}^{-1}$]	0.91
η_{CG}	[%]	73.1
$\eta_{CG,o}$	[%]	70.5

Hydrodeoxygenation of LPP oil

For HDO, a plug flow reactor of Parr instrument GmbH with an inner diameter of 3/8 inch, a heated zone of 12 inch, specified for operation at 200 bar and 550 °C, with a maximum working pressure of 180 bar was used. The reactor was heated by a single zone external electric heater. Temperature was detected by an internal thermowell with a thermocouple with 3 measurement points. The reactor was fed from the top with both gaseous and liquid reactants. Gas flow was controlled by a mass flow controller, type Bronkhorst high – tech B.V., with a bypass valve for flushing the reactor in the startup phase of experiments. The liquid feed, sulfidation agent and LPP oil, was pumped through the reactor with two high pressure pumps. The reaction products were cooled down to 3 °C directly after leaving the reactor with a cooling thermostat. Afterwards, they were collected in two product vessels of Parr Instrument GmbH. The pressure was regulated by a Swagelok pressure regulating valve. Outlet gas flow was measured by a drum-type gas meter of Dr.-Ing. Ritter Apparatebau GmbH & Co. KG. A scheme of the whole setup is shown in Fig. 4.

Experiments were performed at 120 bar. HDO with syngas was performed at 350 °C and LHSV 0.5 h^{-1}, a reference experiment with pure hydrogen was performed at 400 °C and LHSV 1 h^{-1}. Gas flow rate was 1 L min_{stp}^{-1} for hydrogen HDO. The HDO experiment with synthesis gas will be referred to as syngas HDO in this work. To increase the water to synthesis gas ratio and therefore enhance WGS reaction, the gas flow for syngas HDO was set to 0.265 L min_{stp}^{-1}, which results in a hydrogen flow of 0.187 L min_{stp}^{-1}. The catalyst was sulfided *in situ* with a flow rate of 0.18 ml min^{-1}, whereas a temperature program was started to slowly heat up the reactor to 400 °C. In the temperature range of 150 to 350 °C, the temperature was increased with a rate of 100 °C h^{-1}. Then the temperature was increased to 400 °C and sulfidation was carried out for 3 h at this temperature. Afterwards, the pump with the sulfidation agent was stopped, the HDO temperature was adjusted and LPP oil pumping was started. In order to provide enough sulphur during HDO, di-*tert*-butyl-disulfide (DTBDS) equivalent to 1000 ppm of sulphur was added to LPP oil. After 5 hours of lead time, 36 hours of steady state operation mode started. Samples were taken after 12, 28 and 36 hours during syngas feed and every 12 hours in the reference experiment with hydrogen. Therefore, the experiments were divided into three periods. Gas sampling was performed every 4 hours.

Table 4 Synthesis gas composition of the test gas bomb

Product gas composition		Test gas bomb
H_2	[$vol\%_{db}$]	70.5
CO	[$vol\%_{db}$]	8
CO_2	[$vol\%_{db}$]	5.5
CH_4	[$vol\%_{db}$]	14
C_2H_4	[$vol\%_{db}$]	1
C_2H_6	[$vol\%_{db}$]	1

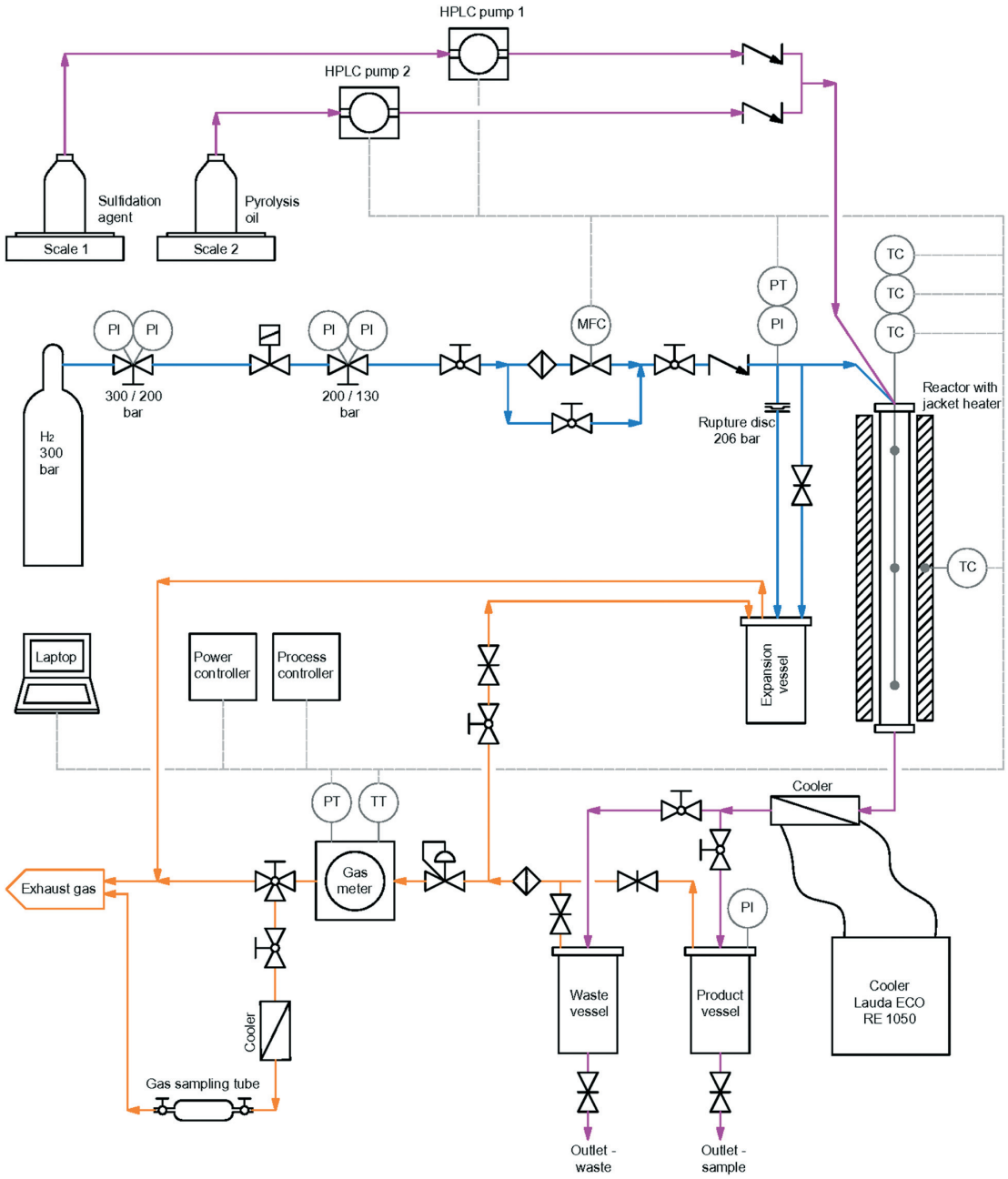

Fig. 4 Schematic overview of the reactor set-up for HDO of LPP oil with H_2 bottle.[62]

Materials

For HDO, LPP oil from the bioCRACK[16,18] pilot plant was used. It was produced by liquid phase pyrolysis of spruce wood at 375 °C. A cobalt molybdenum on aluminium oxide catalyst from Alfa Aesar with a particle size of 200–600 μm was used in sulfided form.

Inline sulfidation was performed with 35 w% DTBDS in an iso-paraffine mixture of C_{15} to C_{20} alkanes.

During sulfidation, hydrogen 5.0 was used, during HDO synthesis gas was used as hydrogen supply. The high pressure synthesis test gas bomb was provided by Airliquide Austria GmbH, based on the TU Wien gasification results, the composition is shown in Table 4. Detailed information of the

catalyst can be found in Table 5. The composition and important parameters of LPP oil are listed in Table 6.

Analytical methods

The ultimate analysis of all streams was carried out by a vario MACRO CHN-analyzer, "Elementar Analysensysteme GmbH". The water content of the aqueous product phase was determined by a gas-phase chromatograph, type Agilent 7890A, with a TCD-detector and a HP-INNOWAX column, 30 m × 0.530 mm × 1 μm. The boiling range of the hydrocarbon product phase was determined by a gas-phase chromatograph, type Agilent 7890A, with a FID-detector and a Restek-column MXT-2887, 10 m × 0.53 mm × 2.65 μm. The total acid number (TAN) was quantified by titration. The water content of the oil fraction was determined by Karl-Fischer-titration with a Schott Titro Line KF-Titrator and Hydranal titration reagent. Density was measured by a digital viscometer, SVM 3000, Anton Paar GmbH. The composition of the hydrocarbon product phase was determined by a gas-phase chromatograph with a quadrupole mass spectrometer (GC-MS), type Schimadzu GCMS QP 2010 Plus, with a VF-1701 MS column, 60 m × 0.25 mm × 0.25 μm.

The composition of the gas phase was analysed by a micro gas-phase chromatograph, type Agilent 3000A, with a TCD-detector, a molecular sieve column and a plot u column. Sulfur content, micro carbon residue, H-NMR, metal screening and surface area of catalysts were determined externally by the "Centralni ispitni laboratorij" of INA industrija nafte d.d. Sulfur content was determined according to ASTM D 2622:2016, micro carbon residue according to HRN EN ISO 10370:2014, catalyst surface area according to ASTM D 3663 modified: 2015 and metal screening was performed by wave dispersive X-ray.

The viscometer has a density reproducibility of 0.0005 g cm^{-3} in the observed density range. GC-MS analysis was used for semi-quantitative determination only. Simulated distillation was performed once. All other internal analyses were performed with 3-fold determination with a maximum deviation of 0.5%, from which the average was built and displayed.

Hydrodeoxygenation of LPP oil results and discussion

For HDO of LPP oil with synthesis gas, a gas to LPP oil weight-ratio of 1 to 1.6 was applied. In the high carbon ratio of synthesis gas to LPP oil in the balance given in Table 7, one can see the high portion of carbon that was fed with the synthesis gas. Assuming, that no carbon is transferred from gas to liquid phase, the carbon yield of the hydrocarbon product phase with respect to LPP oil amounts 44 w%, which is in the range of LPP oil HDO with hydrogen.[51,52]

Table 5 Catalyst details for HDO

Catalyst	
Supplier	Alfa Aesar
Cobalt oxide [w%]	4.4
Molybdenum oxide [w%]	11.9
Surface area [m^2 g^{-1}]	279
Batch number	45 579

Table 6 Composition and physical properties of LPP oil

LPP oil		
Properties	Unit	Value
Water content	[w%]	57.0
Lower heating value	[MJ kg^{-1}]	7.4
Density	[kg m^{-3}]	1092
Viscosity	[mPa s]	3.5
Carbon content	[w%]	22.3
Hydrogen content	[w%]	9.4
Oxygen content (balance)	[w%]	67.8
Nitrogen content	[w%]	<1

Properties of the HDO fuel fraction

The impact of syngas on the HDO of LPP oil was the main challenge. The results of the syngas HDO experiments are compared to an experiment with pure hydrogen, referred to as hydrogen HDO in this work, at 400 °C and LHSV 1 h^{-1}, since it had been observed in former experiments, that the temperature in the range of 350 to 400 °C and the LHSV in the range of 0.5 to 1 h^{-1} has a minor impact on the product quality and technical feasibility. The lower amount of hydrogen applied for HDO might be reflected in the product composition; on the other hand, the *in situ* generated hydrogen could improve HDO. Competing reactions, as discussed later, might also influence the product quality. Through HDO with synthesis gas, organic components in LPP oil were hydrophobized to a degree that led to phase separation. An overview of the product quality can be found in Table 8. Beside the elemental composition, typical fuel parameters such as density, micro carbon residue and metal content are listed. Results of the H-NMR analysis can be found in Table 10. Through water separation and HDO, the water content from LPP oil was decreased drastically to below 0.5 w%. On the other hand, the water fraction contained about 95 w% of water. Carbon content as well as the organic hydrogen content was significantly increased from 22.3 w% to 85.4 w%. LPP oil itself contained about 35 ppm sulphur. Through addition of a sulfidation agent for a more effective HDO, the sulphur content was increased. Compared to the product of hydrogen

Table 7 Overall mass balance and carbon balance of syngas HDO

	Unit	Mass balance	Carbon balance
LPP oil	[w%]	61.27	43.63
Synthesis gas	[w%]	38.73	56.37
Hydrocarbon product phase	[w%]	6.56	19.13
Aqueous phase	[w%]	42.64	3.80
Gaseous phase	[w%]	44.44	61.53
Coking	[w%]	0.93	1.14
Balance inaccuracy	[w%]	5.44	14.39

Table 8 Composition and properties of LPP oil and syngas HDO product compared to hydrogen HDO product and Diesel

Parameter	Unit	LPP oil	HDO syngas	HDO hydrogen	Diesel
C	[w%]	22.3	85.4	86.6	86.3[a]
H	[w%]	9.4	11.9	12.8	13.7[a]
N	[w%]	<1	<1	<1	<1[a]
S	[mg kg^{-1}]	34.6	132.3	42.4	10 (ref. 63)
O (by difference)	[w%]	67.8	2.3	0.0	0.0[a]
Water content	[w%]	56.96	0.28	0.02	≤0.02 (ref. 63)
TAN	[mg g^{-1}]	80.8	0.0	0.0	n.a.
Density	[kg m^{-3}]	1092	877.2	831.1	820–845 (ref. 63)
Lower heating value (equation of Boie[64])	[MJ kg^{-1}]	7.4	40.7	42.2	43.2[a]
Micro carbon residue	[w%]	n.a.	0.04	<0.01	≤0.30 (ref. 63)
Metal content	[w%]	Ni: 0.006	No metals found	No metals found	n.a.

[a] Determined by elemental analysis: Diesel with HVO additives.

Table 9 GC-MS analysis of HDO products-semi quantitative analysis

HDO gas	Syngas			Hydrogen		
Molecule	Period 1	Period 2	Period 3	Period 1	Period 2	Period 3
Pentane	22.2	20.2	n.d.	49.1	43.7	30.7
2-Methylpentane	12.5	9.2	5.1	31.2	24.7	14.8
Cyclopentane	16.8	17.6	n.d.	48.1	41.4	30.5
Hexane	14.2	9.0	4.3	42.3	35.1	22.2
Methylcyclohexane	52.7	27.2	19.8	67.0	46.9	32.9
Ethylcyclopentane	27.3	20.6	14.4	40.4	36.7	29.0
1-Butanol	n.d.	6.7	12.9	n.d.	n.d.	n.d.
1-Ethyl-3-methylcyclopentane	14.1	10.5	9.1	18.5	18.2	14.4
Toluoene	8.3	5.0	5.0	37.2	18.2	13.6
Propylcyclopentane	18.6	17.3	16.1	27.8	26.0	20.7
Ethylcyclohexane	46.8	30.7	25.7	55.0	40.8	35.4
1-Ethylcyclohexene	n.d.	9.7	12.9	n.d.	n.d.	6.8
1-Methyl-2-propylcyclopentane	16.3	11.6	10.5	22.3	20.2	15.0
1-Ethyl-4-methylcyclohexane	15.6	n.d.	n.d.	20.5	15.8	9.2
2-Methyl-1-pentanol	n.d.	n.d.	12.1	n.d.	n.d.	n.d.
Propylcyclohexane	47.7	25.1	18.2	60.2	43.1	29.8
1-Hexanol	n.d.	n.d.	12.8	n.d.	n.d.	n.d.
2-Butyl-1-octanol	18.1	10.6	7.1	n.d.	30.0	19.1
Tetrahydro-2-furanmethanol	95.0	114.7	128.9	26.2	25.4	26.5
3-Methylphenol	n.d.	8.8	9.2	n.d.	n.d.	6.9
3-Ethylphenol	n.d.	6.3	7.7	n.d.	n.d.	15.9
4-Propylphenol	n.d.	16.1	16.9	n.d.	n.d.	16.7

n.d. = not detected.

HDO, slightly inferior product quality was achieved. In both cases a very low micro carbon residue was found in the product compared to EN 590 (ref. 63) standard Diesel. Native LPP oil has a high acid number of 80.8 mg KOH g^{-1}. In the products, no acid was found.

Despite the high corrosivity, catalyst leaching can be excluded as metals were neither found in the organic nor aqueous product phase, controlled by wave dispersive X-ray analysis.

Table 10 H-NMR results of syngas HDO compared to hydrogen HDO

	H aromatic	H phenolic or olefinic	H aliphatic
Unit	[mol%]	[mol%]	[mol%]
HDO syngas	4.62	0.83	94.55
HDO hydrogen	4.90	0.02	95.06

Concerning density and heating value, the quality of diesel was not fully met with syngas HDO. Semi-quantitative GC-MS analysis of the products is shown in Table 9. The most significant molecules found in LPP oil are listed. For comparison, the total ion content peak areas were normalized with the internal standard flouranthene.

LPP oil mainly contains oxygenated components, such as guaiacols, levoglucosan, organic acids, hydroxyacetone and phenolics.[17] The hydrodeoxygenated products are to a big part composed of acyclic and cyclic alkanes, alkenes as well as some acyclic alcohols and phenols. Generally, the amount of alkanes is higher in products of HDO with pure hydrogen, whereas experiments performed with syngas consisted of more alkenes and phenols. With ongoing experiment, more alcohols and phenols were found, such as 1-butanol, 2-methyl-1-pentanol, 1-hexanol and 2-butyl-1-octanol. Several

substituted phenols were found in products of syngas HDO already after the 2nd period, whereas in hydrogen HDO they were not present until the 3rd period of the experiment. Big amounts of tetrahydro-2-furanmethanol were found in the hydrocarbon and aqueous product phases of syngas HDO, as it is soluble in both, polar and non-polar, liquids.

H-NMR results in Table 10 show nearly the same aliphatic hydrogen content, but an interesting difference in the aromatic- and olefinic hydrogen content. Whereas HDO with syngas seems to be more effective concerning cyclic alkene saturation, olefins are more likely to be saturated when pure hydrogen is applied. All in all the differences are minor, but with about 0.02% of phenolic or olefinic hydrogen in the product of pure hydrogen HDO these structures can assumed to be fully hydrogenated in contrast to when syngas is applied.

The boiling range (Fig. 5) shows more high boiling components in the product of syngas HDO, than for pure hydrogen based HDO. For sure, the higher content of alcohols and other oxygen containing high boiling components is remarkable. Less cracking reactions occurred, because of more competing reactions and the lower reaction temperature.

Water-gas shift reaction

During the WGS reaction shown in eqn (3), CO is converted into CO_2 with a stoichiometric ratio of 1. Competing reactions to be considered might be the Boudouard reaction or the Sabatier reaction shown in eqn (9) and (10). According to the Boudouard reaction,[53] two molecules of CO form one molecule of CO_2 and solid carbon. The stoichiometric ratio is therefore 2 : 1 for gaseous components in this reaction. The chemical equilibrium is shifted towards CO_2 with decreasing temperature (below 400 °C) and increasing pressure, as it is an exothermic and volume increasing reaction. At room temperature, CO is fully resistant as a metastable molecule due to the low reaction rate.

$$2CO \leftrightarrow C + CO_2 \quad (9)$$

In the Sabatier reaction, the stoichiometric ratio of CO to CH_4 is 1. This reaction takes place at pressures below 50 bar and at 250 to 300 °C over Nickel catalysts.[53] As formation of methane from CO and H_2 goes along with the formation of water, a high excess of water should shift the chemical equilibrium composition to the left side of the reaction and therefore prevent methanation of CO. In the opposite direction, the reaction might also produce hydrogen from methane and water. This reaction though takes place at higher temperatures (700–830 °C in the presence of a catalyst).

$$CO + 3H_2 \leftrightarrow CH_4 + H_2O \quad (10)$$

The WGS reaction is exothermic with 41.2 kJ mol^{-1},[53] which amounts 1.47 MJ kg^{-1}(CO) compared to 0.84 MJ kg^{-1} (LPP oil)[65] for the exothermic HDO of LPP oil. For the adjusted gas and LPP oil flow for HDO with synthesis gas, the energy output of HDO amounts about 8.4 kJ h^{-1}, the additional energy output of the WGS amounts 2.4 kJ h^{-1}. During the switch from hydrogen for sulfidation to synthesis gas for HDO, a temperature increase of about 20 °C was observed.

WGS reaction is evaluated by the stoichiometry of the reactants. By a high access of water, which is achieved by the usage of LPP oil and a lower gas to liquid ratio, the reaction equilibrium could be forced to the CO_2 and H_2 domain, making more hydrogen available for HDO reactions.

The key figures confirming WGS reaction are listed in Table 11. These are the hydrogen consumption, CO/CO_2 ratio and CH_4 production. The hydrogen consumption was decreased by the usage of synthesis gas by about 28 w%. According to stoichiometry, the CO/CO_2 ratio during Boudouard reaction is 2 : 1, whereas during the HDO experiment with synthesis gas a ratio of 1 : 1.08 was observed, which comes close to the ratio of 1 : 1 for WGS reaction. Therefore, Boudouard reaction can be excluded, although at low temperatures and at high pressure the chemical equilibrium is on the right hand side of solid carbon and CO_2. The molar ratio of CO consumed for methane production was 44.9, which is far off the stoichiometric ratio of 1 during Sabatier reaction. The increase in methane was about 1.22 w%. It was shown, that during HDO of LPP oil methane and CO_2, as well as CO and ethylene, ethane, propane and butane, are produced.[51] The additional methane and CO_2 production, which was observed, is attributed to HDO side reactions. This means, that no methane was produced by hydrogenation of CO, thus the Sabatier reaction can be excluded.

In Fig. 6, the outlet gas composition of HDO of the main components is compared to the inlet gas composition

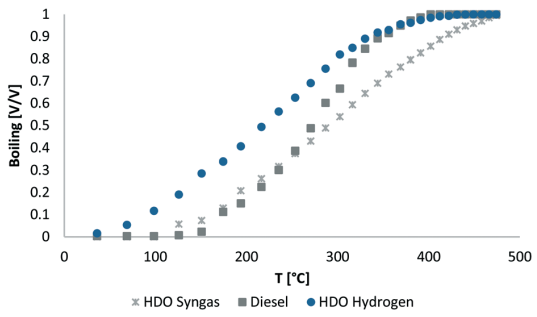

Fig. 5 Boiling range of syngas HDO product phase compared to hydrogen HDO product phase and Diesel.

Table 11 Gas phase changes during HDO of LPP oil with synthesis gas: hydrogen consumption, CO/CO_2 ratio, increase in CH_4 amount

H_2 consumption/LPP oil	[mg g^{-1}]	HDO hydrogen	16.91
		HDO syngas	12.25
CO(consumed)/CO_2(produced)	[mol/mol]	HDO syngas	1.08
CO(consumed)/CH_4(produced)	[mol/mol]	HDO syngas	44.92

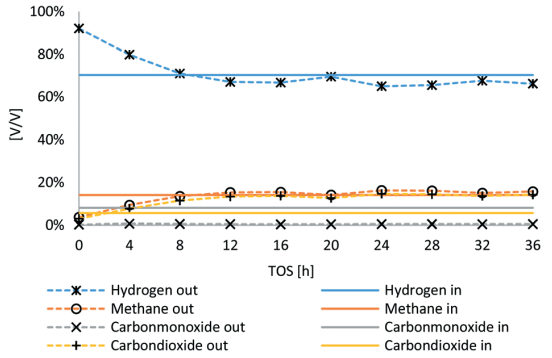

Fig. 6 Gas phase composition of HDO inlet gas (synthesis gas) and outlet gas.

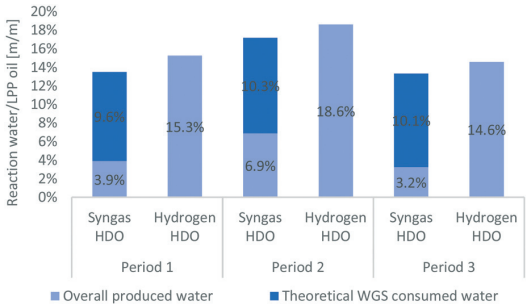

Fig. 7 Formation and consumption of water during HDO using syngas over the WGS reaction compared to HDO with pure hydrogen.

(synthesis gas). TOS is defined as time on stream. In the first 8 hours, the gas phase composition is not stable yet, as the hydrogen used for sulfidation was not fully replaced due to the low gas feed. Therefore, the balance period was made for the experimental time span of 12–36 hours. CO was nearly fully converted, merely about 0.5 vol% were detected in the outlet gas stream of HDO, whereas the portion of CO_2 increased from 5.5 to about 14 vol%. The net hydrogen content increased slightly, whereas the net methane content was nearly untampered with about 14 to 16 vol%.

Subsequently, the water balance was observed, as water is on the one hand produced during HDO and on the other hand consumed during WGS reaction. Following the reaction stoichiometry, the amount of consumed water was calculated for the case that all CO is transferred into CO_2 by WGS reaction according to eqn (11).

$$m(\text{Theroetical WGS consumed } H_2O) = n(CO_{in}) \cdot M(H_2O) \quad (11)$$

m(Theoretical WGS consumed H_2O) = mass of water consumed by WGS reaction if 100% of the introduced CO is consumed in g.

$n(CO_{in})$ = molar amount of fed CO in mol.

$M(H_2O)$ = molar mass of consumed water in g mol^{-1}.

With respect to LPP oil, 3 to 7 w% of water was produced when syngas was applied, whereas it was 14 to 19 w% when hydrogen was applied, as shown in Fig. 7. In comparison to HDO with pure hydrogen, 68.6 w% less water was produced. Considering that water was consumed by WGS reaction when syngas was applied, a higher amount of water must have been originally produced by HDO. This would amount about 65.8 w% more water, assuming that all CO was converted into hydrogen and CO_2 by WGS reaction. With respect to LPP oil, this would mean that between 9.6 to 10.3 w% of water are consumed. This sums up to 13 and 17 w% of water, which must have been produced, before consumed for WGS reaction, which is comparable with the results of hydrogen HDO and again confirms the conversion of water and CO through the WGS reaction.

Catalyst deactivation

A major obstacle in HDO of pyrolysis oil is catalyst deactivation through coke deposition. Table 12 shows the surface area of fresh catalyst compared to that of the used catalysts from syngas and hydrogen HDO. A clear decrease in surface area after HDO can be observed. According to Olarte *et al.*,[29] plugs usually consist of inorganic constituents and polymerized bio-oil condensation products. As LPP oil doesn't contain appreciable amounts of inorganic matter in contrast to fast pyrolysis oils[7] (see metal content in Table 8), the main factor for coke formation is unstable organic matter. Additionally, due to the usage of synthesis gas, a high load of organic matter is introduced to the reactor. While it is highly unlikely that alkanes and alkenes with a small chain length (methane, ethane and ethylene) condense in the reactor and form coke, a main factor could be the Boudouard reaction. If this reaction takes place even in small amounts, the coke formed could still lead to plugging and force the system to break down due to a high pressure drop. It was therefore concluded, that a high excess of water is necessary to force the reaction equilibrium to the side of hydrogen and CO_2 and to suppress Boudouard reaction. This was achieved by the high water content of LPP oil and a nearly triple fold LPP oil to hydrogen ratio compared to previous experiments.

The surface area of the catalyst was reduced by 45% in the experiment with synthesis gas, compared to 41% in an experiment with hydrogen. The difference is negligible considering measurement uncertainty. For more information, the amount of organic matter and carbon on the catalyst were determined. For the determination of combustibles, catalysts were incinerated in a muffle type furnace at 550 °C for 48 h. Thus, the catalyst in the main reaction zone in the middle of the

Table 12 Catalyst surface fresh catalyst as well as used catalyst from syngas and hydrogen HDO

ASTM D3663	[m^2 g^{-1}]
Fresh	239
HDO syngas	131
HDO hydrogen	141

reactor was analysed. The results were quite surprising. The amount of combustibles is the same on both catalysts, but less carbon seemed to be deposited on the catalyst in HDO with syngas, as shown in Table 13. The net carbon content of the coke was about 54 w% in hydrogen HDO but only 38 w% in syngas HDO. A big part of the combustibles is most probably sulphur from sulfidation. About 7 w% is contributed by hydrogen. The difference is assumed to be oxygen. Origin of coke deposition cannot be allocated to Boudouard reaction or standard coking from HDO side reactions only by catalyst analyses.

Coke deposition has a huge impact on product quality, as less catalyst surface is available if plugs are formed. A decreasing product quality was observed for all experiments with LPP oil,[51,52] whereas the rate is different. In Fig. 8, the oxygen content as well as the water content of products from syngas HDO is compared to that of hydrogen HDO. In the first period of both experiments, the oxygen content was zero and water content below 0.1 w%. This indicates the same degree of HDO at the start of the experiment. On the one hand, this can be described by switch from hydrogen to syngas. After 5 hours of lead-time, there was still a higher amount of hydrogen in the system, as can be observed in the product gas composition from HDO experiments in Fig. 6. On the other hand, this might also indicate, that on a freshly sulfided catalyst, syngas and pure hydrogen are more or less equally effective. According to Sheu *et al.*,[66] deoxygenation is a function of the oxygen content and partial hydrogen pressure. This would explain the lower oxygen removal due to the lower hydrogen to LPP oil ratio during Syngas HDO. Grilc *et al.*[48–50] observed comparable oxygen removal when using nitrogen as process gas, conducted with higher decarbonylation and decarboxylation reactions resulting in lower liquid product yield. They also observed high HDO rates for molybdenum sulphide catalysts. In order to enhance the water gas shift reaction, the water to CO ratio was increased, compared to hydrogen based HDO experiments, and therefore only about 35 w% of pure hydrogen was available per g LPP oil for HDO compared to the reference experiment with hydrogen.

According to Wijayapala *et al.*, HDO with synthesis gas seems to be slower, but delivers competitive conversions compared to H_2 (ref. 57). Therefore, an even lower LHSV might be necessary for the same product quality than with hydrogen.

After 36 h TOS, the oxygen content of the product from syngas HDO, determined by difference, amounts 3.7 w%, whereas the oxygen content of the product from hydrogen experiment amounts 0.4 w%. The increasing oxygen content originates mainly in alcohols, as shown in Table 9, which also facilitates water absorption.

Table 13 Organic matter and carbon content of the used catalyst from syngas and hydrogen HDO

	Unit	Syngas HDO	Hydrogen HDO
Combustibles	[w%]	24.4	24.8
Carbon content	[w%]	9.3	13.4
Carbon content/combustibles	[w%]	38.2	54.2

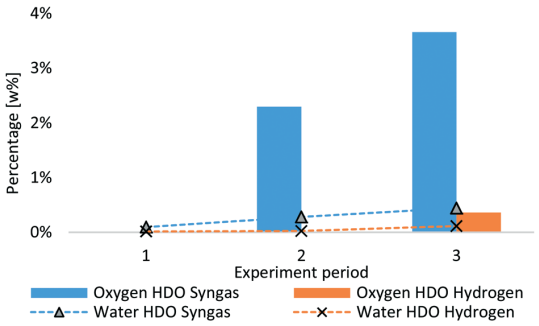

Fig. 8 Oxygen and water content of HDO products from syngas and hydrogen experiment.

Summary and conclusions

By dual fluidized bed steam gasification of softwood, a biogenous synthesis gas with a high hydrogen content of about 70 vol% was produced. A gas with the composition of the synthesis gas was directly used for HDO of LPP oil, produced by LPP of spruce wood. HDO of LPP oil was then performed successfully for 36 h in a first experiment. Pre-treatment of LPP oil was not necessary due to the high water content and negligible particle content. The quality of LPP oil concerning fuel standards was increased significantly. Although high coke deposition can be excluded, product quality still decreased over time. Compared to HDO with pure hydrogen, a slightly lower degree of hydrodeoxygenation was achieved. The reason for this might be the lower hydrogen to LPP oil ratio, which was 37 w% compared to hydrogen HDO, in order to enhance WGS reaction. The consumption of hydrogen for HDO was reduced by 28 w%, while nearly all the CO was consumed for hydrogen production according to stoichiometry. Competing reactions like the Boudouard reaction or Sabatier reaction were not observed. Reasons for that are on the one hand the reaction conditions, especially the temperature when discussing the Sabatier reaction, and on the other hand the surpassingly high water content of LPP oil, which supresses the Boudouard reaction. A synthesis gas with a higher CO content and lower CO_2 content might lead to lower or even zero hydrogen consumption for advanced biofuel production from liquid phase pyrolysis oil.

Conflicts of interest

There are no conflicts to declare.

Acknowledgements

This work was funded by the Austrian Research Promotion Agency (FFG) under the scope of the Austrian Climate and Energy Fund. Furthermore, this work was supported by the

European Union's Horizon 2020 research and innovation programme. The authors want to acknowledge Mario Lukasch, Samir Reiter, Thomas Sterniczky, Sarah Koller and Daniela Grosinger for their outstanding work with HDO experiments, as well as Johannes Schmid, Josef Fuchs and Florian Benedikt for their excellent work regarding the DFB steam gasification process.

Notes and references

1 United Nations, *Kyoto Protocol to the United Nations Framework Convention on Climate Change*, United Nations, 1998.
2 UNFCCC, *ADOPTION OF THE PARIS AGREEMENT: Proposal by the President to the United Nations Framework Convention on Climate Change*, 2015, 21932, 1–32.
3 in *Official Journal of the European Union*, Brussels, Belgium, 2009, pp. 16–62.
4 O. F. T. H. E. *Council*, 2018, 2018.
5 H. Hofbauer, in *Encyclopedia of Sustainability Science and Technology*, Springer, 2017, pp. 459–478.
6 A. V. Bridgwater, D. Meier and D. Radlein, *Org. Geochem.*, 1999, **30**, 1479–1493.
7 A. V. Bridgwater and G. V. C. Peacocke, *Renewable Sustainable Energy Rev.*, 2000, **4**, 1–73.
8 S. Czernik and A. V. Bridgwater, *Energy Fuels*, 2004, **18**, 590–598.
9 A. V. Bridgwater, *J. Anal. Appl. Pyrolysis*, 1999, **51**, 3–22.
10 A. V. Bridgwater, *Biomass Bioenergy*, 2011, **38**, 68–94.
11 K. Klaigaew, P. Wattanapaphawong, N. Khuhaudomlap, N. Hinchiranan, P. Kuchontara, K. Kangwansaichol and P. Reubroycharoen, *Liquid Phase Pyrolysis of Giant Leucaena Wood to Bio-Oil over NiMo/Al2O3 Catalyst*, Elsevier B.V., 2015, vol. 79.
12 W. Ratanathavorn, C. Borwornwongpitak, C. Samart and P. Reubroycharoen, *Chem. Technol. Fuels Oils*, 2016, **52**, 360–368.
13 B. Szabó, M. Takács, A. Domján, E. Barta-rajnai and J. Valyon, *J. Anal. Appl. Pyrolysis*, 2018, 1–9.
14 N. Schwaiger, V. Witek, R. Feiner, H. Pucher, K. Zahel, A. Pieber, P. Pucher, E. Ahn, B. Chernev, H. Schroettner, P. Wilhelm and M. Siebenhofer, *Bioresour. Technol.*, 2012, **124**, 90–94.
15 N. Schwaiger, R. Feiner, K. Zahel, A. Pieber, V. Witek, P. Pucher, E. Ahn, P. Wilhelm, B. Chernev, H. Schröttner and M. Siebenhofer, *BioEnergy Res.*, 2011, **4**, 294–302.
16 J. Ritzberger, P. Pucher and N. Schwaiger, *Chem. Eng. Trans.*, 2014, **39**, 1189–1194.
17 N. Schwaiger, D. C. Elliott, J. Ritzberger, H. Wang, P. Pucher and M. Siebenhofer, *Green Chem.*, 2015, **17**, 2487–2494.
18 K. Treusch, J. Ritzberger, N. Schwaiger, P. Pucher and M. Siebenhofer, *R. Soc. Open Sci.*, 2017, **4**, 171122.
19 A. M. Mauerhofer, F. Benedikt, J. C. Schmid, J. Fuchs, S. Müller and H. Hofbauer, *Energy*, 2018, **157**, 957–968.
20 F. Benedikt, J. Fuchs, J. C. Schmid, S. Müller and H. Hofbauer, *Korean J. Chem. Eng.*, 2017, **34**, 2548–2558.
21 F. Benedikt, J. C. Schmid, J. Fuchs, A. M. Mauerhofer, S. Müller and H. Hofbauer, *Energy*, 2018, **164**, 329–343.
22 J. Fuchs, J. C. Schmid, F. Benedikt, S. Müller, H. Hofbauer, H. Stocker, N. Kieberger and T. Bürgler, *Energy*, 2018, **162**, 35–44.
23 S. Koppatz, C. Pfeifer, R. Rauch, H. Hofbauer, T. Marquard-Moellenstedt and M. Specht, *Fuel Process. Technol.*, 2009, **90**, 914–921.
24 J. C. Schmid, J. Fuchs, F. Benedikt, A. M. Mauerhofer, S. Müller, H. Hofbauer, H. Stocker, N. Kieberger and T. Bürgler, 2017.
25 S. Oh, H. Hwang, H. S. Choi and J. W. Choi, *Fuel*, 2015, **153**, 535–543.
26 S. Oh, H. S. Choi, I.-G. Choi and J. W. Choi, *RSC Adv.*, 2017, **7**, 15116–15126.
27 C. Boscagli, C. Yang, A. Welle, W. Wang, S. Behrens, K. Raffelt and J. D. Grunwaldt, *Appl. Catal., A*, 2017, **544**, 161–172.
28 C. Boscagli, K. Raffelt and J. D. Grunwaldt, *Biomass Bioenergy*, 2017, **106**, 63–73.
29 M. V. Olarte, A. H. Zacher, A. B. Padmaperuma, S. D. Burton, H. M. Job, T. L. Lemmon, M. S. Swita, L. J. Rotness, G. N. Neuenschwander, J. G. Frye and D. C. Elliott, *Top. Catal.*, 2016, **59**, 55–64.
30 D. C. Elliott, *Energy Fuels*, 2007, **21**, 1792–1815.
31 D. Carpenter, T. Westover, D. Howe, S. Deutch, A. Starace, R. Emerson, S. Hernandez, D. Santosa, C. Lukins and I. Kutnyakov, *Biomass Bioenergy*, 2017, **96**, 142–151.
32 P. A. Meyer, L. J. Snowden-Swan, K. G. Rappé, S. B. Jones, T. L. Westover and K. G. Cafferty, *Energy Fuels*, 2016, **30**, 9427–9439.
33 D. C. Elliott, T. R. Hart, G. G. Neuenschwander, L. J. Rotness and A. H. Zacher, *Environ. Prog. Sustainable Energy*, 2009, **28**, 441–449.
34 M. V. Olarte, A. B. Padmaperuma, J. R. Ferrell, E. D. Christensen, R. T. Hallen, R. B. Lucke, S. D. Burton, T. L. Lemmon, M. S. Swita, G. Fioroni, D. C. Elliott and C. Drennan, *Fuel*, 2017, 620–630.
35 D. Howe, T. Westover, D. Carpenter, D. Santosa, R. Emerson, S. Deutch, A. Starace, I. Kutnyakov and C. Lukins, *Energy Fuels*, 2015, **29**, 3188–3197.
36 D. Carpenter, T. Westover, D. Howe, S. Deutch, A. Starace, R. Emerson, S. Hernandez, D. Santosa, C. Lukins and I. Kutnyakov, *Biomass Bioenergy*, 2016, **96**, 142–151.
37 G. Kim, J. Seo, J. W. Choi, J. Jae, J. M. Ha, D. J. Suh, K. Y. Lee, J. K. Jeon and J. K. Kim, *Catal. Today*, 2017, 0–1.
38 K. Routray, K. J. Barnett and G. W. Huber, *Energy Technol.*, 2017, **5**, 80–93.
39 S. Oh, H. S. Choi, I.-G. Choi and J. W. Choi, *RSC Adv.*, 2017, **7**, 15116–15126.
40 S. Cheng, L. Wei, J. Julson and M. Rabnawaz, *Energy Convers. Manage.*, 2017, **150**, 331–342.
41 F. De Miguel Mercader, P. J. J. Koehorst, H. J. Heeres, S. R. A. Kersten and J. A. Hogendoorn, *AIChE J.*, 2011, **57**, 3160–3170.
42 J. Neumann, N. Jäger, A. Apfelbacher, R. Daschner, S. Binder and A. Hornung, *Biomass Bioenergy*, 2016, **89**, 91–97.
43 I. Kim, A. A. Dwiatmoko, J. W. Choi, D. J. Suh, J. Jae, J. M. Ha and J. K. Kim, *J. Ind. Eng. Chem.*, 2017, **56**, 74–81.

44 W. Yin, A. Kloekhorst, R. H. Venderbosch, M. V. Bykova, S. A. Khromova, V. A. Yakovlev and H. J. Heeres, *Catal. Sci. Technol.*, 2016, **6**, 5899–5915.

45 J. Michl, J. Neumann, H. Rottengruber and M. Wensing, *Appl. Therm. Eng.*, 2016, **98**, 502–512.

46 S. A. Rezzoug and R. Capart, *Appl. Energy*, 2002, **72**, 631–644.

47 M. Kunaver, E. Jasiukaityte and N. Čuk, *Bioresour. Technol.*, 2012, **103**, 360–366.

48 M. Grilc, B. Likozar and J. Levec, *Biomass Bioenergy*, 2014, **63**, 300–312.

49 M. Grilc, B. Likozar and J. Levec, *Appl. Catal., B*, 2014, **150–151**, 275–287.

50 M. Grilc, G. Veryasov, B. Likozar, A. Jesih and J. Levec, *Appl. Catal., B*, 2015, **163**, 467–477.

51 K. Treusch, N. Schwaiger, K. Schlackl, R. Nagl, A. Rollett, M. Schadler, B. Hammerschlag, J. Ausserleitner, A. Huber, P. Pucher and M. Siebenhofer, *React. Chem. Eng.*, 2018, 258–266.

52 K. Treusch, N. Schwaiger, K. Schlackl, R. Nagl and P. Pucher, *Front. Chem.*, 2018, **6**(297), 1–8.

53 A. F. Holleman, E. Wiberg and N. Wiberg, *Holleman-Wiberg: Lehrbuch der Anorganischen Chemie*, de Gruyter, Berlin, 102nd edn., 2007.

54 P. H. Steele, S. K. Gajjela, T. E. Mlsna, C. U. Pittman and F. Yu, *Pat. US* 2014/0073827A1, 2014.

55 S. K. Tanneru and P. H. Steele, *Renewable Energy*, 2015, **80**, 251–258.

56 Y. Luo, E. B. Hassan, V. Guda, R. Wijayapala and P. H. Steele, *Energy Convers. Manage.*, 2016, **115**, 159–166.

57 R. Wijayapala, A. G. Karunanayake, D. Proctor, F. Yu, C. U. Pittman and T. E. Mlsna, in *Handbook of Climate Change Mitigation and Adaptation*, ed. W.-Y. Chen, T. Suzuki and M. Lackner, Springer New York, New York, NY, 2016, pp. 1–34.

58 S. Müller, J. Fuchs, J. C. Schmid, F. Benedikt and H. Hofbauer, *Int. J. Hydrogen Energy*, 2017, **42**, 29697–29707.

59 T. Pröll and H. Hofbauer, *Int. J. Chem. React. Eng.*, 2008, **6**, A89.

60 M. Kolbitsch, *Doctoral thesis*, TU Wien, 2016.

61 S. Müller, *Doctoral thesis*, TU Wien, 2013.

62 M. Lukasch, *Master thesis*, Graz University of Technology, 2018.

63 *EN 590*, 2004.

64 K.-H. Grote and J. Feldhusen, *Dubbel Taschenbuch für Maschinenbau, Springer*, 22nd edn., 2007.

65 K. Schlackl, *Master thesis*, Graz University of Technology, 2016.

66 Y.-H. E. Sheu, R. G. Anthony and E. J. Soltes, *Fuel Process. Technol.*, 1988, **19**, 31–50.

Chapter 9

Summary and Conclusions

9. Summary and Conclusions

Production of advanced biofuels via liquid phase pyrolysis, as applied in the bioCRACK process, and subsequent product upgrading through hydrodeoxygenation of liquid phase pyrolysis oil was shown in this thesis.

During the bioCRACK process, spruce wood was pyrolysed in vacuum gas oil as heat carrier oil in the temperature range of 350 to 390°C with the objective of a high cracking rate and maximum carbon transfer into the carrier oil. In the pilot plant, which had a capacity of 100 kg h^{-1} wood and 600 kg h^{-1} vacuum gas oil, spruce wood was liquefied to an extent of 50 to 65 wt% with respect to the biogenous carbon. Increasing temperature resulted in increasing liquefaction. Between 30 and 39 wt% of the carbon contained in spruce wood was transferred into residual and cracked phases of the carrier oil, which could be directly upgraded in existing petroleum refinery units. Another 20 to 26 wt% were converted to liquid phase pyrolysis oil.

Liquid phase pyrolysis oil was then hydrodeoxygenated in a lab scale plug flow reactor in the presence of a sulfided $CoMo/Al_2O_3$ catalyst under 120 bar hydrogen pressure. The influence of the temperature and residence time was examined. In all cases, a phase separation was achieved, yielding in a hydrocarbon product phase and an aqueous phase. It was shown that the temperature has a minor influence in the range between 350 and 400°C with only slightly inferior product properties at lower temperature, apparent by residual oxygen with ongoing experiment duration. Water content was below 0.05 wt% and lower heating value was between 42 and 43 MJ kg^{-1}.

Liquid hourly space velocity was negligible between 0.5 and 1 h^{-1}, but showed decreasing product properties such as increasing oxygen content and decreasing H/C ratio and thus decreasing heating value at LHSV 2 and 3 h^{-1}.

Feasibility of integrating liquid phase pyrolysis oil hydrodeoxygenation into petroleum refineries was investigated. In a two-step process, consisting of mild hydrotreatment at 300°C and co-hydrotreatment with heavy gas oil at 400°C, liquid phase pyrolysis oil was upgraded to a fuel with 8 to 9 wt% of renewable carbon at 120 and 80 bar, respectively, as depicted in Figure 1. In the second and hence co-processing step, constant product quality over the experiment duration of 36 h in stationary operation mode was achieved. No catalyst deactivation was observed. In the first step though, product quality decreased rapidly, indicating catalyst deactivation when liquid phase pyrolysis oil is processed at lower temperatures.

Finally, synthesis gas was applied to reduce reliance on precious pure hydrogen. Therefore, liquid phase pyrolysis oil was hydrodeoxygenated with a hydrogen rich synthesis gas from TU Wien, produced by biomass gasification. By making use of the water-gas shift reaction, hydrogen consumption was reduced and the necessity of highly purified hydrogen was contradicted.

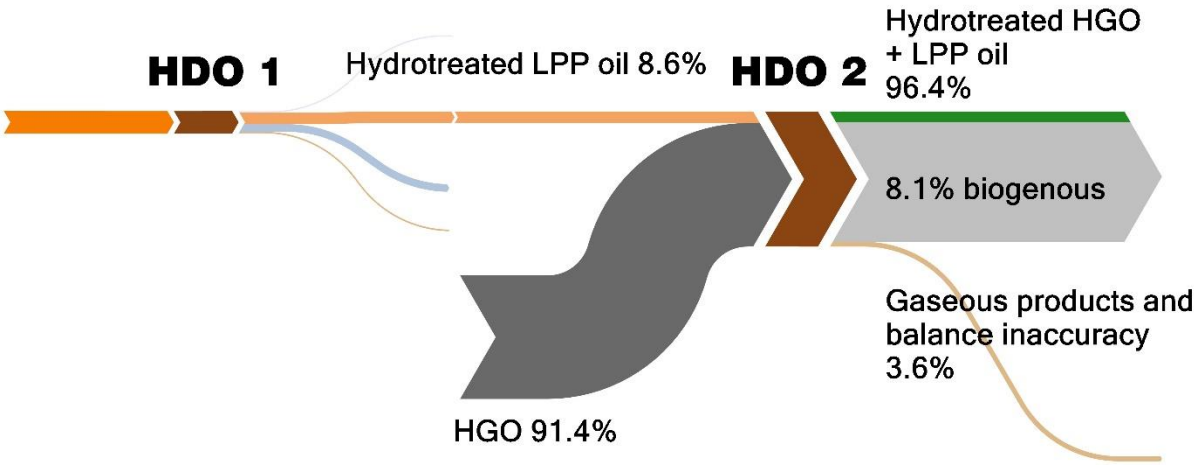

Figure 1: Carbon balance of the 2-step hydrodeoxygenation of liquid phase pyrolysis oil (LPP oil) and heavy gas oil (HGO) at 120 bar

The properties of liquid phase pyrolysis oil showed some unexpected advances compared to fast pyrolysis oil, which is the most common bio-oil to be upgraded via hydrodeoxygenation:

1. The high water content lowers viscosity, making high liquid hourly space velocities operable.
2. The high water content buffers heat of reaction and thus lowers coke formation reactions, which allows hydrodeoxygenation to be performed in one step.
3. The high water content allows for the usage of synthesis gas through in situ water-gas shift reaction.
4. The low particle load significantly reduces coke formation.

Continuous hydrodeoxygenation of liquid phase pyrolysis oil at different temperatures and liquid hourly space velocities as well as co-processing with refinery intermediates and substitution of hydrogen through synthesis gas were shown to be feasible in lab scale. The next steps would include long term experiments and upscaling of the process.

Appendix

APPENDIX

Publications

ARTICLES

Kontinuierliche Hydrodeoxygenierung von Flüssigphasenpyrolyseöl
Treusch, K., Schlackl, K., Nagl, R. & Schwaiger, N.
CEET Konkret, TU Graz, 2016

Co-Hydrodeoxygenierung von Flüssigphasenpyrolyseöl und Erdölraffinationsintermediaten
Treusch, K., Schwaiger, N., Huber, A., Hammerschlag, B., Ausserleitner, J.
CEET Konkret, TU Graz, 2017

Biogene Treibstoffe aus Biomassepyrolyse
Schwaiger, N., Treusch, K. & Siebenhofer, M.
BIOspektrum, Springer-Verlag 2017; DOI: 10.1007/s12268-017-0803-7

Continuous Hydrocarbon Production by Hydrodeoxygenation of Liquid Phase Pyrolysis Oil
Treusch, K., Schwaiger, N., Schlackl, K., Nagl, R., Pucher, P. & Siebenhofer, M.
SEEP Conference Proceeding, Bioenergy and Biofuels, 27.-30. Juni 2017, Bled (Slowenien); DOI: 10.18690/978-961-286-048-6.28; ISBN: 978-961-286-048-6

Diesel Production from Lignocellulosic Feed – The bioCRACK Process
Treusch, K., Ritzberger, J., Schwaiger, N., Pucher, P., Siebenhofer, M.
Royal Society Open Science, 2017, 4: 171122; DOI: 10.1098/rsos.171122

High Throughput Continuous Hydrodeoxygenation of Liquid Phase Pyrolysis Oil
Treusch, K., Schwaiger, N., Schlackl, K., Nagl, R., Rollett, A., Schadler, M., Hammerschlag, B., Ausserleitner, J., Huber, A., Pucher, P., Siebenhofer, M.
Reaction Chemistry and Engineering, 2018, 3, 258-266; DOI: 10.1039/c8re00016f

Temperature Dependence of Single Step Hydrodeoxygenation of Liquid Phase Pyrolysis Oil
Treusch, K., Schwaiger, N., Schlackl, K., Nagl, R., Pucher, P., Siebenhofer, M.
Frontiers in Chemistry, 2018, 6:297, DOI: 10.3389/fchem.2018.00297

Kontinuierliche Hydrodeoxygenierung von Flüssigphasenpyrolyseöl mit Synthesegas über die Wassergas-Shift-Reaktion
Treusch, K., Schwaiger, N., Mauerhofer, A., Painer, D.
CEET Konkret, TU Graz, 2018

Hydrocarbon production by continuous hydrodeoxygenation of liquid phase pyrolysis oil with biogenous hydrogen rich synthesis gas
Treusch, K., Mauerhofer, A., Schwaiger, N., Pucher, P., Müller, S., Painer, D., Hofbauer, H., Siebenhofer, M.
Reaction Chemistry and Engineering, 2019, DOI: 10.1039/c9re00031c

Refinery integration of lignocellulose for automotive fuel production
Treusch, K., Schwaiger, N., Huber, A., Reiter, S., Lukasch, M., Hammerschlag, B., Ausserleitner, J., Pucher, P., Siebenhofer, M.
Prepared for submission

Simultane Hydrodeoxygenierung von Flüssigphasenpyrolyseöl und Erdölraffinationsintermediaten zu Treibstoffen mit biogenem Anteil
Treusch, K., Schwaiger, N., Huber, A., Hammerschlag, B., Außerleitner, J., Pucher, P., Siebenhofer, M.
Chemie-Ingenier-Technik, 2018, 90(9), 1151-1151, DOI: 10.1002/cite.201855042

PRESENTATIONS

Liquid phase pyrolysis based biomass liquefaction
Schwaiger, N., Siebenhofer, M., Pucher, P., Nagl, R., Schlackl, K., Pichler, T. M., Menapace, M., Heinrich, D., Treusch, K., Mauerhofer, A. M. & Tandl, M. J.
ProcessNet Jahrestagung, 2016, Aachen (Germany)

High throughput single stage continuous hydrodeoxygenation of liquid phase pyrolysis oil
Schwaiger, N., Mauerhofer, A. M., Schlackl, K., Siebenhofer, M., Tandl, M. J., Nagl, R., Pichler, T. M., Pucher, P., Heinrich, D. & Menapace, M.
COST Action, 2016, Lissabon (Portugal)

Continuous Hydrodeoxygenation of Liquid Phase Pyrolysis Oil
Treusch, K., Schwaiger, N., Pichler, T. M., Siebenhofer, M., Mauerhofer, A. M., Schadler, M., Schlackl, K., Nagl, R., Rollett, A. T., Menapace, M. & Pucher, P.
AIChE Annual Meeting, 2016, San Francisco (USA)

The bioCRACK Process - a refinery integrated biomass-to-liquid concept to produce diesel from biogenic feedstock
Treusch, K., Ahn, E., Schwaiger, N. & Pucher, P.
Mitteleuropäische Biomassekonferenz, 2017, Graz (Austria)

Einfluss der Raumgeschwindigkeit auf die Hydrodeoxygenierung von Flüssigphasenpyrolyseöl
Schwaiger, N., Schlackl, K., Nagl, R., Treusch, K., Außerleitner, J., Hammerschlag, B., Pichler, T., Ritzberger, J., Pucher, P. & Siebenhofer, M.
TTTK, 2017, Canazei (Italy)

Hydrocarbon formation during hydrodeoxygenation of liquid phase pyrolysis oil
Schwaiger, N., Hammerschlag, B., Außerleitner, J., Nagl, R., Schlackl, K., Treusch, K., Pichler, T., Pucher, P. & Siebenhofer, M.
FP 1306 COST Action 2017, 2017, Torremolinos (Spain)

High throughput single stage continuous hydrodeoxygenation of liquid phase pyrolysis oil
Schwaiger, N., Schlackl, K., Hammerschlag, B., Außerleitner, J., Nagl, R., Treusch, K., Pichler, T., Pucher, P. & Siebenhofer, M.
ISGC, 2017, La Rochelle (France)

Continuous Hydrocarbon Production by Hydrodeoxygenation of Liquid Phase Pyrolysis Oil
Schwaiger, N., Hammerschlag, B., Ausserleitner, J., Nagl, R., Schlackl, K., Treusch, K., Pichler, T., Pucher, P., Siebenhofer, M.
SEEP, 2017, Bled (Slovenia)

Continuous Hydrodeoxygenation of Pyrolysis Oil from the bioCRACK Process
Huber, A., Treusch, K., Schwaiger, N., Ausserleitner, J., Hammerschlag, B., Nagl, R., Sterniczky, T., Siebenhofer, M.
WCCE, 2017, Barcelona (Spain)

Liquid Phase Pyrolysis based Biomass Liquefaction and Hydrodeoxygenation
Siebenhofer, M., Treusch, K., Schwaiger, N.
TIChE, 2017, Bangkok (Thailand)

Co-Processing of Liquid Phase Pyrolysis Oil and Refinery Intermediates in a Continuous Hydrodeoxygenation Reactor
Treusch, K., Schwaiger, N., Nagl, R., Hammerschlag, B., Ausserleitner, J., Huber, A., Pucher, P., Siebenhofer, M.
AIChE Annual Meeting, 2017, Minneapolis (USA)

Downstream Processing of Liquid Products of the BioCRACK Process with Refinery Unit Operations
Schwaiger, N., Pucher, P., Treusch, K., Ahn, E., Siebenhofer, M.

FASTCARD seminar, 2018, Madrid (Spain)

Co-Processing of Liquid Phase Pyrolysis Oil with Refinery Intermediates for Fuel Production

Schwaiger, N., Treusch, K., Huber, A., Hammerschlag, B., Ausserleitner, J., Pucher, P., Siebenhofer, M.

COST, 2018, Thessaloniki (Greece)

Co-Hydrodeoxygenation of Liquid Phase Pyrolysis Oil with Refinery Intermediates for Fuel Production

Treusch, K., Schwaiger, N., Huber, A., Hammerschlag, B., Ausserleitner, J., Nagl, R., Schlackl, K., Pucher, P., Siebenhofer, M.

ACHEMA, 2018, Frankfurt (Germany)

Simultane Hydrodeoxygenierung von Flüssigphasenpyrolyseöl & Erdölraffinationsintermediaten zu Treibstoffen mit biogenem Anteil

Treusch, K., Schwaiger, N., Huber, A., Hammerschlag, B., Ausserleitner, J., Pucher, P., Siebenhofer, M.

ProcessNet-Jahrestagung, 2018, Aachen (Germany)

Refinery Integrated Hydrocarbon Production – the BioCRACK Process and Liquid Product Upgrading

Treusch, K., Schwaiger, N., Pucher, P., Siebenhofer, M., Soprek, H., Kurte, L.

GOMA Symposium – Fuels, 2018, Opatija (Croatia)

Low Pressure Hydrodeoxygenation of Liquid Phase Pyrolysis Oil and Refinery Intermediates

Pichler, T., Treusch, K., Schwaiger, N., Huber, A., Siebenhofer, M., Pucher, P.

AIChE Annual Meeting, 2018, Pittsburgh (USA)

POSTERS

Continuous hydrodeoxygenation of liquid phase pyrolysis oil

Schwaiger, N., Mauerhofer, A. M., Schlackl, K., Tandl, M. J., Siebenhofer, M., Pichler, T. M., Nagl, R., Treusch, K. & Pucher, P.

Symposium on Seperation Science and Technology for Energy Applications, 2016, Wien (Austria)

Continuous Single-Step Hydrodeoxygenation of Liquid Phase Pyrolysis Oil

Treusch, K., Schwaiger, N., Pichler, T., Hammerschlag, B., Ausserleitner, J., Pucher, P. & Siebenhofer, M.

Minisymposium Verfahrenstechnik, 2017, Innsbruck (Austria)

High throughput single stage continuous hydrodeoxygenation of liquid phase pyrolysis oil

Treusch, K., Schwaiger, N., Nagl, R., Schlackl, K., Pichler, T., Dirninger, E., Siebenhofer, M. & Pucher, P.

Jahrestreffen Reaktionstechnik, 2017, Würzburg (Germany)

Low Temperature Hydrodeoxygenation of Liquid Phase Pyrolysis Oil

Treusch, K., Schwaiger, N., Huber, A., Pucher, P., Siebenhofer, M.

Minisymposium Verfahrenstechnik, 2018, Linz (Austria)

Supervised and Co-supervised theses

MASTER THESES

Temperatureinfluss und Einfluss der Raumgeschwindigkeit auf die Produktverteilung bei der kontinuierlichen Hydrodeoxygenierung von Flüssigphasenpyrolyseöl
Klaus Schlackl
TU Graz, 2016

Simultane Hydrierung von sauerstoffhaltigen Kohlenwasserstoffen und Schwerölkomponenten zur Herstellung von biogenen Treibstoffen der zweiten Generation
Berndt Hammerschlag
TU Graz, 2017

Einfluss des Katalysators auf die Produkteigenschaften bei der Hydrodeoxygenierung von Flüssigphasenpyrolyseöl
Roland Nagl
TU Graz, 2017

Sulfidisierung von Übergangsmetallkatalysatoren für die Hydrodeoxygenierung von Flüssigphasenpyrolyseöl
Julia Außerleitner
TU Graz, 2017

Hydrophobierung von Flüssigphasenpyrolyseöl durch partielle kontinuierliche Hydrodeoxygenierung
Anna Huber
TU Graz, 2017

Niederdruck-Hydrodeoxygenierung von Flüssigphasenpyrolyseöl
Mario Lukasch
TU Graz, 2018

Niederdruck-Co-Hydrodeoxygenierung von Erdölraffinationsintermediaten und Flüssigphasenpyrolyseöl
Samir Reiter
TU Graz, 2018

BACHELOR THESES

Variation der Durchflussrate bei der kontinuierlichen Hydrodeoxygenierung von Pyrolyseöl
Dominik Heinrich
TU Graz, 2017

Einfluss der Sulfidisierungszeit eines Metalloxidkatalysators auf die Hydrodeoxygenierung von Flüssigphasenpyrolyseöl
Thomas Sterniczky
TU Graz, 2018

Milde kontinuierliche Hydrodeoxygenierung von Flüssigphasepyrolyseöl über einem Halbmetall Katalysator
Julian Schwingshackl
TU Graz, in progress

PROJECT REPORTS

Einfluss von Temperatur und Sulfidisierungsdauer auf die Katalysatoralterung bei der kontinuierlichen Hydrodeoxygenierung von Flüssigphasenpyrolyseöl
Elisabeth Dirninger
TU Graz, 2017

Hydropyrolyse und Hydrothermale Verflüssigung von Biomasse – Ein Überblick
Julia Ausserleitner
TU Graz, 2017

Auswirkung von Temperatur und Durchflussrate auf die kontinuierliche Niederdruck-Hydrodeoxygenierung von Pyrolyseöl
Dominik Heinrich
TU Graz, 2018

Co-Hydrierung von Flüssigphasenpyrolyseöl und Erdölraffinationsintermediaten
Martin Dalvai Ragnoli
TU Graz, 2018

Regeneration eines Metalloxid Katalysators für die Hydrodeoxygenierung von Flüssigphasenpyrolyseöl
Daniela Grosinger
TU Graz, 2018

Temperaturvariation bei der Niederdruck Hydrodeoxygenierung von Flüssigphasenpyrolyseöl
Martina Kotzent
TU Graz, 2018

Biotreibstoff aus Flüssigphasenpyrolyseöl: ein kontinuierlicher zweistufiger Hydrodeoxygenierungsprozess
Maximilian Karre
TU Graz, 2018

Niederdruck-Co-Hydrodeoxygenierung von Flüssigphasenpyrolyseöl und schwerem Gasöl
Sarah Koller
TU Graz, 2018

Einfluss der Druckreduzierung auf die Hydrodeoxygenierung von Flüssigphasenpyrolyseöl und schwerem Gasöl
Thomas Sterniczky
TU Graz, 2018